ABSTRACT

Benjamin Thompson. IDENTIFICATION OF FACTORS ASSOCIATED WITH THE DEVELOPMENT AND DECAY OF HETEROLOGOUS TOLERANCE TO MORPHINE IN THE GUINEA PIG. (Under the direction of David A. Taylor) Department of Pharmacology and Toxicology, April 2016

It is believed that the heterologous tolerance that develops upon chronic exposure to morphine is the result of adaptive changes in the cellular signaling pathways associated with the μ opioid receptor. Proposed adaptive changes that occur in these signaling elements should occur as the changes in function appear in the whole animal and should spontaneously reverse as function returns to normal. The length of time it takes for these adaptations to reverse should be proportional to the magnitude of tolerance that has developed. To test these hypotheses, it is necessary to establish a complete time course for the development and decay of heterologous tolerance. Such a time course has been documented in the LM/MP of the guinea pig following pellet implantation. However, that method of administration only allows for a qualitative assessment of the nature of the decay of tolerance because the time at which morphine exposure ends is unknown. We therefore, assessed the capacity of two different twice daily injection administrations (subcutaneous and intraperitoneal) to generate a time course for the development and decay of heterologous tolerance that was reproducible. Animals were treated for 1, 2, 4, 7, or 10 days and then assessed for the appearance of tolerance via paw pressure testing in the whole animal and by measuring the response of the LM/MP to DAMGO and 2-CADO either 0, 1, 2, or 4 days after the last treatment day. Administration of morphine via intraperitoneal injection was found to produce tolerance that was highly variable, presumably due to variable absorption from the gut, making it unsuitable for the time course study. Subcutaneous injection was shown to reproducibly induce tolerance in both the whole animal via paw pressure analgesic testing and in the response of the guinea pig LM/MP to DAMGO and 2-CADO. The results of

this study indicated that a significant level of tolerance begins to develop by 2 days of treatment which appears to become maximal and plateau by 4 days of treatment. In addition, the tolerance observed after 2 days is not heterologous as evidenced by the lack of a significant change in the IC_{50} value for 2-CADO in the LM/MP. By 4 days of treatment tolerance had become heterologous. Despite the plateau after 4 days of treatment, LM/MP responses from animals treated for 7 or 10 days of treatment took longer (4 days) to return to baseline than animals treated for 4 days (2 days). These data suggest that more extensive adaptations occur as treatment length increases despite the fact that the magnitude of change in the responses from the LM/MP and whole animal were not significantly different from each other after 4, 7, or 10 days of treatment. Western blot analysis of LM/MP and brainstem homogenates from these same animals revealed that heterologous tolerance in these tissues is not the result of a decrease in the receptor number of either the μ, A_1, A_{2a}, or α_{2b} receptors. A trend was observed for the α_3 subunit isoform of the Na^+/K^+ ATPase in the LM/MP to decrease in abundance as tolerance develops and return to baseline as tolerance decays. Although it was not statistically significant, the change in abundance is of a similar magnitude to significantly changed values previously reported in the literature. A trend for an increase in the abundance of PKC_ε was also observed in the LM/MP. This trend, though not significant, is in agreement with reported literature values in other tissues. Contrary to the LM/MP results, PKC_γ and PKC_ε showed a trend for a decrease in the brainstem while there was no change in the abundance of the α_3 subunit of the Na^+/K^+ ATPase there. No change was observed in the brainstem for the α_1 and β_1 subunits of the Na^+/K^+ ATPase as well. The trends observed may indicate that the brainstem and the LM/MP develop tolerance by distinct mechanisms but more research will be necessary elucidate the role of the α_3 subunit of the Na^+/K^+ ATPase and PKC in the development of tolerance to morphine.

IDENTIFICATION OF FACTORS ASSOCIATED WITH THE DEVELOPMENT AND DECAY OF HETEROLOGOUS TOLERANCE TO MORPHINE IN THE GUINEA PIG

A Dissertation

Presented to the Faculty of the Department of Pharmacology and Toxicology

Brody School of Medicine at East Carolina University

In Partial Fulfillment of the Requirements for the Degree

Doctor of Philosophy in Pharmacology and Toxicology

by

Benjamin Thompson

April, 2016

IDENTIFICATION OF FACTORS ASSOCIATED WITH THE DEVELOPMENT AND DECAY OF HETEROLOGOUS TOLERANCE TO MORPHINE IN THE GUINEA PIG

by
Benjamin Thompson

APPROVED BY:

DIRECTOR OF DISSERTATION
AND CHAIR OF THE DEPARTMENT
OF PHARMACOLOGY AND TOXICOLOGY _____
Dr. David A. Taylor Ph.D.

COMMITTEE MEMBER _____
Dr. Abdel A. Abdel-Rahman Ph.D.

COMMITTEE MEMBER _____
Dr. Brian A. McMillen Ph.D.

COMMITTEE MEMBER _____
Dr. Raymond Dionne Ph.D.

COMMITTEE MEMBER _____
Dr. Kori L. Brewer Ph.D.

DEAN OF THE GRADUATE SCHOOL _____
Dr. Paul Gemperline Ph.D

ACKNOWLEDGEMENTS

I do not believe that there are many individuals who can truthfully say they accomplished any worthwhile endeavor without the assistance and support of others. I would like to thank my parents for all of the love and support they have given me over the years. It is unlikely that I would be who I am today without them.

The faculty and staff at the Brody School of Medicine at East Carolina University also should be recognized for the educational opportunity they have provided me. Everyone has always been more than willing to take the time help further explain a concept that I was not clear on or to show me how to perform a laboratory technique. I could not have asked for a better environment in which to complete my graduate studies and to begin my career as a scientist.

I would like to thank the members of my dissertation committee, Dr. David A. Taylor, Dr. Abdel A. Abdel-Rahman, Dr. Brian A. McMillen, Dr. Raymond Dionne, and Dr. Kori L. Brewer. Dr. Taylor served as the chair of my dissertation committee and was gracious enough to allow me the opportunity to complete my research in his laboratory. He is an excellent mentor, educator, and scientist who has always sought to provide the best opportunities for growth possible for any student he has had contact with, myself included. He and the other members of my committee have given me valuable advice and feedback which has helped shape my project into what you will see in the coming pages.

Some members of the technical staff in the Pharmacology and Toxicology department also deserve special recognition. In particular, I would like to thank Jackie McKeel, Kathleen Thayne, and Barbara Davis. Jackie was the technician in Dr. Taylor's lab and helped me perform many of the experiments necessary for the completion of my project. Kathleen taught me many of the experimental techniques that were used in my project and helped me

troubleshoot them when they went wrong. She has also used her artistic talents to create some the figures in this document. Barbara assisted me with experiments when Jackie could not be there to do so. She and Jackie both have given me advice with matters, both personally and professionally, that has allowed me to grow beyond who I was when I entered this department.

Last but not least, I would like to thank the other graduate students in the department, both past and present, which have served as a source of encouragement and friendship throughout my time in the program.

TABLE OF CONTENTS

LIST OF TABLES

LIST OF FIGURES

LIST OF ABREVIATIONS

2-CADO	2-chloroadenosine
5-HT	Serotonin
A_1 receptor	Adenosine A_1 receptor
A_{2a} receptor	Adenosine A_{2a} receptor
ACTH	Adrenocorticotropic hormone
Akt	Protein kinase B
AUC	Area under the curve
BCA	Bicinchoninic acid
BSA	Bovine serum albumin
cAMP	Cyclic adenosine monophosphate
CNS	Central nervous system
DAMGO	[D-Ala^2, MePhe^4, Gly(ol)^5] enkephalin
DOP	Delta opioid peptide receptor
EC_{50}	Excitatory concentration required to elicit 50% of the max response
G Protein	Guanine nucleotide binding protein
GAPDH	Glyceraldehyde 3-phosphate dehydrogenase
GDP	Guanine diphosphate
GI	Gastrointestinal
GIRK	G protein coupled inwardly rectifying K^+ channels
GPCR	G protein coupled receptor
GRK	G protein coupled receptor kinase
GTP	Guanine triphosphate

HINT1	Histidine triad nucleotide-binding protein 1
HPA axis	Hypothalamic-pituitary-adrenal axis
IC_{50}	Inhibitory concentration required to inhibit 50% of the max response
IP	Intraperitoneal
KOP	Kappa opioid peptide receptor
LM/MP	Longitudinal smooth muscle/myenteric plexus
M3G	Morphine-3-glucuronide
M6G	Morphine-6-glucuronide
MOP	Mu opioid peptide receptor
N/OFQ	Nociceptin/orphanin FQ receptor
NMDA	N-methyl-D-aspartate receptor
nNOS	Neuronal nitric oxide synthase
ORL1	Opioid receptor-like 1
PBS	Phosphate buffered saline
PBS-T	Phosphate buffered saline with 0.1% tween 20
PI3K	Phosphatidylinositol-4,5-bisphosphate 3-kinase
PKA	Protein kinase A
PKC	Protein kinase C
POMC	Prepro-opiomelanocortin
PVDF	Polyvinylidene fluoride
sc	Subcutaneous
α_{2b} receptor	Alpha 2b adrenergic receptor
β-LPH	β-lipotrophin

γ-LPH γ-lipotrophin

CHAPTER ONE: INTRODUCTION

1.1 General Introduction

Opium is the dried resin found in the seed pod of the opium poppy (*papaver somniferum*). The first undisputed reference to opium is found in the writings of Theophrastus but its therapeutic use likely predates recorded history. It was historically used to treat a wide range of illness, including some for which it had no indication based on the medical knowledge of the time. It was lauded by Sir Thomas Sydenham in 1680 that "Among the remedies which it has pleased almighty God to give to man to relieve his sufferings, none is so universal and so efficacious as opium." An entire class of drugs, opioids, has been developed based on alkaloids isolated from opium. Opioids are among the most potent analgesic drugs known to man. The term opioid refers to opiates, which are natural alkaloids present in opium, as well as synthetic substances derived from opiates and endogenous opioid peptides.

Morphine (see figure 1.1) is the most abundant alkaloid found in opium. It was first isolated from opium in 1804 by Friedrich Sertürner in what is believed to be the first isolation of a natural plant alkaloid in history. Sertürner originally named the compound *morphium* after the Greek god of dreams, Morpheus, because it tended to cause drowsiness. In 1817 Sertürner began distributing morphine and Merck began marketing the drug 10 years later in 1827. After the hypodermic syringe came into use in 1857, the use of morphine became more widespread. Referred to as "God's own medicine" by Sir William Osler (Osler, 1910), morphine was used in the civil war for its potent analgesic effect, during which time it was called "soldier's joy (Yaksh & Wallace, 2011)." It has since become, and remains today, the gold standard for analgesic drugs. Unfortunately, the use of "soldier's joy" for chronic war wounds often led to the "soldier's disease (Yaksh & Wallace, 2011)" or opioid addiction. Morphine's beneficial effects

are subject to the development of tolerance and the drug possesses a number of toxic side effects as well as the potential to cause addiction leading Francis Peabody to revise Osler's description of the drug based on his own experience with it saying that "depending upon how it is used it may be either 'God's Own Medicine' or 'The Devil's Own Poison (Paul, 1999).'"

The less favorable effects of morphine and other opiates prompted scientists to synthesize new compounds in search of one that had potent analgesic properties but lacked the side effects and abuse potential. That search has yielded a number of new drugs (see table 1.1) that included agonists, antagonists, partial agonists, drugs with mixed agonist/antagonist properties, each having varying side effect profiles and efficacies. While these new compounds have provided a wider range of therapeutic options, they also share many of the same liabilities that morphine has. Opioids are also subject to the development of cross tolerance such that individuals tolerant to one opioid drug will likely display some degree of tolerance to other opioids as well. Research into the cellular mechanisms by which opioids act on biological systems and the mechanism(s) by which tolerance to their actions develops is still ongoing. By understanding these mechanisms it may yet be possible to develop an opioid drug that is not subject to developing tolerance and does not cause addiction.

1.2 The Endogenous Opioid System

1.2.1 Opioid Receptors

Although there was a vast amount of knowledge about the effects morphine and other opioids on living organisms, it wasn't until the 1970s that any real understanding of how they function at a cellular level was ascertained. Radioligand binding studies in the early 1970s revealed multiple binding sites for opiates on brain cell membranes (Goldstein, Lowney & Pal, 1971; Pert & Snyder, 1973). In the mid to late 1970s the three classic opioid receptors (mu, kappa, and

delta) were characterized (Lord, Waterfield, Hughes & Kosterlitz, 1977; Martin, Eades, Thompson, Huppler & Gilbert, 1976). Although the Greek letter nomenclature is still prevalent in the literature, in 2000 the Committee on Receptor Nomenclature and Drug Classification of the International Union of Pharmacology adopted and encourages the use of the terms MOP, DOP, and KOP (**M**u **O**pioid **P**eptide receptor etc.)

The sigma receptor was proposed as an opioid receptor and was discovered at the same time as the classic receptors. However, it was later shown that naloxone, an opioid antagonist, did not act as an antagonist at the sigma receptor (Manallack, Beart & Gundlach, 1986; Su, London & Jaffe, 1988). More recently, cloning experiments have shown that the sigma receptor does not share the 7 transmembrane spanning domain structure typical of canonical G-protein coupled receptors that the mu, kappa, and delta receptors display (Hanner et al., 1996). As a result of these findings, the sigma receptor is no longer considered to be an opioid receptor.

In the 1990s a fourth receptor was recognized as an opioid receptor based on sequence homology to the other opioid receptors. It was called either ORL1 (Mollereau et al., 1994) or LC132 (Bunzow et al., 1994) when it was initially cloned. At the time it was an orphan receptor with no known endogenous ligand. The endogenous ligand was later isolated and characterized by two groups independently who called it either orphanin FQ (Reinscheid et al., 1995) or nociceptin (Meunier et al., 1995). Since the isolation of the endogenous ligand, the receptor has also been called the nociceptin/orphanin FQ receptor (N/OFQ) by some authors. At the present time, the functions of the N/OFQ receptor are not well understood. The receptor is expressed in a number of systems that endogenous opioids play a regulatory role in, thus it is hypothesized that it may play a similar regulatory type role.

A number of other opioid receptors have been proposed, but at the present time they are poorly characterized and their existence is not as widely accepted as the classic opioid receptors or the N/OFQ receptor. These receptors include epsilon (Wüster, Schulz & Herz, 1979), iota (Oka, 1980), lambda (Grevel & Sadée, 1983), and zeta (Zagon, Goodman & McLaughlin, 1989). Additionally, it was suggested that via alternative splicing there may exist at least two receptor subtypes for each of the mu, kappa, and delta classes of receptors. However, at the present time, cloning studies do not support the existence of these receptors as distinct classes. It is believed that the modified specificity for opioid ligands could be accounted for by several underlying events as opposed to a difference in the receptor subtype (Yaksh & Wallace, 2011).

Opioid receptors are found in the cell membrane where it is known that they can form both homo- and heterodimers. Receptor heterodimers have different pharmacological properties than the specific type of receptors that compose them. For example, mu-delta and delta-kappa dimers tend to have less affinity for highly selective agonists, show reduced agonist-induced receptor trafficking, and display a mutual synergy between receptor-selective agonists (Gupta, Décaillot & Devi, 2006). Receptor dimerization is also thought to play a role in opioid tolerance.

Opioid receptors are widely expressed both centrally and peripherally where they mediate several functions, including analgesia, behavioral responses such as reward reinforcement, and inhibition of respiration (see table 1.2). Mu, kappa, and delta receptors are found in several regions of the brain and spinal cord linked to pain transmission and analgesia such as the periaqueductal gray, the rostral ventral medulla, and the dorsal horn of the spinal cord. For a more detailed review of the anatomical distribution of opioid receptors and endogenous peptides see (Mansour, Khachaturian, Lewis, Akil & Watson, 1988; Sim & Childers, 1997).

1.2.2 Endogenous Opioid Ligands

Around the same time as the characterization of the opioid receptors, their endogenous ligands were isolated. Several classes of endogenous ligands exist. The main three classes are endorphins, enkephalins, and dynorphins. None are absolutely specific to a particular receptor, but the enkephalins appear to be somewhat selective for delta receptors, dynorphins are selective for kappa receptors, and endorphins are selective to mu receptors. In addition to these there are also the endomorphins, which are fairly mu selective, and N/OFQ, the ligand for the N/OFQ receptor. The endogenous ligands are as widely distributed as the receptors and mediate a number of functions (see table 1.2). All of these endogenous peptides are derived from larger precursor proteins. Each of these precursor proteins is subject to digestion by trypsin-like enzymes resulting in a multitude of smaller peptides, some of which are active. Most of the active peptides share a common sequence of amino acids, the opioid motif (Tyr-Gly-Gly-Phe-(Met or Leu)) at the N-terminal end of the peptide (see table 1.3). Notable exceptions to this are the endomorphins which have an atypical structure and N/OFQ which is lacking a hydroxyl group from the motif, which renders it inactive at mu, kappa, or delta receptors (Yaksh & Wallace, 2011).

Endorphins are cleaved from prepro-opiomelanocortin (POMC). POMC contains sequences for several non-opioid peptides as well. Proteolytic cleavage of POMC yields adrenocorticotropic hormone (ACTH), β-lipotropin (β-LPH), and one of the melanocyte stimulating hormones (γ-MSH). Further processing of β-LPH will produce γ-LPH and the opioid peptide β-endorphin. Although β-endorphin does contain the sequence for met-enkephalin, it is not converted this peptide. POMC is mainly expressed in the arcuate nucleus of the hypothalamus and the nucleus tractus solitarius but it is also found in the anterior and

intermediate lobes of the pituitary and in pancreatic islet cells. Most of the circulating β-endorphin is released from the pituitary with other pituitary hormones (Yaksh & Wallace, 2011).

Enkephalins are derived from proenkephalin which contains several copies of met-enkephalin and one copy of leu-enkephalin. Proenkephalin peptides are expressed in areas of the central nervous system (CNS) that are thought to be related to the processing of pain information, to the modulation of affective behavior, motor control, and the autonomic nervous system, as well as neuroendocrinological functions. Most of the circulating enkephalins are released from the chromaffin cells of the adrenal medulla and from nerve plexuses and exocrine glands of the stomach and intestines (Yaksh & Wallace, 2011).

Dynorphins are derived from prodynorphin. This precursor protein contains the sequences for dynorphin A and B as well as the sequence for neoendorphin. These peptides are distributed widely in neurons and are frequently co-expressed with other opioid peptides (Yaksh & Wallace, 2011). N/OFQ is widely distributed in the CNS though its physiological role is less understood than that of the endorphins, enkephalins, and dynorphins. A more complete review of N/OFQ distribution and functions was published in 2013 (Donica, Awwad, Thakker & Standifer, 2013). Endomorphins, like the other opioid peptides, are widely distributed in the CNS and are thought to be involved in a multitude of processes (Fichna, Janecka, Costentin & Do Rego, 2007).

A few other general points can be made regarding the endogenous opioid peptides. Not all cells that make a given opioid precursor will release the same mixture of opioid peptides because of differences in the peptidases present in each cell. A given cell may release a different mixture of opioid peptides depending on the current physiological demands the cell is experiencing. And lastly opioid peptides can be released both centrally and peripherally. The concentration of peptides in the plasma reflects release from peripheral systems and not release from neuraxial

systems. The reverse is also true, the concentration of peptides in the cerebral spinal fluid are a reflection of release from neuraxial systems and are not associated with release from the periphery (Yaksh & Wallace, 2011).

1.3 Basic Opioid Pharmacology

1.3.1 Opioid Pharmacokinetics

Opioids are fairly well absorbed but most are subject to extensive first-pass metabolism (Yaksh & Wallace, 2011). As a result, when given orally, the therapeutically effective dose may be much higher than would be required if the drug were administered via some other route (subcutaneously, intramuscularly, etc.) In addition, there is great variability in first-pass metabolism from person to person, making determining an effective oral dose difficult. Therefore, opioids are generally administered through other routes of administration including intravenous or subcutaneous injection, oral mucosa via lozenges, and transdermal patches. There are some opioids such as codeine and oxycodone that are more resistant to first-pass metabolism that are commonly administered orally (Yaksh & Wallace, 2011).

Opioids bind to plasma proteins with varying affinity, but they tend to rapidly leave the blood and localize in high concentrations in highly perfused tissues such as the brain, lungs, liver, kidneys, and spleen (Schumacher, Basbaum & Way, 2012). Despite the fact that the concentration of opioids that can be found in skeletal muscle is much lower than other tissues, skeletal muscle serves as the main reservoir due to the greater mass of skeletal muscle. Fatty tissue can also serve as a reservoir, especially after high-dose or chronic administration of lipophilic opioids that are slowly metabolized such as fentanyl (Schumacher, Basbaum & Way, 2012).

Opioids are primarily metabolized by hepatic P450 enzymes to more polar compounds which are then excreted. Most often, opioids undergo glucuronidation reactions. Morphine has two glucuronide metabolites, morphine-3-glucuronide (M3G) and morphine-6-glucuronide (M6G), both of which exert other effects (Yaksh & Wallace, 2011). M3G has neuroexcitatory effects that do not appear to be mediated through the μ receptor and are currently undergoing further analysis (Schumacher, Basbaum & Way, 2012). M6G does act through the μ receptor and has an analgesic potency 4-6 times that of its parent compound (Schumacher, Basbaum & Way, 2012). These metabolites are much more polar than the parent compound and therefore do not readily cross the blood brain barrier, so it is thought that they do not contribute much to the CNS effects observed after a single dose of morphine. In addition to hepatic metabolism, some opioids such as heroin or remifentanil that contain esters are metabolized by plasma esterases (Schumacher, Basbaum & Way, 2012).

The polar metabolites of opioids, as well as small amounts of the unchanged drugs, are primarily excreted in urine. Glucuronide conjugates can also be found in bile but the enterohepatic circulation only accounts for a small portion of the excretory process (Schumacher, Basbaum & Way, 2012).

1.3.2 Mechanism of Opioid Action

All opioid receptors belong to the superfamily of G-protein coupled receptors. This type of receptor is characterized by 7 transmembrane spanning domains coupled to a heterotrimeric G protein. G proteins consist of an alpha and a beta/gamma subunit. There are several types of alpha subunits, but opioid receptors are predominately coupled to pertussis toxin-sensitive G_i/G_o alpha subunits. All three of the major opioid receptors respond similarly when activated but since morphine and most of the other clinically relevant opioids act primarily at the mu receptor,

this section will focus on mu receptor activation. Upon acute receptor activation by an opioid, the GDP bound to the alpha subunit is replaced by GTP. This causes a conformational change in the alpha subunit which destabilizes the heterotrimer causing it to dissociate into an alpha and a beta/gamma subunit, both of which have signaling consequences (see figure 1.2). Being coupled to G_i/G_o alpha subunits, one of the major consequences of opioid receptor activation is an inhibition of adenylyl cyclase, leading to a reduction in intracellular cyclic adenosine monophosphate (cAMP) levels. G_i/G_o alpha also leads to an activation of protein kinase C (PKC) and phospholipase C-beta (PLC_β) as well as reducing the opening frequency of voltage-gated Ca^{2+} channels. Additionally, the beta/gamma subunit enhances K^+ efflux from the cell by opening G-protein coupled inwardly rectifying K^+ channels (GIRKs). There is also a Na^+ component to opioid hyperpolarization that been suggested to be due to an increase in the function of the Na^+/K^+ ATPase (Masocha, González, Baeyens & Agil, 2002). These signaling events are terminated via hydrolysis of the GTP to GDP on the alpha subunit allowing it to re-associate with the beta/gamma subunit (Yaksh & Wallace, 2011).

Mu receptors are present on both pre- and post-synaptic neurons and the activation at both sites results in an inhibition of signal transmission (see figure 1.3). The closing of voltage-gated Ca^{2+} channels on pre-synaptic neurons prevents the release of neurotransmitters. Post-synaptic neurons are hyperpolarized by the opening of GIRK channels and enhanced function of the Na^+/K^+ ATPase at the soma, thus dampening signal transmission, making it more difficult for these cells to generate action potentials (Schumacher, Basbaum & Way, 2012). Given that opioid receptors are widely distributed and they operate on both pre- and post-synaptic neurons, it is not surprising that opioids produce such a potent analgesic effect. Opioids act on the ascending pain transmission pathway starting at specialized nerve terminals in the periphery,

inhibiting the transmission of pain signals directly at the inflamed tissue (Schumacher, Basbaum & Way, 2012). They also act in the dorsal horn of the spinal cord at what is sometimes referred to as the pain gate (see figure 1.4), dampening the transmission of pain signals to the brain. Opioids also enhance the activity of the descending inhibitory pathways which help to dampen pain signals at the spinal cord (Schumacher, Basbaum & Way, 2012).

1.4 Clinical Application of Opioids

Opioids are predominately used for their potent analgesic effect to treat severe or chronic pain but there are a few other indications for them as well. Morphine has been used clinically in patients with acute pulmonary edema associated with left ventricular heart failure to relieve dyspnea. Several mechanisms have been proposed as to how morphine produces this effect. These mechanisms include reducing anxiety, which is thought to reduce the perception of shortness of breath, and by reducing cardiac preload and afterload. Morphine is also useful in treating painful myocardial ischemia associated with pulmonary edema. Dextromethorphan and codeine are useful as antitussives at doses lower than those required for analgesia. The mechanism of antitussive action is not clearly understood at the present time but it is thought that both central and peripheral effects have a role. Diarrhea from almost any cause can be controlled with opioids, most commonly diphenoxylate or loperamide employed due to their more selective GI effects with little to no CNS effects. However, if the underlying cause of diarrhea is an infection, opioids are not to be considered a substitute for the appropriate chemotherapeutic agents. Opioids, meperidine in particular, are also reported to reduce shivering. This particular response appears to be mediated through effects on α_2 adrenoceptor subtypes as opposed to effects generated from one of the opioid receptors (Schumacher, Basbaum & Way, 2012). Opioids are also frequently used as premedicant drugs before anesthesia for their sedative,

anxiolytic, and analgesic properties. They are also used as adjuncts to anesthetic agents or in higher doses as a primary component of an anesthetic regimen. Opioids are commonly used with anesthetics in cardiovascular surgeries and other types of high risk surgeries where minimizing cardiovascular depression is a priority (Schumacher, Basbaum & Way, 2012).

1.5 Adverse Effects of Opioids

Given that opioid receptors are widely distributed, it should not be surprising that in addition to the clinical benefits that opioids provide, they are also responsible for a number of adverse effects. One of the largest concerns with acute opioid administration is marked respiratory depression, which becomes more severe as the dose increases. At high enough doses this effect can be fatal. Although opioid actions in the GI system can relieve diarrhea in people suffering from this condition, opioids will cause constipation in patients who have normal GI function. This effect is also more severe with greater doses. Opioids can activate the chemoreceptor trigger zone in the brainstem resulting in nausea and vomiting. Endogenous opioid peptides also play a role in the homeostatic regulation of body temperature and thus administration of centrally active opioids may result in alterations of body temperature. Morphine can act in the anterior hypothalamus at μ receptors to produce hyperthermia while other opioids acting at κ receptors can produce hypothermia. Most of the beneficial and adverse effects of opioids are subject to the development of tolerance. However, the miosis that occurs with virtually all opioid agonists seems to develop little to no tolerance. Constriction of the pupils can be seen in even the most tolerant addicts.

Prolonged use of opioids may lead to the development of tolerance, physical dependence/withdrawal, and psychological dependence/addiction. Tolerance is defined as the loss of responsiveness to an agent that occurs as a result of repeated exposure to that agent.

Tolerance to the analgesic effect can be overcome by increasing the dose of the drug. The problem with this solution is that not all of the side effects will develop tolerance at the same rate as the analgesic effect and some effects do not develop an appreciable level of tolerance at all. As a result, higher doses will result in greater toxicity. Opioid tolerance is an extremely complex phenomenon. The degree of tolerance that develops and how long that tolerance persists after withdrawal of the drug depends on the effect, which opioid is used, and a number of genetic and epigenetic factors. Tolerance develops to the agonistic effects of opioids, but not to antagonists or to the antagonistic properties of mixed agents. There is also a degree of cross tolerance that occurs with opioids, particularly with opioids that are primarily μ selective, but this tolerance is often partial or incomplete. This incomplete tolerance among opioids is the basis behind the "opioid rotation" strategy that is used clinically to overcome tolerance. Despite years of research the cellular mechanism(s) underlying the development of tolerance are still not fully understood. This topic will be discussed in detail in section 1.6.

Physical dependence on an opioid is defined as requiring an opioid drug in order to maintain normal physiological function. This should not be confused with psychological dependence/addiction as it is possible for someone to be physically dependent on an opioid but not addicted to it. Physical dependence almost invariably occurs as a patient develops tolerance to the opioids that act primarily on the μ receptor. The withdrawal syndrome that occurs is a result of an exaggerated rebound from the acute effects of the opioid. Symptoms of withdrawal can include rhinorrhea, lacrimation, yawning, chills, gooseflesh (piloerection), hyperventilation, hyperthermia, mydriasis, muscular aches, vomiting, diarrhea, anxiety, and hostility. Which of these symptoms manifest, and the intensity of the symptoms, will be dependent on the extent to which physical dependence has developed. Giving an opioid agonist to a patient suffering from

opioid withdrawal will quickly ameliorate any symptoms. Similarly, giving an opioid antagonist such as naloxone to someone who has developed physical dependence, but who has not stopped taking an opioid, will precipitate withdrawal symptoms. The time of onset, intensity, and duration of withdrawal symptoms depend on the opioid used as well as the setting in which it is used and appears to be associated with the half-life of the drug. For example, the withdrawal symptoms associated with chronic methadone exposure take longer to peak and are less severe than those seen with morphine or heroin. This fact was the basis for using methadone in clinics to aid in the detoxification of heroin addicts. However, even once the physical dependence has subsided; there still remains the possibility of psychological dependence or addiction.

Addiction is defined by the American Society of Addiction Medicine as a primary, chronic disease of brain reward, motivation, memory, and related circuitry. Dysfunction of these circuits leads the affected person to pathologically seek reward and relief through substance abuse. Psychological dependence/addiction is characterized by the inability to consistently abstain from using a drug, impairments in behavioral control, drug craving, diminished ability to recognize significant problems with one's behaviors and interpersonal relationships, and a dysfunctional emotional response. Opioids are associated with high risk of developing addiction, but despite this risk, opioids are not to be withheld if there are no other options to adequately control a patient's pain (Schumacher, Basbaum & Way, 2012).

1.6 Cellular Mechanisms of Opioid Tolerance

As stated previously, the development of tolerance to the analgesic effect of opioids that occurs when they are used for prolonged periods of time is a serious obstacle to the successful management of chronic pain, such as pain associated with cancer. Despite many years of research, the mechanisms that underlie the development of tolerance have still not been fully

elucidated. It is believed that tolerance is the result of cellular adaptations that occur as part of a homeostatic response to the constant presence of opioid agonists in the body (Collier, 1966; Johnson & Fleming, 1989; Koob & Bloom, 1988). There are five criteria that have been proposed that must be met in order for a potential cellular mechanism to be identified as accounting for the observed change in responsiveness (i.e. tolerance): "The proposed cellular change must: 1) be induced by experimental procedures identical to those that induce tolerance and/or dependence; 2) follow a similar time course as the tolerance and/or dependence in that tissue; 3) quantitatively account for the tolerance and/or dependence; 4) account for the qualitative characteristics of the tolerance and/or dependence; and 5) occur in the very cells upon which the opioid is acting (Taylor & Fleming, 2001)". Opioid tolerance is a complex phenomenon in part because several forms of tolerance are known to exist. These different forms of tolerance can occur independently or simultaneously depending on the method used to induce tolerance.

Homologous tolerance is a form of reduced responsiveness that is confined to a single receptor system, in this case the μ receptor system. It typically occurs over a short period of time (seconds to hours) after exposure to high concentrations of agonist. One example of this form of tolerance is the receptor desensitization that occurs within seconds upon acute exposure to high concentrations of agonist (Johnson & Fleming, 1989; Law & Loh, 1999). Another form of homologous tolerance that has been proposed appears to be due to changes in the adenylyl cyclase cascade and develops more slowly over a few hours after agonist exposure (Nestler & Aghajanian, 1997; Nestler, Alreja & Aghajanian, 1994). In contrast, heterologous tolerance is a form of tolerance that extends beyond the single receptor system that the agonist responsible for its development acts on. This form of tolerance can take days to develop and decay. An

example of this form of tolerance has been proposed to be due to a partial depolarization of the cell membrane potential that can be accounted for by a down-regulation of the sodium pump and a corresponding decrease in its electrogenic contribution to the membrane potential (Fleming, 1999; Fleming & Taylor, 1995). This section will describe several of the mechanisms proposed by various laboratories.

1.6.1 Receptor Desensitization and β-arrestin mediated Internalization

Receptor desensitization is a fairly common mechanism by which signaling from many G-protein coupled receptors can be terminated acutely. Desensitization can be distinguished from longer lasting cellular tolerance by its quick reversal upon removal of the opioid agonist that induced the desensitization. Some of the first works that examined this phenomenon in the opioid receptor system were conducted in the early 1980s by Gahwiler and Law (Gähwiler, 1981; Law, Hom & Loh, 1982). A general mechanism for desensitization of G-protein coupled receptors has been described by Lefkowitz that is consistent with what has been observed with the μ receptor (Pierce, Premont & Lefkowitz, 2002). Briefly, this mechanism consists of the agonist binding the receptor, after which the receptor is phosphorylated allowing β-arrestin to bind to the receptor causing G protein uncoupling, desensitization, and/or internalization. If the receptor is internalized, it is either marked for degradation or it is recycled back to the membrane where it can become reactivated. A relatively new concept that has been developed from pharmacological studies of G-protein coupled receptors is that of biased agonism or functional selectivity (Kenakin, 2011). Functional selectivity is the observation that different ligands for a given receptor stabilize slightly different conformations of the receptor such that certain signaling pathways may be favored depending on which agonist is used. Functional selectivity has been observed in opioid receptor pharmacology in the context of desensitization at the steps

of receptor phosphorylation, endocytosis, and trafficking after endocytosis (Kelly, 2013; Pradhan, Smith, Kieffer & Evans, 2012; Raehal, Schmid, Groer & Bohn, 2011). This concept may also help explain the partial tolerance between opioids that is the basis for the opioid rotation strategy used in chronic pain patients. It may also help explain why very little internalization occurs upon acute morphine exposure when compared to acute DAMGO exposure as well (Patierno, Anselmi, Jaramillo, Scott, Garcia & Sternini, 2011).

Phosphorylation of the μ receptor is known to occur at numerous sites and is mediated by a number of different proteins (see figure 1.5). Fitting with the concept of biased agonism/functional selectivity, Lau et al. were able to characterize two such regions on the C terminal tail of the μ receptor that are quantitatively differentially phosphorylated by the μ selective peptide DAMGO and morphine (Lau et al., 2011). As seen in figure 1.5, there is evidence to support the involvement of a number of different protein kinases in μ receptor phosphorylation. G protein coupled receptor kinases (GRKs) 2, 3, and 5 appear to mediate phosphorylation upon exposure to morphine and DAMGO (Doll, Pöll, Peuker, Loktev, Glück & Schulz, 2012). In addition, PKC isoforms α, βII, γ, and ε have been shown to phosphorylate the μ receptor (Doll, Konietzko, Pöll, Koch, Höllt & Schulz, 2011; Feng, Li & Wang, 2011). Phosphorylation of the μ receptor by GRK appears to be a prerequisite to the binding of β-arrestin (Johnson et al., 2006; Whistler & von Zastrow, 1998). Both β-arrestin 1 and 2 (also called arrestin 2 and 3) have been implicated in the desensitization and internalization of μ receptor (Johnson et al., 2006) although β-arrestin 2 may be more involved with morphine mediated desensitization (Bohn, Dykstra, Lefkowitz, Caron & Barak, 2004). The μ receptor can also be desensitized via another mechanism independent of β-arrestin that does not result in receptor internalization and appears to be mediated by PKC phosphorylation (see figure 1.6)

(Allouche, Noble & Marie, 2014; Johnson et al., 2006). Once the μ receptor has been internalized it can be sequestered into endosomes, recycled back to the cell surface and reactivated, or targeted for degradation. Unlike other types of GPCRs, trafficking of the μ receptor for recycling or lysosomal degradation does not depend completely on ubiquitination (Hislop, Henry & von Zastrow, 2011). The recycling of the receptor to the membrane surface was enhanced upon treatment with the non-selective kinase inhibitor staurosporine, indicating that some of the kinases sensitive to staurosporine inhibition are involved with μ receptor recycling (Arttamangkul, Lau, Lu & Williams, 2012). Resensitization of μ receptor after morphine induced desensitization appears to involve dephosphorylation-mediated by protein phosphatases sensitive to calyculin A but not okadaic acid (Levitt & Williams, 2012).

1.6.2 Receptor Down-regulation

Receptor down-regulation is another common mechanism by which GPCR signaling is reduced in response to exposure to high concentrations of agonists. β adrenergic receptors, for example, are known to be down-regulated when chronically exposed to short acting β adrenoceptor agonists, which limits their use clinically to short term applications. There are conflicting reports about whether chronic treatment with opioids may or may not lead to changes in receptor abundance. Some labs report that chronic morphine treatment down-regulates the μ receptor (Bernstein & Welch, 1998; Yoburn, Billings & Duttaroy, 1993) while others report no change in receptor abundance (De Vries, Tjon Tien Ril, Van der Laan, Mulder & Schoffelmeer, 1993; Klee & Streaty, 1974). In contrast, there are a few reports suggesting that up-regulation of the receptors occurs with chronic treatment (Fábián, Bozó, Szikszay, Horváth, Coscia & Szücs, 2002; Rothman et al., 1991). Although there are instances where receptor down-regulation and cellular tolerance have been observed concomitantly, it is generally accepted that receptor down-

regulation is not required for the development of cellular tolerance (Gomes, Shen, Stafford, Patel & Yoburn, 2002). In addition, it appears the opioid used to induce tolerance has an important impact on whether or not receptor down-regulation occurs. For example, it has been shown that chronic treatment with morphine results in little to no down-regulation while chronic treatment with etorphine or other high-intrinsic-efficacy agonists does (Stafford, Gomes, Shen & Yoburn, 2001; Yabaluri & Medzihradsky, 1997). While receptor down-regulation is not required for the development of tolerance, the Yoburn group has suggested that down-regulation does contribute to the magnitude of tolerance that develops to those opioid agonists that have been shown to cause down-regulation (i.e. etorphine) (Gomes, Shen, Stafford, Patel & Yoburn, 2002; Shen, Benedict Gomes, Gallagher, Stafford & Yoburn, 2000; Stafford, Gomes, Shen & Yoburn, 2001). As morphine is not an agonist that tends to cause μ receptor down-regulation, it follows that down-regulation likely does not play a significant role in the cellular tolerance that develops as a result of chronic morphine treatment.

1.6.3 Adenylyl Cyclase, cAMP, and G-Protein Coupling

As discussed in section 1.3.2, activation of μ receptors results in hyperpolarization of neurons by opening GIRK channels. However, the opening of GIRK channels cannot completely explain the hyperpolarization that occurs. Opioid exposure has also been shown to suppress a resting Na^+ dependent inward current (Alreja & Aghajanian, 1993). One of the other signaling events that occurs after acute μ receptor activation is an inhibition of adenylyl cyclase (see figure 1.2), reducing the level of cAMP that is produced and thus reducing signaling within this cascade. The decrease in signaling of the adenylyl cyclase cascade has been suggested by the Nestler group to be responsible for the Na+ dependent component of opioid action (Nestler, Alreja & Aghajanian, 1994). They have been able to show that chronic opioid exposure leads to

an up-regulation of the adenylyl cyclase cascade in several brain regions thought to mediate the opioid analgesic response (Nestler & Aghajanian, 1997; Nestler, Alreja & Aghajanian, 1994). A homeostatic increase in the activity of adenylyl cyclase to counter the constant inhibition caused by chronic opioid presence, such as the Nestler group has suggested, is consistent with the hypothesis that tolerance to chronic morphine exposure is mediated by adaptive changes in a number of proteins. Indeed, they have been able to show that chronic morphine treatment increases the abundance of adenylyl cyclase I and VIII isoforms in the rat locus coeruleus (Nestler & Aghajanian, 1997). Similar changes in the adenylyl cyclase cascade have been reported in the guinea pig LM/MP as well (Chakrabarti, Wang, Tang & Gintzler, 1998). In addition to an increase in adenylyl cyclase isoforms, the Nestler group has also been able to demonstrate increases in the $G_{i/o}$ and G_s alpha subunits in the rat locus coeruleus in response to chronic morphine treatment (Nestler, Alreja & Aghajanian, 1994; Nestler, Erdos, Terwilliger, Duman & Tallman, 1989).

Also of note is that the changes in the adenylyl cyclase cascade in the LM/MP have been reported by the Gintzler group to be due to a shift in G-protein coupling from a $G_{i/o}$ alpha subunit to a G_s alpha subunit (Chakrabarti, Chang & Gintzler, 2010; Chakrabarti, Regec & Gintzler, 2005; Chakrabarti, Wang, Tang & Gintzler, 1998). In addition to this, work from the Gintzler laboratory has suggested that the adaptations responsible for the development of tolerance are not simply a hard-wired response to prolonged exposure to opioids (Gintzler & Chakrabarti, 2008; Shy, Chakrabarti & Gintzler, 2008). In fact, the nature of the adaptations that occur depend on the state of the cell and whether or not the consequence of μ receptor activation is inhibition or stimulation of adenylyl cyclase. Experiments conducted by this group in which the investigators overexpressed adenylyl cyclase II along with a constitutively active G_s alpha

subunit created an environment in which the activation of the μ receptor resulted in an increase instead of a decrease in cAMP. The increase in adenylyl cyclase and shift to G_s alpha signaling that occurs in a cellular environment that is inhibitory as far as adenylyl cyclase is concerned does not occur in the stimulatory environment.

While it is clear that changes occur in the adenylyl cyclase system during the development of opioid tolerance, it is unclear what this change contributes to the development of tolerance in the LM/MP. It has been shown that cAMP has no direct impact on the electrical properties of neurons in the LM/MP in untreated animals (Johnson & Pillai, 1990). Although cAMP does not directly impact the electrical properties in untreated neurons, over time alterations in signaling within this cascade could possibly change the expression of proteins that play a role in the establishment/maintenance of membrane potential, such as the Na^+/K^+ ATPase.

1.6.4 Protein Kinase C

As mentioned in section 1.6.1, a number of protein kinases are thought to play a role in receptor desensitization and internalization by directly phosphorylating the mu receptor. Protein kinase C has generated some interest in the context of the long lasting cellular tolerance to opioids. It is known that chronic administration of opioids leads to an increase in PKC activation (Granados-Soto, Kalcheva, Hua, Newton & Yaksh, 2000) and translocation of PKC to the membrane (Kramer & Simon, 1999). Additionally, inhibiting PKC before long-term morphine treatment prevents the development of analgesic tolerance (Gabra, Bailey, Kelly, Smith, Henderson & Dewey, 2008). Administration of either non-specific or subtype specific inhibitors of the α, γ, and ε isoforms of PKC reverses antinociceptive tolerance after it has developed (Javed, Dewey, Smith & Smith, 2004; Smith, Gabra, Smith, Redwood & Dewey, 2007). Because PKCγ is only expressed centrally (Aley & Levine, 1997; Wang & Wang, 2006), it was

suggested that the α and ε isoforms mediate peripheral nociception while PKCγ mediates central nociception (Velázquez, Mohammad & Sweitzer, 2007).

Work done by the Rodríguez-Muñoz group suggested a mechanism by which opioids can disinhibit signals from the periaqueductal gray, a part of the descending inhibitory pathway, and how acute tolerance can arise from this brain region. They suggested that in this brain region the μ receptor is coupled to the NR1 subunit of the NMDA receptor (Rodríguez-Muñoz, Sánchez-Blázquez, Vicente-Sánchez, Berrocoso & Garzón, 2012). They further suggest that under normal conditions this association is of little consequence, but after stimulation by morphine, a negative feedback loop is triggered whereby NMDA receptors reduce the signaling capacity of μ receptors (Rodríguez-Muñoz, Sánchez-Blázquez, Vicente-Sánchez, Berrocoso & Garzón, 2012). Activation of μ receptors by morphine initiates a signaling cascade where the βγ subunit of the receptor acts through PI3K-Akt-nNOS to produce nitric oxide (Sánchez-Blázquez, Rodríguez-Muñoz & Garzón, 2010). Nitric oxide releases zinc ions from endogenous stores that recruit PKCγ and Raf-1 to the HINT1 protein at the μ receptor C-terminus (Rodríguez-Muñoz, de la Torre-Madrid, Sánchez-Blázquez & Garzón, 2011; Rodríguez-Muñoz, de la Torre-Madrid, Sánchez-Blázquez, Wang & Garzón, 2008). PKCγ is then proposed to separate the μ receptor and NMDA receptor complex and activate Src, producing enhanced Ca^{2+} influx by NMDA receptors (Sánchez-Blázquez, Rodríguez-Muñoz, de la Torre-Madrid & Garzón, 2009). This enhanced Ca^{2+} influx opposes the effect of μ receptor activation, thus reducing the efficacy of morphine at the periaqueductal gray. This group has also shown that PKA, but not PKC, inhibition reduces the NMDA-induced antagonism of the analgesic effects of morphine (Rodríguez-Muñoz, Sánchez-Blázquez, Vicente-Sánchez, Berrocoso & Garzón, 2012). This mechanism could potentially explain the observation by Zeitz and colleagues that PKCγ null

mice develop tolerance to the analgesic effects of morphine and clonidine to a lesser degree than wild-type littermates (Zeitz, Malmberg, Gilbert & Basbaum, 2001).

Interestingly, Lin and colleagues recently took a different approach and demonstrated that increasing PKCα or PKCε activity at the pre-Bötzinger complex increases the level of tolerance to the respiratory depression that occurs as a result of opioid exposure (Lin, Law & Loh, 2012). The depressive effect opioids have on respiration does not develop tolerance as quickly or to the same extent to which the analgesic effect does, which causes it to be a significant problem when higher doses are used to overcome analgesic tolerance. Given the extensive body of work that exists, PKC may play an integral part in the development of tolerance to morphine.

1.6.5 μ-δ Heterodimerization

Over the past decade it was demonstrated that GPCRs can form homomers or heteromers and that doing so has an effect on the ligand binding, signaling, and trafficking properties of the receptors (Smith & Milligan, 2010). It was shown in the early 2000s that opioid receptors can form heterodimers, particularly κ-δ and μ-δ dimers (George et al., 2000; Gomes, Jordan, Gupta, Trapaidze, Nagy & Devi, 2000; Jordan & Devi, 1999). Since this time μ-δ heteromerization has been studied extensively. The dimerization of these two receptors plays a role in some of the adverse effects associated with opioids, including the development of tolerance (Gupta et al., 2010; He et al., 2011). Mice lacking the δ receptor do not develop tolerance to morphine (Zhu et al., 1999). Following chronic morphine treatment, it was observed that there is an increased abundance of μ-δ heteromers (Gupta et al., 2010). The μ-δ heteromers activate β-arrestin 2 mediated signaling which targets the heteromer for degradation (Rozenfeld & Devi, 2007). Disruption of heteromer appears to increase the analgesic effect of morphine by preventing the co-degradation of the heteromer (He et al., 2011). There is also evidence to suggest that μ-δ

heteromers are associated with $G_z\alpha$ subunits as opposed to the $G_i\alpha$ subunit usually associated with either receptor independently (George et al., 2000).

The μ-δ heteromers respond to drugs differently than homomers of either of these receptors. Signaling assays with classical μ agonists such as morphine, DAMGO, fentanyl, and methadone in cells expressing the μ-δ heteromer or homomers of each receptor revealed that the potency of these drugs was approximately 7-12 fold greater in cells expressing the μ-δ heteromer than in cells expressing μ receptor homomers and no activity in cells expressing the δ receptor homomer (Yekkirala, Banks, Lunzer, Negus, Rice & Portoghese, 2012; Yekkirala, Kalyuzhny & Portoghese, 2010). The same authors also found that the δ selective antagonist naltrindole antagonized the signaling mediated by morphine, fentanyl, and methadone only in cells that expressed the μ-δ heteromer and it antagonized the antinociceptive effect of these drugs in monkeys (Yekkirala, Banks, Lunzer, Negus, Rice & Portoghese, 2012). These findings led the Portoghese group to suggest that the μ-δ heteromers are the primary target for the antinociceptive effects of morphine, fentanyl, and methadone as well as for the development of analgesic tolerance. Inhibitors of δ receptors of μ-δ heteromers enhances the cellular response of the μ receptor, resulting in a greater antinociceptive effect upon activation by morphine (Gomes, Gupta, Filipovska, Szeto, Pintar & Devi, 2004). These results have prompted efforts to synthesize drugs that can target the μ-δ heteromers. These efforts led to generation of the bivalent ligand MDAN21, a compound comprised of the δ selective antagonist DN20 separated by a 21 atom spacer from the μ selective agonist MA19 (Daniels, Lenard, Etienne, Law, Roerig & Portoghese, 2005). MDAN21 has a potency 100 times greater than morphine and develops little tolerance or dependence (Daniels, Lenard, Etienne, Law, Roerig & Portoghese, 2005). Other compounds have also been generated, but their properties have yet to be adequately

assessed and at the present time there are no bivalent ligands in clinical trials (Fujita, Gomes & Devi, 2015).

1.6.6 Na^+/K^+ ATPase α_3 subunit

The Na^+/K^+ ATPase has been of interest in the context of morphine tolerance since the 1970s. Goldstein and his group used the LM/MP preparation to demonstrate morphine tolerance in the ileum of guinea pigs and observed that the LM/MP from tolerant animals were subsensitive to the inhibitory effects of morphine and supersensitive to the stimulatory effects of 5-hydroxytryptamine (Schulz & Goldstein, 1973). However, the magnitude of the hyperpolarization produced by receptor activation was similar in neurons from either placebo treated or morphine treated animals (Meng, Malanga, Kong, Taylor & Fleming, 1997). Based upon work done in the guinea pig vas deferens, Fleming and his group proposed that the results obtained by Goldstein et al. could be explained by an adaptive partial depolarization of the myenteric neurons similar to the depolarization observed in supersensitive smooth muscle cells of the vas deferens (Fleming, 1999; Wong, Westfall, Fedan & Fleming, 1981). There are two main contributors to basal membrane potential: the diffusion potential, of which the outward diffusion of K+ is the main component, and the electrogenic activity of the Na^+/K^+ ATPase. Of these two contributors, it was determined that the Na^+/K^+ ATPase was responsible for the adaptive partial depolarization observed in tolerant myenteric neurons (Kong, Leedham, Taylor & Fleming, 1997; Leedham, Kong, Taylor, Johnson & Fleming, 1992). The proposed mechanism by which the Na^+/K^+ ATPase contributes to morphine's activity on neurons involves the activation of the μ receptor by morphine which inhibits adenylyl cyclase and decreases PKA activation, leading to a decrease in the level of phosphorylation at Na^+/K^+ ATPase α_3 subunit, increasing its activity (Blanco & Mercer, 1997; Masocha, González, Baeyens & Agil, 2002; Wu,

Li, Chen, Chi & Liu, 2006). The increase in activity contributes to the overall hyperpolarization produced by μ receptor activation.

The Na^+/K^+ ATPase is composed of two subunits, an α subunit which contains the binding sites for Na^+ and K^+ as well as cardiac glycosides such as ouabain, and a β subunit which is responsible for trafficking and insertion into the membrane (Sweadner, 1989). There are four α subunits: the α_1 subunit is expressed ubiquitously, the α_2 subunit is mainly found in muscle and the nervous system, the α_3 subunit is expressed predominately in neurons, and the α_4 subunit which is expressed only in the testis (Tokhtaeva, Clifford, Kaplan, Sachs & Vagin, 2012). There are three β subunits: the β_1 subunit is expressed ubiquitously, the β_2 subunits are expressed mainly in skeletal muscle and brain, and the β_3 subunit is found in the testis, skeletal muscle, lung, and liver (Tokhtaeva, Clifford, Kaplan, Sachs & Vagin, 2012). The $\alpha_3\beta_1$ subunit combination has been implicated in the action of cardiac glycosides and is a form of the sodium pump thought to be specific to neurons (Schwinger et al., 1999).

After chronic morphine treatment, there is some debate as to the nature of the adaptation that occurs. In the LM/MP it has been shown that there is a decrease in the α_3 subunit that correlates with the development of tolerance in that tissue, but not in the α_1 subunit (Li, Maguma, Thayne, Davis & Taylor, 2010). In agreement with this finding it was also shown by another laboratory that there was about a 40% decrease in the abundance of the α_3 subunit found in the synaptosomes isolated from the cerebral cortex of morphine tolerant rats (Prokai, Zharikova & Stevens, 2005). Other authors observed a decrease in the activity of the pump, specifically the α_3 subunit, without a decrease in the protein level (Gonzalez et al., 2012). It has been suggested that the cause of this discrepancy may be due to differences in the way different tissues develop tolerance (Gonzalez et al., 2012). Activation of PKC leads to a decrease in the activity of the

$\alpha_3\beta_1$ subunit combination as well as others (Blanco & Mercer, 1997). As stated in previous sections, some of the adaptations that occur with chronic morphine exposure are enhanced activation of PKA and PKC, both of which can negatively modulate Na^+/K^+ ATPase activity by altering its phosphorylation state. As such, this may explain the decrease in activity noted by Gonzalez et al. and may contribute to the reduction in activity observed in the guinea pig LM/MP.

Table 1.1 Common Opioid Drugs

This table lists a number of the opioid agonists and antagonists with their selectivity for the main three receptor types. This table was adapted from (Yaksh & Wallace, 2011). [a]μ-preferring; [b]δ-preferring; [c]κ-preferring; [d]Universal ligand; [e]Irreversible ligand; + = agonist; - = antagonist; P = partial agonist. The greater the number of symbols, the greater the potency. The ratio of these symbols is representative of the selectivity of these agents. The values were calculated from in vivo/in vitro animal pharmacological work and may not extrapolate to humans.

	Opioid Receptor Types		
Agonists	μ	δ	κ
Morphine[a]	+++		+
Etorphine	+++	+++	+++
Fentanyl	+++		
Hydromorphone	+++		+
Methadone	+++		
Sufentanil	+++	+	+
DAMGO[a] ([D-Ala^2, MePhe^4, Gly(ol)^5]enkephalin)	+++		
DPDPE[b] ([D-Pen^2, D-Pen^5]enkephalin)		++	
Bremazocine	+++	++	+++
Buprenorphine	P		--
Butorphanol	P		+++
Ethylketocyclazocine	P	+	+++
Nalbuphine	--		++
Spiradoline[c]	+		+++

Antagonists	μ	δ	κ
Naloxone[d]	---	-	--
Naltrexone[d]	---	-	---
CTOP[a]	---		
Diprenorphine	---	--	---
β-Funaltrexamine[a,e]	---	-	++
Naltrindole[b]	-	---	-
Naloxone benzoylhydrazone	---	-	-

Table 1.2: Summary of central and peripheral effects caused by opioid agonists

This table, adapted from (Al-Hasani & Bruchas, 2011) summarizes the effect an opioid agonist has on various organ systems.

Organ Systems	Effects	
	Increase	**Decrease**
Central Nervous System	Analgesia	Rate of respiration
	Euphoria	Cough reflex
	Sedation	
	Miosis-Constriction of pupils	
	Truncal Rigidity	
	Nausea and vomiting	
Gastrointestinal System	Constipation	Gastric motility
	Constriction of biliary smooth muscle	Digestion in the small intestine
	Esophageal reflux	Peristaltic waves in the colon
Other Smooth Muscle	Depression of renal function	Uterine tone
	Urinary retention	
Skin	Itching and sweating	
	Flushing of the face, neck, and thorax	
Cardiovascular System		Blood pressure and heart rate if cardiovascular system is stressed
Immune System		Formation of rosettes by human lymphocytes
		Cytotoxic activity of natural killer cells

Table 1.3 Selected Endogenous Opioid Peptide Sequences

This table contains the sequences for some of the common opioid peptides from each class. For each peptide the opioid motif is bolded and the selectivity is noted. This table is adapted from Table 18-1 found in (Yaksh & Wallace, 2011). + = agonist; - = antagonist; P = partial agonist. The greater the number of symbols, the greater the potency. The ratio of these symbols is representative of the selectivity of these agents. The values were calculated from in vivo/in vitro animal pharmacological work and may not extrapolate to humans.

		Receptor type		
Peptide Name	Sequence	Mu (μ)	Delta (δ)	Kappa (κ)
Met-enkephalin	(**Tyr-Gly-Gly-Phe-Met**)	++	+++	
Leu-enkephain	(**Tyr-Gly-Gly-Phe-Leu**)	++	+++	
β-Endorphin	(**Tyr-Gly-Gly-Phe-Met**-Thr-Ser-Glu-Lys-Ser-Gln-Thr-Pro-Leu-Val-Thr-Leu-Phe-Lys-Asn-Ala-Ile-Ile-Lys-Asn-Ala-Tyr-Lys-Lys-Gly-Glu)	+++	+++	
Dynorphin A	(**Tyr-Gly-Gly-Phe-Leu**-Arg-Arg-Ile-Arg-Pro-Lys-Leu-Lys-Trp-Asp-Asn-Gln)	++		+++
Dynorphin B	(**Tyr-Gly-Gly-Phe-Leu**-Arg-Arg-Gln-Phe-Lys-Val-Val-Thr)	+	+	+++
Nociceptin/Orphanin FQ	(Phe-**Gly-Gly-Phe**-Thr-Gly-Ala-Arg-Lys-Ser-Ala-Arg-Lys-Leu-Ala-Asn-Gln)	-	-	-

Figure 1.1 Chemical Structure of Morphine

Chemical formula: $C_{17}H_{19}NO_3$

IUPAC Name: (4R,4aR,7S,7aR,12bS)-3-methyl-2,4,4a,7,7a,13-hexahydro-1H-4,12-methanobenzofuro[3,2-e]isoquinoline-7,9-diol

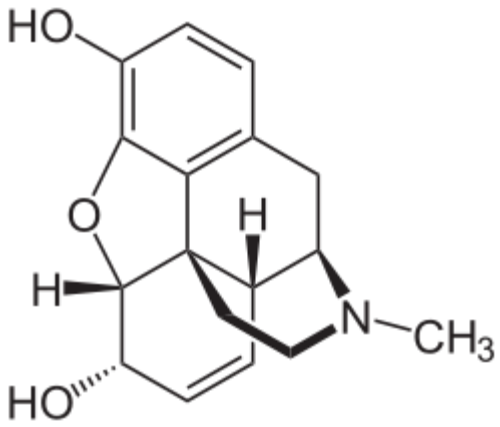
HO
O
H
H
N
CH3
HO

Figure 1.2 Acute mu opioid receptor signaling

This figure is a schematic representation of the signaling consequences that result from acute mu receptor activation. Drawn by Kathleen Thayne.

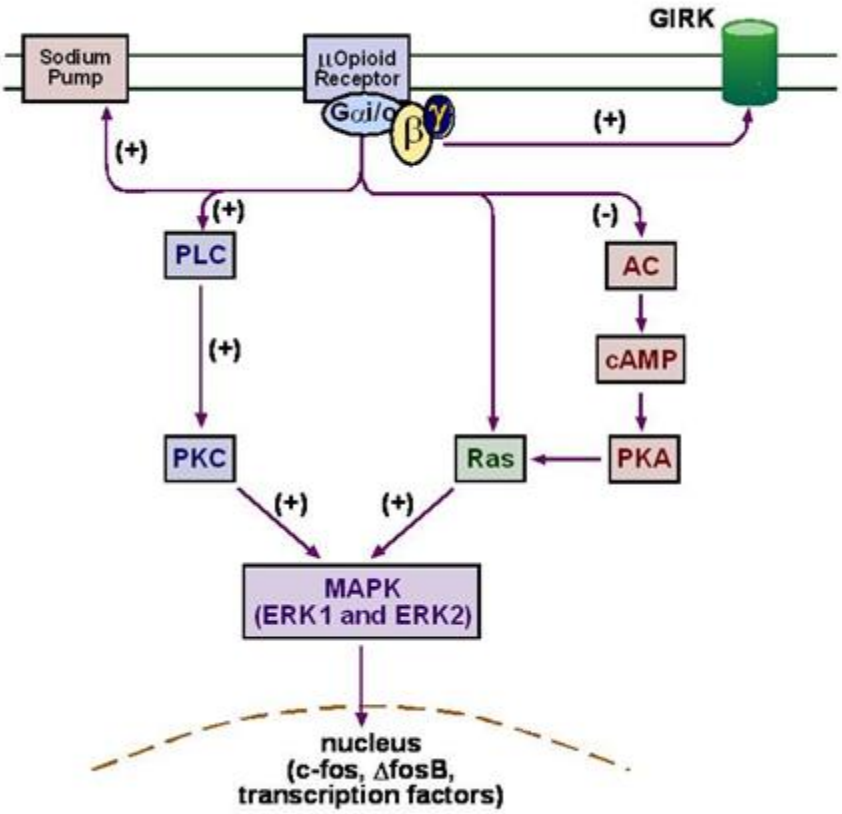
GIRK
Sodium Pump
μOpioid Receptor
Gαi/o
βγ
(+)
(+)
(+)
(-)
PLC
AC
(+)
cAMP
PKC
Ras
PKA
(+)
(+)
MAPK
(ERK1 and ERK2)
nucleus
(c-fos, ΔfosB,
transcription factors)

Figure 1.3 Mu receptor function at pre- and post-synaptic neurons

This figure depicts the effect of mu receptor activation on both pre- and post-synaptic neurons. Receptor activation on pre-synaptic neurons prevents release of neurotransmitter while post-synaptic neurons are hyperpolarized. Drawn by Kathleen Thayne, based on information found in (Schumacher, Basbaum & Way, 2012).

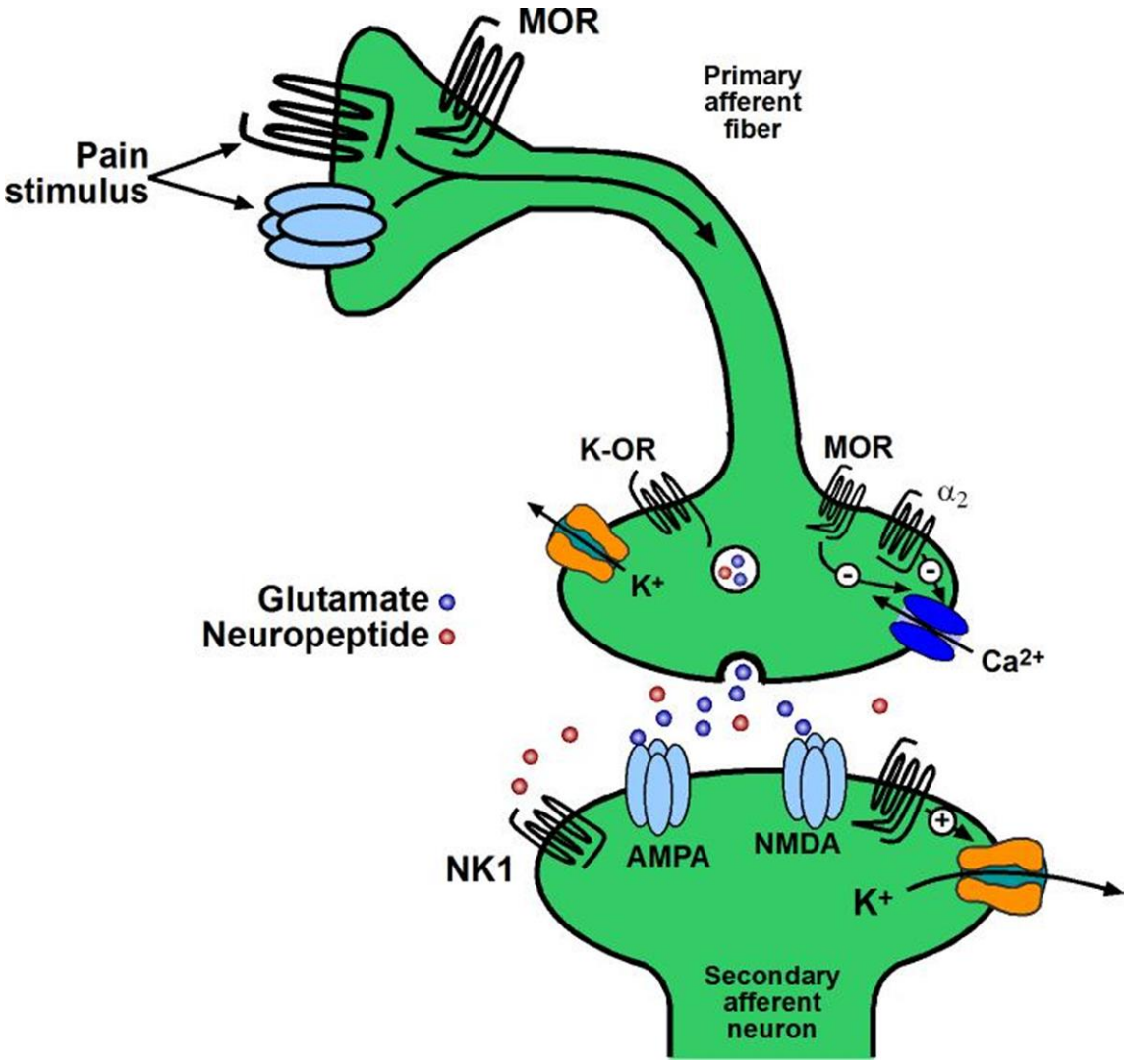
MOR
Primary afferent fiber
Pain stimulus
K-OR
MOR
α_2
K+
Glutamate
Neuropeptide
Ca2+
NK1
AMPA
NMDA
K+
Secondary afferent neuron

Figure 1.4 Sites of Opioid Action that Produce Analgesia

Opioids act in the periphery and at the "pain gate" neurons in the dorsal horn of the spinal cord. If the neurons in the dorsal horn of the spinal cord do not fire action potentials, the pain signal does not get transmitted to the brain and the sensation of pain is not experienced by the person. Opioids also enhance the activity of descending inhibitory pathways that dampen transmission of pain signals at the dorsal horn. Drawn based on information found in (Fields & Basbaum, 2005). PAG = periaqueductal gray; NRM = nucleus raphe magnus; NRPG = nucleus reticularis paragigantocellularis; DLF = dorsal longitudinal fasciculus

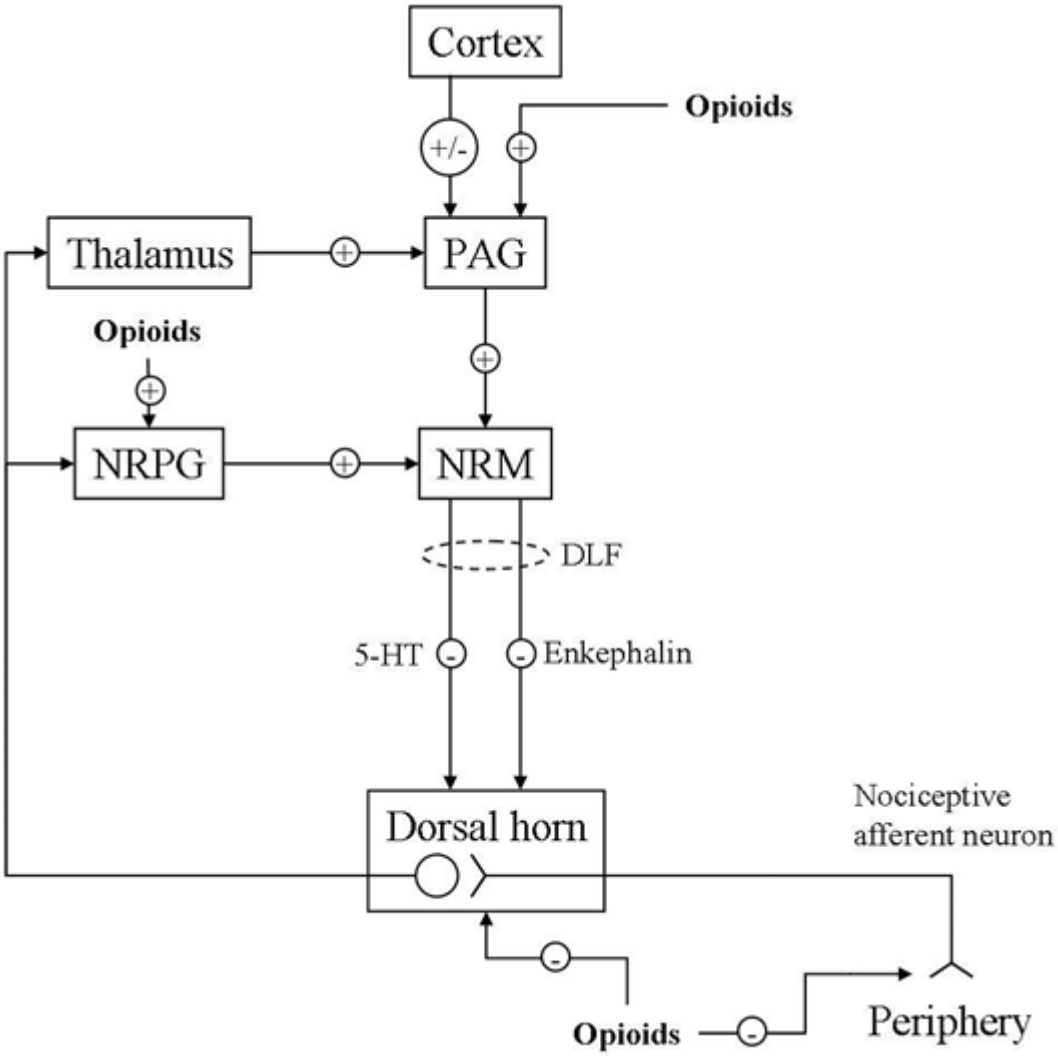
Cortex
Opioids
+/-
Thalamus
PAG
Opioids
NRPG
NRM
DLF
5-HT
Enkephalin
Dorsal horn
Nociceptive
afferent neuron
Opioids
Periphery

Figure 1.5 Sites of Phosphorylation on the Rat μ receptor

This figure was adapted from figure 1 found in the review article by (Allouche, Noble & Marie, 2014). This figure shows some of the sites that the rat μ receptor is phosphorylated at under basal conditions as well as sites that are phosphorylated after exposure to agonists. In cases where it is known, the kinase(s) that mediates the phosphorylation of each site is shown. For more detail, see (Allouche, Noble & Marie, 2014).

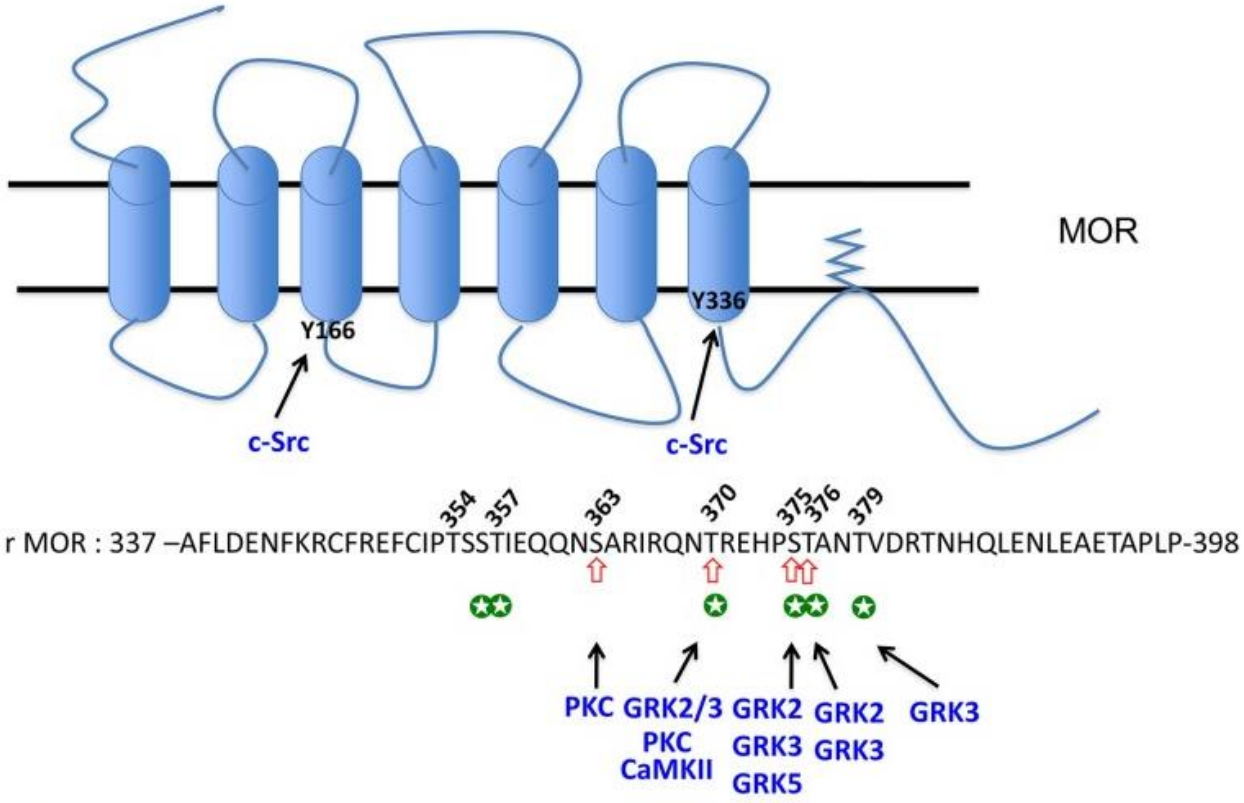

⇧ : basal phosphorylation

✪ : agonist-mediated phosphorylation

Figure 1.6 Mechanisms of Opioid Desensitization

This figure was adapted from figure 2 found in the review article by (Allouche, Noble & Marie, 2014). This figure depicts the arrestin dependent form of desensitization of the μ receptor that is seen with DAMGO exposure and the arrestin independent form that results in very little receptor internalization caused by morphine exposure.

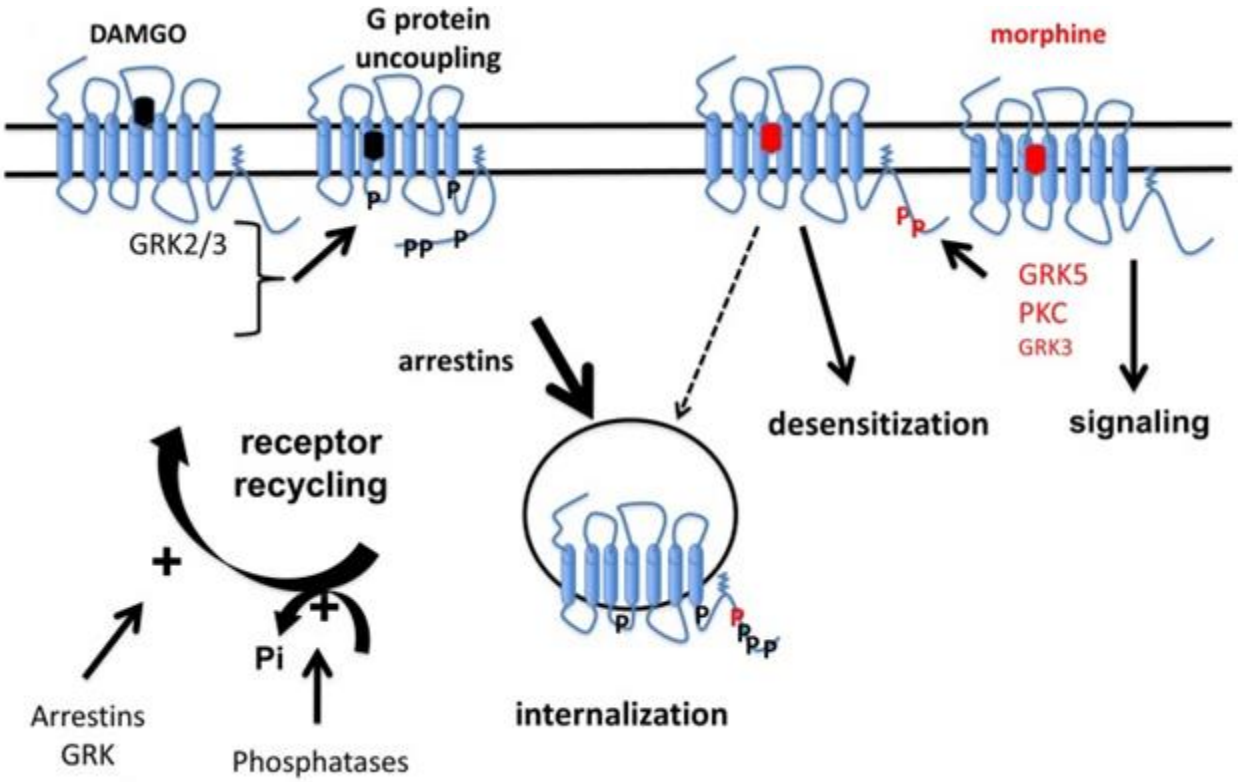
DAMGO
G protein
uncoupling
morphine
GRK2/3
arrestins
GRK5
PKC
GRK3
desensitization
signaling
receptor
recycling
Pi
Arrestins
GRK
Phosphatases
internalization

CHAPTER TWO: MATERIAL AND METHODS

2.1 Animals

All experimental procedures employing animals were reviewed and approved by the Institutional Animal Care and Use Committee of the Brody School of Medicine at East Carolina University and were conducted in accordance with the guidelines for the humane use of animals in research [NIH "Public Health Service Policy on Humane Care and Use of Laboratory Animals" (revised 2011)]. Dunkin-Hartley guinea pigs (Charles-River labs; Raleigh, NC, USA) of either sex weighing 200–450g were used in the study. The animals were housed 4 per cage with access to food and water *ad libitum*. The guinea pigs were kept in the animal facility for 1 week to permit acclimation prior to initiation of any treatment. Every effort was made to reduce the use of animals to the minimum number required to achieve sufficient statistical power.

2.2 Drugs

Morphine sulfate pentahydrate, ([D-Ala^2, MePhe^4, Gly(ol)^5]enkephalin) DAMGO, 2-chloroadenosine (2-CADO), and nicotine hydrogen tartrate salt were purchased from Sigma Chemical Company (St. Louis, MO). The dose of all drugs was corrected to exclude the conjugated salt. Isoflurane was purchased from the Department of Comparative Medicine at East Carolina University.

2.3 Animal Treatment

Animals were treated using a subcutaneous or intraperitoneal injection schedule adapted from Li et. al (Li, Maguma, Thayne, Davis & Taylor, 2010). Drugs or vehicle were injected in the housing room of the animal facility. For intraperitoneal injections animals were wrapped in cloth such that their front paws were restricted and they could not see the needle. Because the animals resist subcutaneous injections, risking injury to themselves during the process and

commercially available restrainers did not adequately restrain animals as small as those that we were using, a custom restrainer made from PVC pipe was used to prevent the animal from thrashing around during the injection procedure. The restrainer itself is simply a PVC pipe with one end capped off. A hole was cut into the top to allow access to the nape of neck of the animals. Depending on the size of the animal additional pieces of pipe were used to raise the animal closer to the hole in the pipe. Once the animal was inside a stopper obtained from a commercially available restrainer was placed inside the open end to prevent the animal from escaping. With the restrainer the animals were not able to move forward or backwards and their side to side movement was minimal. Drugs were injected twice daily at approximately 10:00 AM and 10:00 PM. The injections were made in the peritoneal cavity (intraperitoneal) or at the nape of the neck (subcutaneous) using a standard 1 mL tuberculin syringe with a 25 gauge needle obtained from the medical storeroom at East Carolina University Brody School of Medicine. In an attempt to minimize the amount of inflammation due to repeated injections, the site of injection was randomized. Occasionally on some of the older animals, the hair at the back of the neck was long enough to make it difficult to inject the animal. To prevent this from being an issue the hair at the back of the neck was shaved. Treated animals received morphine (free base) according to the following schedule: 10 mg/kg on day 1, 20 mg/kg on days 2 and 3, 40 mg/kg on days 4-7, and 80 mg/kg on days 8-10. Placebo animals received an equivalent volume of saline based on the weight of the animal. To examine the onset of tolerance animals were treated for 1, 2, 4, 7, or 10 days and assessed for tolerance 0 days after the last full treatment day. To examine the decay of heterologous tolerance animals that were treated for 4, 7, and 10 days were assessed for tolerance 1, 2 or 4 days after the last full treatment day. All experiments were done with

pairs of animals (1 morphine treated and 1 placebo treated) in order to account for some of the daily variability that may occur with paw pressure testing and/or the organ bath experiments.

2.4 Randal-Selitto Paw Pressure Test

Behavior assessment was performed early on the day of the experiment. Each animal was acclimated to the observation room for 1 h prior to the initiation of any assessment. Although it was discovered after these experiments were performed, this acclimation period should be sufficient to prevent any stress related analgesia by exposure to male experimenters according to Sorge et al. (Sorge et al., 2014). The Randall and Selitto (1957) test was used to assess mechanical nociception (Randall & Selitto, 1957). In this test, pressure was manually applied to the plantar surface of the hind paw using a cone-shaped pusher with a rounded tip (Randall-Selitto analgesimeter model 2500 [IITC Life Sciences, Woodlands Hills, CA]) (see figure 2.2). Pressure was applied gradually until the guinea pig either vocalized or withdrew its paw. The force (in *grams*) at which the guinea pig withdrew its hind paw or vocalized was defined as the paw pressure threshold. A cut-off was set at 600 grams of pressure to prevent tissue damage. Baseline analgesia was determined prior to injecting the challenge drug. Subsequent mean response thresholds were determined at the following time intervals after acute drug administration: 15, 30, 45, 60, and 90. Occasionally the test was performed at 120 minutes after the challenge dose if the animal's response was still not back to baseline. Tolerance was defined as a reduction in the antinociceptive effect (decreased threshold for withdrawal) of the challenge dose of agonist such that the maximum amount of pressure required to elicit a paw withdrawal was decreased. The challenge dose employed (morphine, 10 mg/kg s.c.) was selected based on preliminary studies done to assess the optimum dose required to produce an adequate and quantifiable analgesic response. The magnitude of the tolerance that developed was assessed by

calculating the area under the curve (AUC) for the time versus pressure threshold graphs using Graph Pad Prism 5. There was no apparent difference in locomotor activity displayed by the subjects in the treatment group in response to the acute drug administration.

2.5 Longitudinal Smooth Muscle/Myenteric Plexus Preparations

The LM/MP from morphine treated and placebo animals was used as an ex-vivo model to assess tolerance. The procedure to remove and isolated LM/MP segments was established previously by Paton (Paton, 1957). Animals were euthanized by decapitation following isoflurane anesthesia. The abdomen was opened to expose the cecum. The 10 cm section of ileum closest to the cecum was removed and discarded, and 2–4 cm segments of ilea from the adjacent 10 cm of ileum (see figure 2.3) were used for the LM/MP preparations. The segments of ilea were threaded on to a glass rod and, using a cotton swab moistened with Krebs–Henseleit buffer (see Appendix B), the LM/MP were carefully stripped tangentially from the point of mesenteric attachment until the muscle–nerve preparation was detached from the total area of the ileum.

The resulting sheet of LM/MP was tied at each end with surgical silk, passed through platinum-ring electrodes, and placed in a 10-ml organ bath containing Krebs-Henseleit buffer solution. One thread was tied to a Grass FT.03 force transducer and the other fixed to a tissue holder on the electrode, making sure that the thread was not touching the sides of the organ bath and as close to the center as possible (see figure 2.1). The output of the force transducer was delivered to a computer and digitized using the Power Lab/Chart 7 computer program (AD Instruments, Colorado Springs, CO, USA) through a four channel power lab system using a four channel Quad bridge converter interface (AD instruments, Colorado Springs, CO, USA). Force transducers were calibrated with a 1 g weight prior to attaching the tissues and electrodes. Two

tissues from each animal were placed in organ baths for these experiments. In order to control for the variation in organ bath temperature due to the distance away from the water bath as well as other factors associated with placement in the organ baths, the morphine and placebo tissues were alternated with each experiment such that for a given time point there were experiments in which the morphine tissues were closest to the water bath and vice versa.

The tissues were maintained at 37˚C in a physiological Krebs-Henseleit buffer solution (see Appendix B) bubbled continuously with a mixture of 95% O_2/ 5% CO_2. A basal tension of 1.0 g was set for each tissue and isometric tension generated by the muscle was recorded and stored using the Power Lab/Chart 7 program. Tissues were allowed to rest for 15 min before beginning neurogenic contractions. Neurogenic contractions were elicited via transmural electrical stimulation using supramaximal voltage delivered to the tissue through platinum-ring electrodes using a stimulation system consisting of a Grass S48 stimulator connected to the electrodes by a Med Lab Attenuator and Stimu-splitter. To ensure only nerve endings were stimulated, the following parameters were used: voltage (50V); impulse duration (<1 ms); delay setting (zero); and frequency (0.1Hz). To allow for equilibration, the tissues were stimulated for 1 hour before exposure to inhibitory drugs. During the equilibration period the buffer solution was replaced at 15 min intervals.

2.5.1 Ex-Vivo Assessment of Tolerance

To assess tolerance in the LM/MP, concentration response curves were constructed by exposing the tissues to cumulatively increasing concentrations of the inhibitory drugs DAMGO and 2-CADO (final concentrations in the organ bath ranging between 1 nM and 10 μM) (see figure 2.4). To minimize the impact of acute tolerance, the order the in which drugs were administered was randomized. Three 5 min washes followed by three 15 min washes with drug

free Krebs–Henseleit solution were performed between concentration–response curves of different drugs permitting full recovery of the amplitude of neurogenic contractions. In each experiment, two LM/MP preparations from each test group of animals were studied simultaneously and the responses of the tissues from the same animal averaged. The Lab Chart 7 software automatically constructed an average concentration response curve for each treatment group and calculated a number of parameters, including an IC_{50} value for each drug. A daily morphine to placebo ratio of the –log (IC_{50}) for DAMGO, 2-CADO, and in some cases nicotine was obtained from each pair of animals and used for statistical analysis. Graph Pad Prism 5® (Graph Pad Software, Inc.) was used for all statistical analyses.

2.6 Tissue Preparation

The LM/MP of both control and treated guinea pigs were removed as detailed in section 2.5. In addition to the LM/MP, the heart, diaphragm, and brain (sectioned into the cortex, midbrain, brainstem, and cerebellum) were also taken from the animals as soon as possible after euthanasia. The tissues that were not to be used immediately for the organ bath experiments were placed in labeled aluminum foils, frozen in liquid nitrogen, and stored at -80°C until they were used for western blot analysis. For western blot analysis, tissues were homogenized and a protein assay was performed to determine the amount of protein in each sample after homogenization.

2.6.1 Tissue Homogenization

Tissues were removed from the -80°C freezer and weighed. An amount of protease inhibitor buffer (see Appendix C) was added to a ground glass homogenizer (PowerGen 125; Fisher Scientific, Pittsburgh, PA) depending on the wet weight of the tissue (1 mL of buffer per 100 mg of wet weight). Tissues were then placed in the homogenizer and homogenized until there were

no visible pieces of tissue left. The homogenate was then placed into a 1.5 mL microcentrifuge tube and centrifuged for 5 seconds and maximum speed (14000 rpm). The supernatant was transferred to a clean 1.5 mL microcentrifuge tube and spun for 10 minutes at maximum speed at 4°C. The supernatant was aliquoted into the necessary number of microcentrifuge tubes to ensure that there was only enough sample to be used for a protein assay and a western blot in each tube. This process of preparation prevented wasting sample and reduced protein damage by excessive freezing and thawing of the sample. The tubes were stored at -20°C for later use.

2.6.2 BCA Protein Assay

Spectrophotometric determination of protein concentration in samples was determined using a Pierce® BCA Protein assay kit (Pierce Biotechnology, Rockford, Illinois). Bovine serum albumin (BSA) was made at a concentration of 1 mg per 1 mL of phosphate buffered saline (PBS – see Appendix D). Serial dilutions (0.5, 0.25, 0.1, and 0.05 mg/mL) of this BSA solution were made to create the standard curve that was used extrapolate the protein concentration of the samples. Samples were diluted 1:20 with PBS. In a 96 well plate, 10 µL of the samples, the standards, and a blank (PBS) were loaded in triplicate. 200 µL of BCA dye reagent was added to each well and mixed. The dye reagent is made by mixing 50 parts dye reagent A with 1 part dye reagent B and should be green in color. In the presence of protein, the dye should change from green to purple. The reaction will occur at room temperature, but to increase the reaction rate the plate was incubated at 37°C for 15 minutes. If the color had not developed sufficiently after 15 minutes, the plate was incubated for another 15 minutes. The absorbance of each well at a wavelength of 562 nm was read using the Infinite M200 PRO plate reader (Tecan US, Research Triangle Park, NC). Calculation of the standard curve and interpolation of concentration of the samples were done using Graph Pad Prism 5 software.

2.7 Western Blot

To assess the relative abundance of specific proteins in each sample, western blots were performed. Prior to western blotting, the samples to be examined were homogenized and the concentration of total protein in each sample was determined using a BCA protein assay as detailed in section 2.6. The protocol for western blotting was similar to one that was used in the lab previously by Biser et al (Biser, Thayne, Fleming & Taylor, 2002). Tissue homogenates were diluted 1:1 with a working sample buffer solution (see Appendix D). These samples were loaded onto a Bio Rad Criterion 10% TGX pre-cast polyacrylamide gel (Bio-Rad Laboratories, Inc., Hercules, CA) at a concentration of 20 µg of protein per well. The concentration of protein per well was determined based on preliminary experiments and was deemed suitable to detect the proteins of interest. In addition, each gel was also loaded with 3 µL of the Kaleidoscope ladder (Bio-Rad Laboratories, Inc., Hercules, CA). Samples were then size fractionated via electrophoresis at 200 V using a Criterion cell (Bio-Rad Laboratories, Inc., Hercules,CA). Proteins were transferred from the gel to a pre-made polyvinylidene fluoride (PVDF) membrane transfer pack from Bio-Rad using the Trans-Blot Turbo from Bio-Rad using the appropriate setting depending on the number of gels being run. After transfer, membranes were prehybridized in Odyssey Blocking Buffer (Li-cor Biosciences, Lincoln, NE) overnight at 4°C. Following this step, the membranes were rinsed with phosphate buffered saline with 0.1 % Tween-20 (PBS-T, see Appendix D) and then washed 3 times for 15 minutes each with PBS-T. After washing, the primary antibody was added at the appropriate concentration for each protein of interest (see Appendix E for details). Previous experiments were performed in order to optimize the antibody concentrations for each protein of interest (see figures 2.5-2.13). Primary antibody incubation lasted 1 hour. After primary antibody incubation the membrane was washed

3 times with PBS-T for 10 minutes each. Following these washes, the secondary antibody was added at previously optimized dilutions (see Appendix E) for 1 hour. After secondary antibody incubation, the membrane was washed 4 times for 10 minutes with PBS (not PBS-T). Membranes were allowed to dry completely before imaging with the Odyssey CLX® near-infrared imaging system (Li-Cor Biosciences, Lincoln, NE). Densitometry analysis was performed using the Image Studio 5.2 software (Li-Cor Biosciences, Lincoln, NE).

Figure 2.1 Anatomy of the Ileum

Most of the tissue work was done in this project using the outermost layer of the ileum consisting of the longitudinal smooth muscle and the myenteric plexus. The next layer going inward is the circular muscle and submucosal plexus. The innermost layer is the mucosal layer.

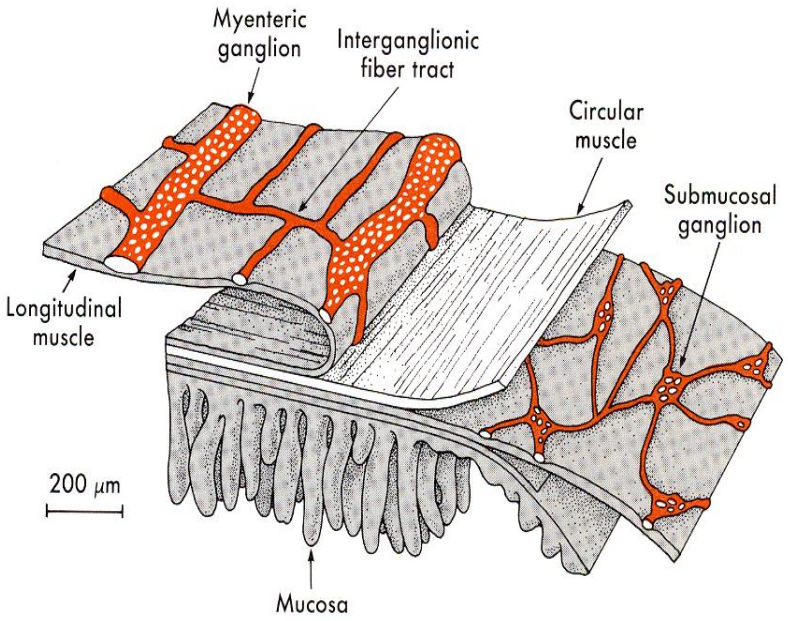
Myenteric ganglion
Interganglionic fiber tract
Circular muscle
Submucosal ganglion
Longitudinal muscle
200 μm
Mucosa

Figure 2.2 Randall-Selitto Analgesimeter 2500

In the context of the paw pressure test this device measures and records the amount of force required to cause pain great enough to elicit a paw withdraw response from the animal. The hind paw of the guinea pig is placed in the apparatus such that the rubber cone will press down on the plantar surface. Force is manually applied and increased gradually until the animal feels pain and withdraws its paw or vocalizes.


ALMEMO 2590-5

Figure 2.3 Organ Bath Schematic Diagram

Schematic diagram depicting the organ bath set up used to obtain concentration response curves for DAMGO and 2-CADO for the ex-vivo assessment of tolerance. Adapted from (Taylor, 2011).

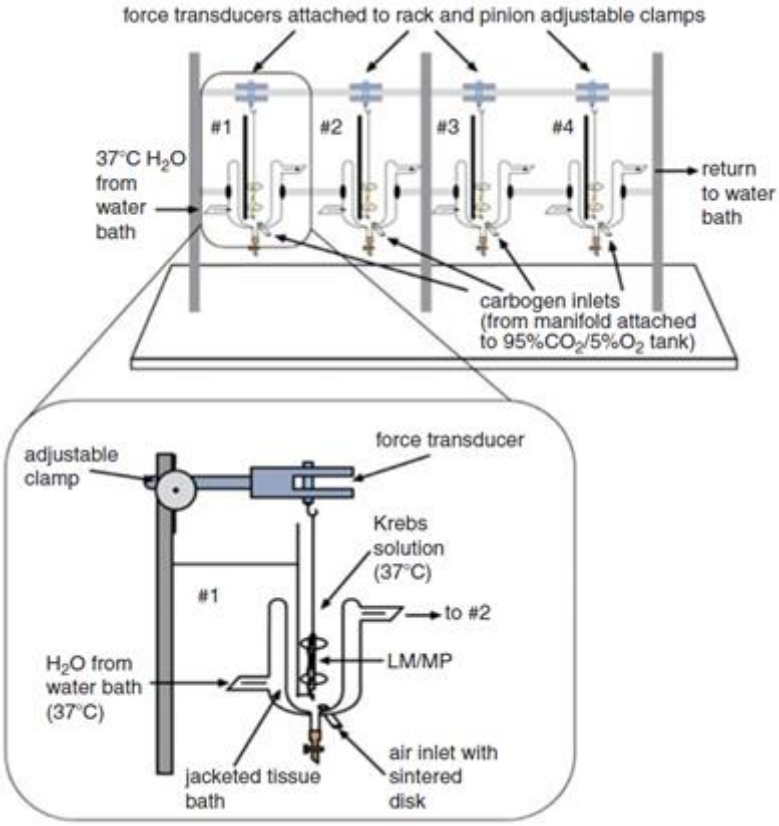
force transducers attached to rack and pinion adjustable clamps
#1
#2
#3
#4
37°C H_2O from water bath
return to water bath
carbogen inlets (from manifold attached to 95%CO_2/5%O_2 tank)
adjustable clamp
force transducer
Krebs solution (37°C)
#1
to #2
H_2O from water bath (37°C)
LM/MP
air inlet with sintered disk
jacketed tissue bath

Figure 2.4 Representative tracing depicting the concentration dependent reduction in the amplitude of neurogenic twitches of the LM/MP.

A) In this tracing the LM/MP was exposed to cumulatively increasing concentrations of the inhibitory drug DAMGO (final cumulative concentration in the bath ranging between 1 nM and 3 μM). The effect of DAMGO on the neurogenic twitches is calculated as a percent inhibition of the initial amplitude. IC_{50}s are defined here as the concentration of drug required to reduce the amplitude of the contractions by 50%.

B) A continuation of the tracing in A depicing the return of the electrogenic twitches after washing out the drug.

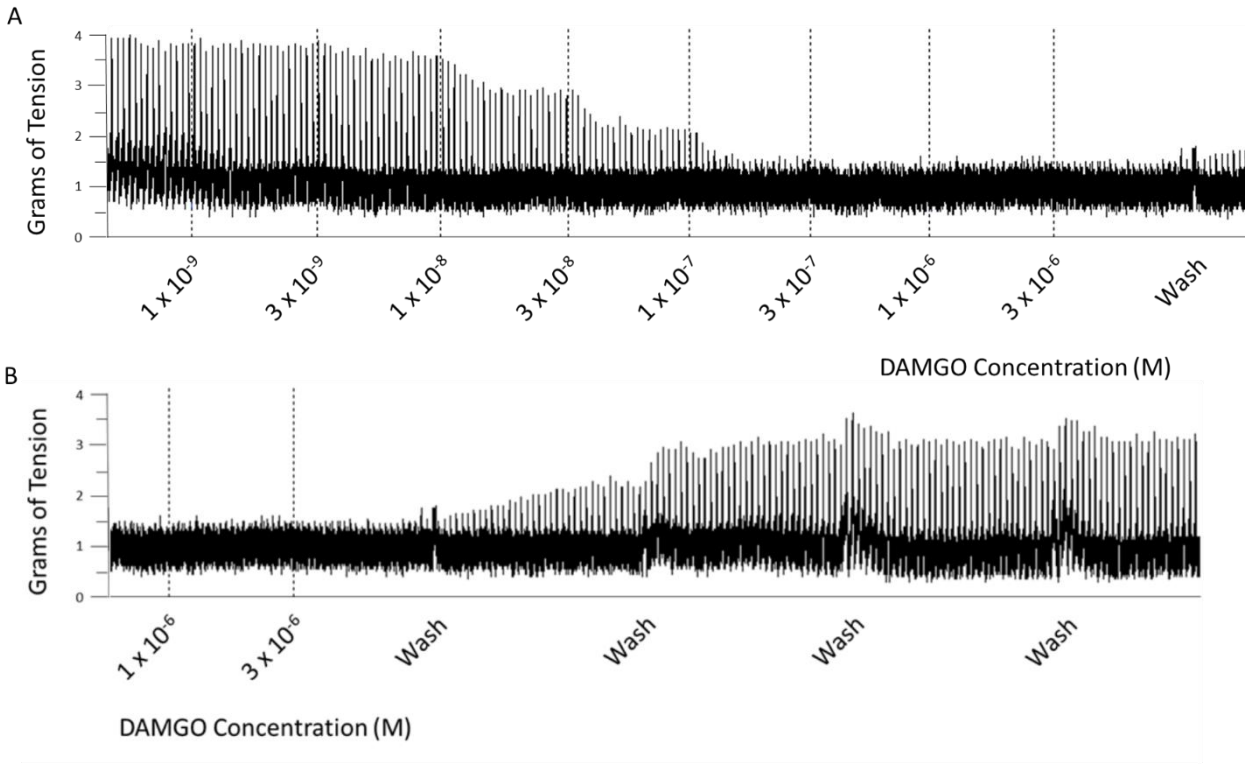
A
Grams of Tension
0
1
2
3
4
1 x 10-9
3 x 10-9
1 x 10-8
3 x 10-8
1 x 10-7
3 x 10-7
1 x 10-6
3 x 10-6
Wash
DAMGO Concentration (M)
B
Grams of Tension
0
1
2
3
4
1 x 10-6
3 x 10-6
Wash
Wash
Wash
Wash
DAMGO Concentration (M)

Figure 2.5 Verification of μ opioid receptor antibody

A representative image of a western blot using LM/MP homogenates from a naïve guinea pig and brainstem homogenates from a placebo treated guinea pig using the antibody concentration displayed in Appendix E and following the protocol described in section 2.7. The μ receptor appears at 45 kDa in the 680 nM channel (red) and the housekeeper protein, GAPDH, is shown in the 800 nM channel (green) at 36 kDa.

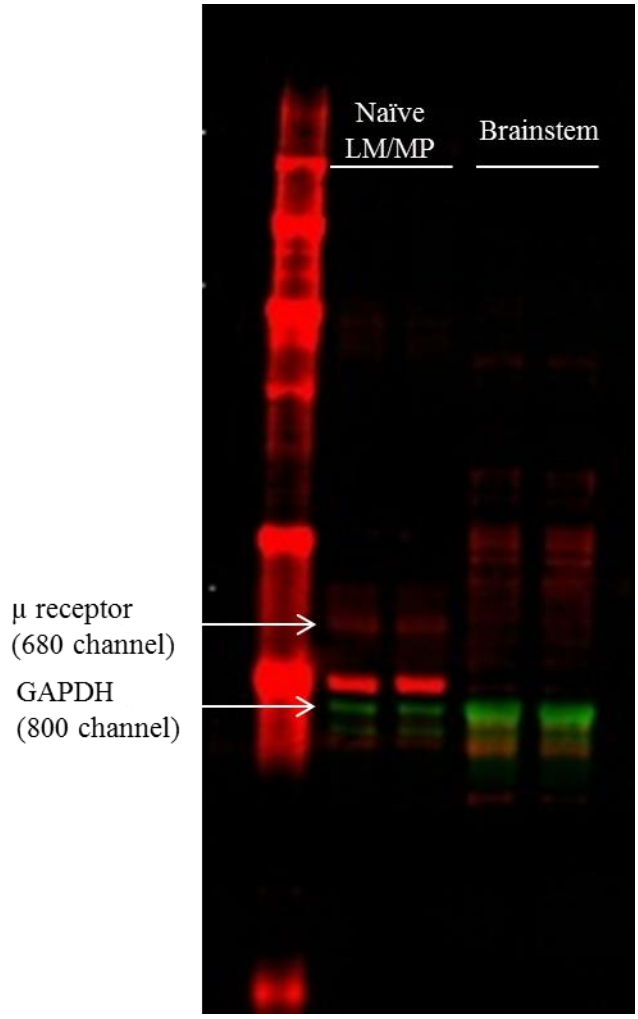
Naïve
LM/MP
Brainstem
μ receptor
(680 channel)
GAPDH
(800 channel)

Figure 2.6 Verification of Adenosine 1 (A_1) receptor antibody

A representative image of a western blot using LM/MP homogenates from a naïve guinea pig and brainstem homogenates from a placebo treated guinea pig using the antibody concentration displayed in Appendix E and following the protocol described in section 2.7. The A_1 receptor appears at 45 kDa in the 680 nM channel (red) and the housekeeper protein, GAPDH, is shown in the 800 nM channel (green) at 36 kDa.

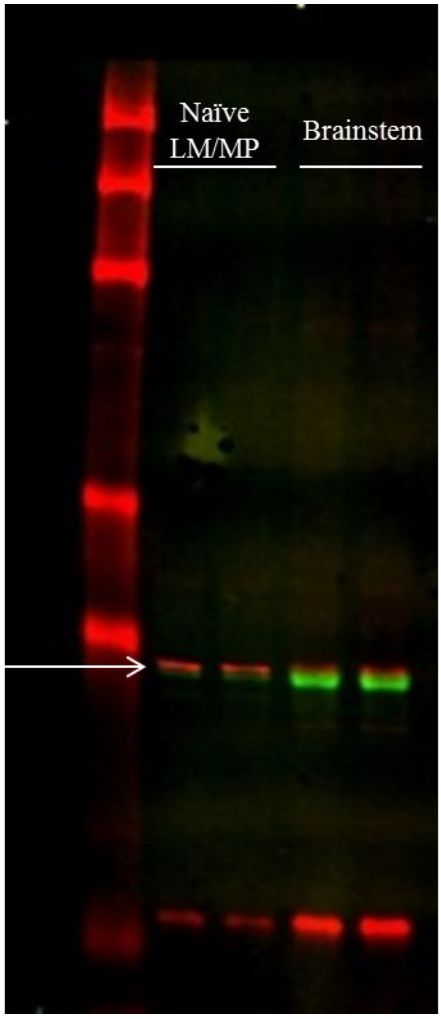
Naïve
LM/MP
Brainstem
A1 receptor
(680 channel)
GAPDH
(800 channel)

Figure 2.7 Verification of Adenosine 2a (A_{2a}) receptor antibody

A representative image of a western blot using LM/MP homogenates from a naïve guinea pig and brainstem homogenates from a placebo treated guinea pig using the antibody concentration displayed in Appendix E and following the protocol described in section 2.7. The A_{2a} receptor appears at 45 kDa in the 680 nM channel (red) and the housekeeper protein, GAPDH, is shown in the 800 nM channel (green) at 36 kDa.

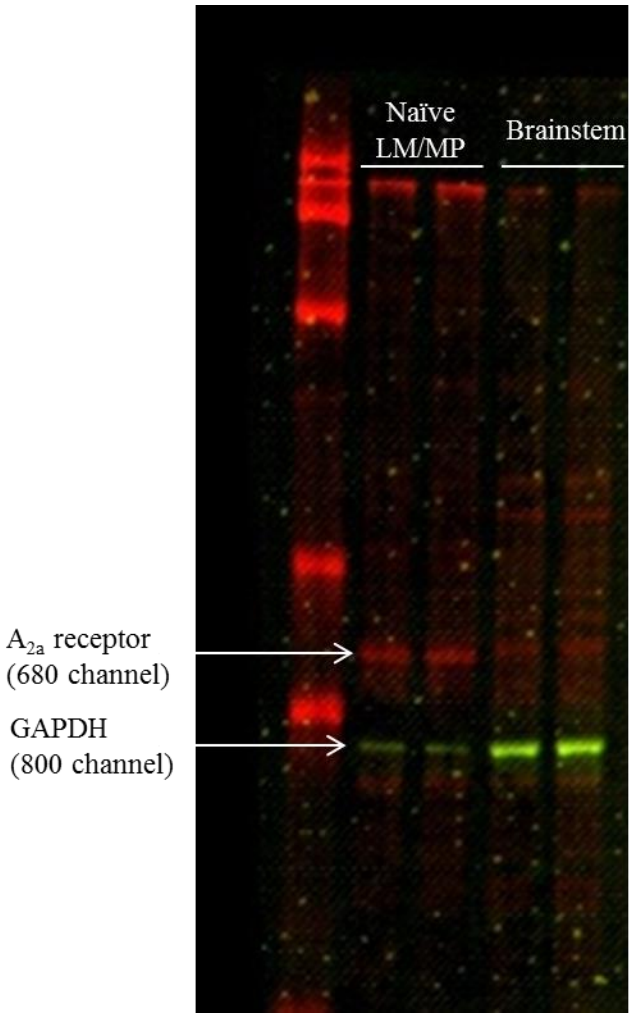
Naïve
LM/MP
Brainstem
A_{2a} receptor
(680 channel)
GAPDH
(800 channel)

Figure 2.8 Verification of Alpha 2b Adrenergic (α_{2b}) receptor antibody

A representative image of a western blot using LM/MP homogenates from a naïve guinea pig and brainstem homogenates from a placebo treated guinea pig using the antibody concentration displayed in Appendix E and following the protocol described in section 2.7. The α_{2b} receptor appears at 45 kDa in the 680 nM channel (red) and the housekeeper protein, GAPDH, is shown in the 800 nM channel (green) at 36 kDa.

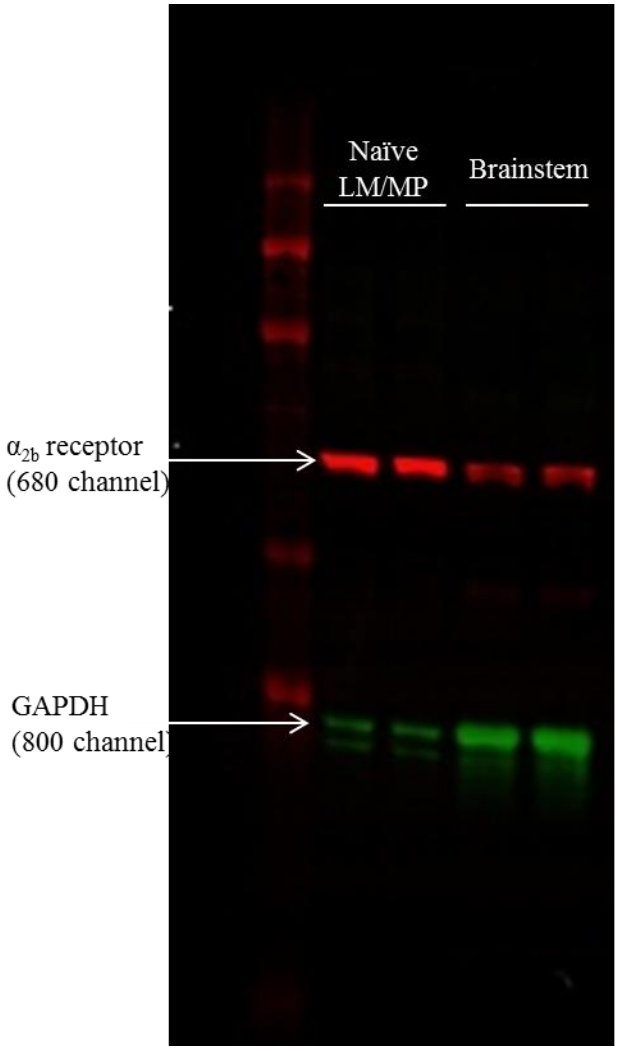
Naïve
LM/MP
Brainstem
α_{2b} receptor
(680 channel)
GAPDH
(800 channel)

Figure 2.9 Verification of PKC_{γ} antibody

A representative image of a western blot using LM/MP homogenates from a naïve guinea pig and brainstem homogenates from a placebo treated guinea pig using the antibody concentration displayed in Appendix E and following the protocol described in section 2.7. The PKC_{γ} appears at 45 kDa in the 680 nM channel (red) and the housekeeper protein, GAPDH, is shown in the 800 nM channel (green) at 36 kDa.

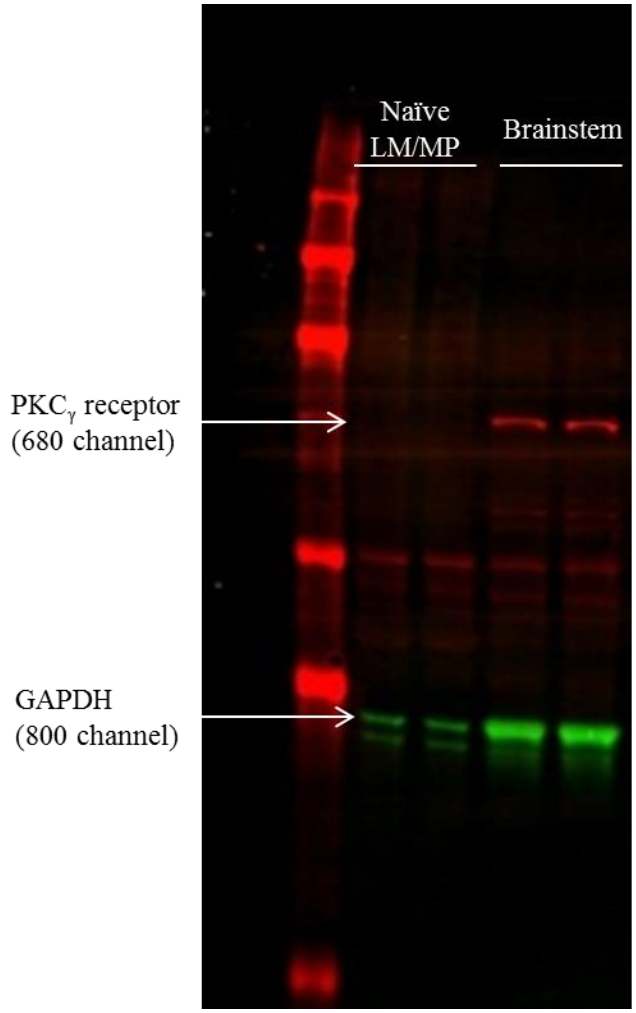
Naïve
LM/MP
Brainstem
PKCγ receptor
(680 channel)
GAPDH
(800 channel)

Figure 2.10 Verification of PKC_{ε} antibody

A representative image of a western blot using LM/MP homogenates from a naïve guinea pig and brainstem homogenates from a placebo treated guinea pig using the antibody concentration displayed in Appendix E and following the protocol described in section 2.7. The PKC_{ε} appears at 45 kDa in the 680 nM channel (red) and the housekeeper protein, GAPDH, is shown in the 800 nM channel (green) at 36 kDa.

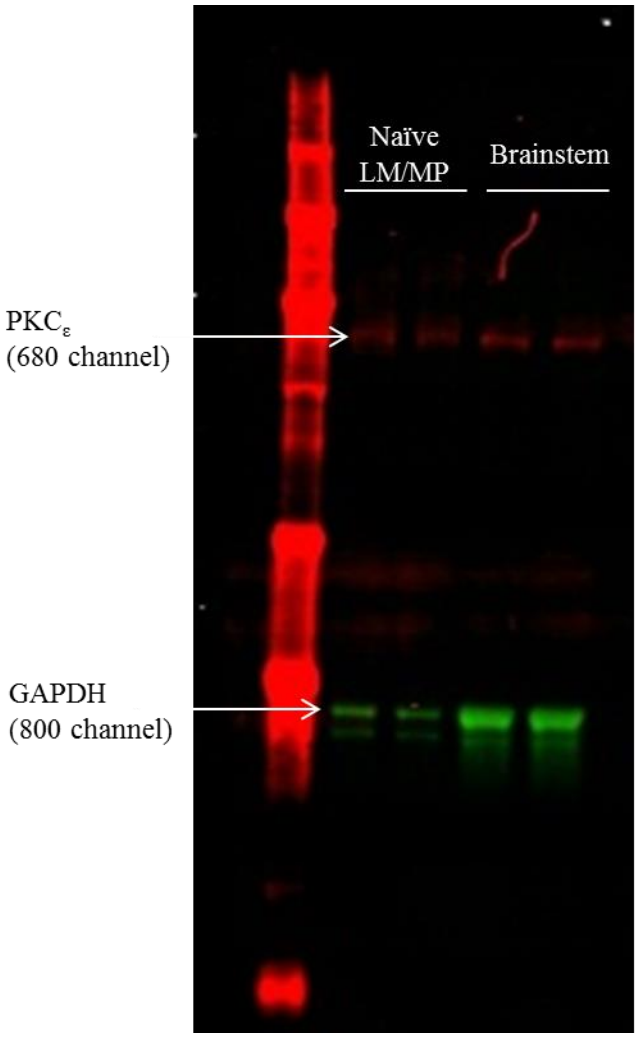
Naïve
LM/MP
Brainstem
PKCε
(680 channel)
GAPDH
(800 channel)

Figure 2.11 Verification of Na^+/K^+ ATPase α_1 antibody

A representative image of a western blot using LM/MP homogenates from a naïve guinea pig and brainstem homogenates from a placebo treated guinea pig using the antibody concentration displayed in Appendix E and following the protocol described in section 2.7. The α_1 subunit of the Na^+/K^+ ATPase appears at 45 kDa in the 680 nM channel (red) and the housekeeper protein, GAPDH, is shown in the 800 nM channel (green) at 36 kDa.

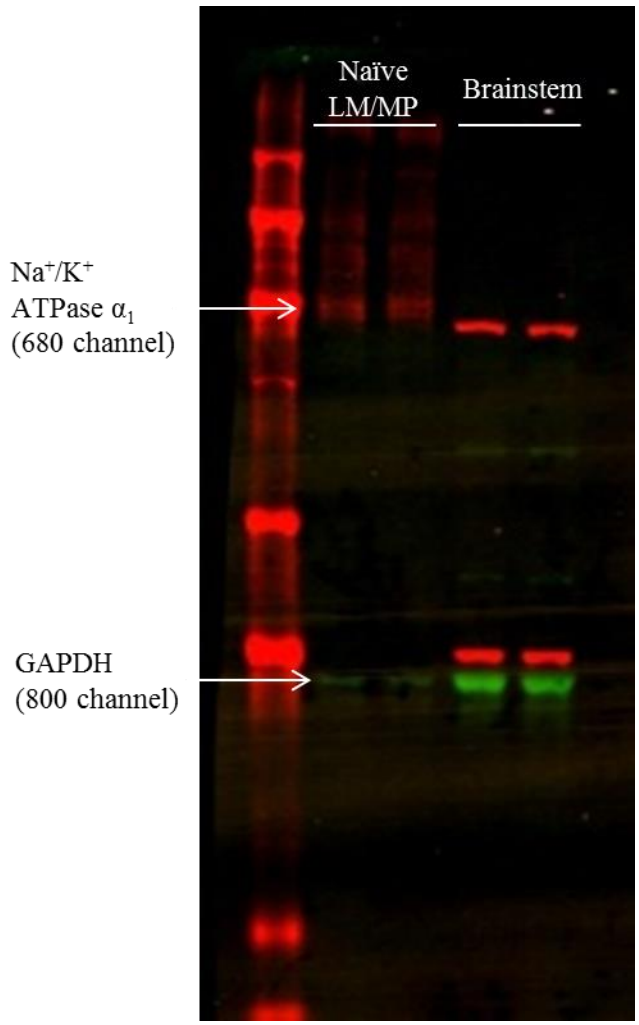
Naïve
LM/MP
Brainstem
Na+/K+
ATPase α1
(680 channel)
GAPDH
(800 channel)

Figure 2.12 Verification of Na^+/K^+ ATPase α_3 antibody

A representative image of a western blot using LM/MP homogenates from a naïve guinea pig and brainstem homogenates from a placebo treated guinea pig using the antibody concentration displayed in Appendix E and following the protocol described in section 2.7. The α_3 subunit of the Na^+/K^+ ATPase appears at 45 kDa in the 680 nM channel (red) and the housekeeper protein, GAPDH, is shown in the 800 nM channel (green) at 36 kDa.

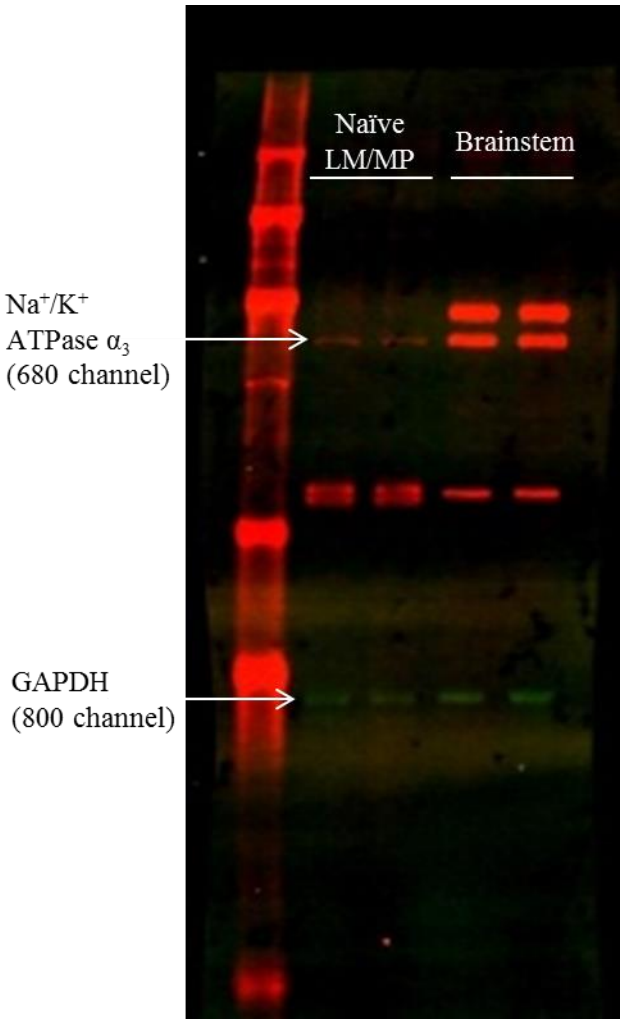
Naïve
LM/MP
Brainstem
Na+/K+
ATPase α3
(680 channel)
GAPDH
(800 channel)

Figure 2.13 Verification of Na^+/K^+ ATPase β_1 antibody

A representative image of a western blot using LM/MP homogenates from a naïve guinea pig and brainstem homogenates from a placebo treated guinea pig using the antibody concentration displayed in Appendix E and following the protocol described in section 2.7. The β_1 subunit of the Na^+/K^+ ATPase appears at 45 kDa in the 680 nM channel (red) and the housekeeper protein, GAPDH, is shown in the 800 nM channel (green) at 36 kDa.

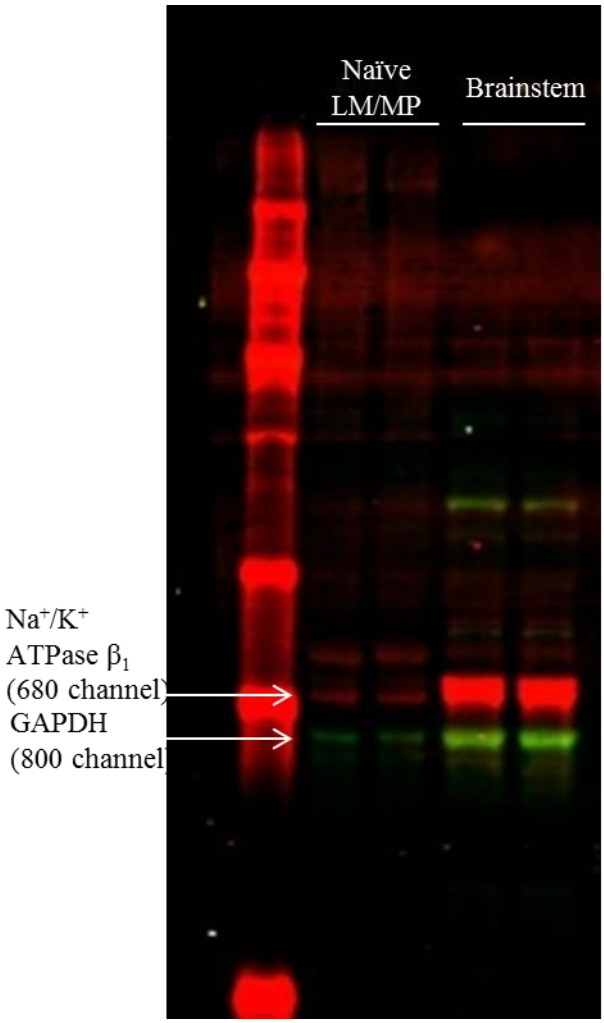
Naïve
LM/MP
Brainstem
Na+/K+
ATPase β1
(680 channel)
GAPDH
(800 channel)

CHAPTER THREE: TIME COURSE FOR THE ONSET AND DECAY OF HETEROLOGOUS TOLERANCE TO MORPHINE INTRAPERITONEALLY INJECTED INTO GUINEA PIGS

3.1 Abstract

It is believed that opioid tolerance results from adaptive changes in cellular signaling pathways associated with the μ opioid receptor. The adaptive changes develop in these signaling elements as the changes in function occur and should reverse as the function returns to normal. The extent of these changes should be proportional to the magnitude of tolerance that develops. More extensive adaptations resulting from a greater magnitude of tolerance require longer periods of time to reverse after dosing stops and function returns to normal. To test these hypotheses it is necessary to have a complete time course for the development and decay of tolerance to morphine. Previous work has established a time course for the onset of tolerance in guinea pigs implanted with morphine pellets. However, this method of administration is not adequate to examine the decay of tolerance because a time zero cannot be established due to the uncertainty surrounding the exact time when morphine has left the pellet. To establish a complete time course a parenteral injection administration protocol would be more appropriate because the time when dosing stops can be controlled and identified more accurately. Therefore, guinea pigs were treated with bi-daily intraperitoneal injections of escalating doses of morphine for 4, 7, or 10 days to induce tolerance. Tolerance was then assessed at 0, 1, 2, or 4 days after treatment cessation via paw pressure testing in the whole animal and by measuring the responsiveness of the LM/MP to nicotine, DAMGO, and 2-CADO ex-vivo. The results of these experiments were subject to higher variability than that reported for either subcutaneous or pellet implantation administrations which prevented the achievement of statistical significance. This

variability was attributed to variable absorption and/or metabolism of the drug due to the route of administration. Intraperitoneal injections allow the drug to be subjected to first pass hepatic metabolism. Paw pressure results indicated no changes between morphine and placebo animals regardless of treatment length. After further examination it was determined that the lack of responsiveness was due to using 10 mg/kg of morphine sulfate pentahydrate. Despite the lack of statistical significance in the whole animal studies, a trend for the IC_{50} of DAMGO and 2-CADO to be significantly greater in animals treated for 4, 7, or 10 days was observed in the LM/MP. For animals treated for 4 days, only 1 day was required to return the morphine to placebo ratio of the IC_{50}s of DAMGO and 2-CADO back to ~1 after treatment ceased. This took 2 days for the 7 and 10 day treated animals. No statistically significant results or trends were obtained with nicotine contractions in the LM/MP. These results suggest that intraperitoneal injection is not the optimal route of administration to study the onset and decay of tolerance to morphine.

3.2 Introduction

Despite many years of research, the mechanisms underlying the development of tolerance to morphine are still not fully understood. Tolerance is defined as the loss of responsiveness to a given agent that occurs as a result of repeated exposure to that agent. Multiple forms of tolerance are known to exist and can be expressed independently or simultaneously (Johnson & Fleming, 1989). The general consensus is that tolerance to morphine is an adaptive response that occurs due to chronic exposure to morphine. As discussed in section 1.6, there are many different hypotheses regarding the mechanism(s) by which opioids, morphine in particular, develop tolerance. In order for any of these proposed mechanisms to truly account for the observed changes in responsiveness, they must meet five criteria: "The proposed cellular change must: 1) be induced by experimental procedures identical to those that induce tolerance and/or

dependence; 2) follow a similar time course as the tolerance and/or dependence in that tissue; 3) quantitatively account for the tolerance and/or dependence; 4) account for the qualitative characteristics of the tolerance and/or dependence; and 5) occur in the very cells upon which the opioid is acting (Taylor & Fleming, 2001)". Of the model animals that are commonly used to study morphine tolerance guinea pigs were chosen. There are several reasons for this choice. Firstly, guinea pigs have a distribution of opioid receptors in the brain that is much more similar to that of humans than of the other commonly used animals (Mansour, Khachaturian, Lewis, Akil & Watson, 1988). In addition, guinea pigs display a pharmacological response to morphine that is more similar to humans than that observed in mice or rats. Furthermore, like humans, guinea pigs do not display a motor response to morphine (Bot, Chahl, Brent & Johnston, 1992). Guinea pigs also allow access to the LM/MP model system that has been used since the 1970s to evaluate the characteristics and mechanism of tolerance to morphine (Goldstein & Schulz, 1973).

Over the past several years this laboratory has focused on studying the second criteria. Since tolerance develops over time, any adaptive change that occurs as a result of chronic morphine exposure should occur along a similar time course as the observed changes in function. Conversely, when chronic morphine exposure ends, the adaptation(s) should spontaneously reverse over a similar time course as the changes in function. A time course for the onset of tolerance has been developed using pellet implanted guinea pigs (Barrett, Maguma & Taylor, 2011; Li, Maguma, Thayne, Davis & Taylor, 2010). While using pellet implanted animals does allow for adequate study of the development of tolerance, the decay of that tolerance cannot be accurately assessed because of the time at which the morphine has completely diffused out of the pellet cannot be ascertained; therefore a time zero for the initiation of the decay cannot be defined. To study the decay of tolerance, a parenteral method of administration would be more

adequate. It has already been shown that subcutaneous injection and pellet implantation administrations both develop a tolerance that is quantitatively and qualitatively similar (Li, Maguma, Thayne, Davis & Taylor, 2010). Intraperitoneal injections have not been used to chronically treat animals with morphine. The main goal of this work was to establish a time course for the onset and decay of tolerance to morphine in the guinea pig using intraperitoneal injections. One hypothesis for this work is that chronic morphine treatment via intraperitoneal injection would produce a tolerance that is quantitatively and qualitatively similar to subcutaneous injection and/or pellet implantation. A second hypothesis is that the decay of tolerance will be proportional to the magnitude of tolerance that develops. The basis for these hypotheses lies in the fact that it has already been established that morphine administration by various methods all produced a tolerance that is similar in magnitude (Li, Maguma, Thayne, Davis & Taylor, 2010). It is expected that a greater magnitude of tolerance is the result of more extensive adaptive changes and that it will take longer to reverse.

3.3 Experimental Protocol

All of the methods used here are detailed in chapter 2. Dunkin-Hartley guinea pigs were treated via intraperitoneal (IP) injection for either 4, 7, or 10 days with either morphine sulfate pentahydrate or saline. The dosing schedule employed (see table 3.1) was adapted from previous work in this laboratory (Li, Maguma, Thayne, Davis & Taylor, 2010). Some of the animals for each of the treatment lengths were allowed to remain in the animal facility for specified lengths of time after the last dose of morphine in order to assess the decay of the developed tolerance. Animals treated for 4 days were assessed at 0, 1, or 2 days after the last treatment day. Because it was expected that a greater degree of tolerance would take longer to fade, the animals treated for 7 or 10 days were assessed at 0, 2, or 4 days after the last treatment day. To help control for

daily variations animals were dosed in pairs, a treated and a control, and a daily morphine to placebo ratio was calculated. All statistics were done on these ratios. For the sake of simplicity animals treated for 4 days and assessed 0 days after the last treatment day will be referred to as 4 day – 0 day animals while animals treated for 4 days and assessed 1 day after the last treatment day will be referred to as 4 day – 1 day animals and so forth.

Tolerance assessment consisted of paw pressure testing followed by euthanasia after isoflurane anesthesia. At this point tissues were collected and segments of the LM/MP were prepared for the organ bath apparatus (see figure 2.3). Because the nicotine concentration response curves needed to be done in the absence of electrical stimulation, non-cumulative nicotine concentration response curves were performed first. After a washing period, electrical stimulation was applied and the tissue was allowed to reacclimate. Cumulative concentration response curves for either DAMGO or 2-CADO (the order was randomized) were performed next, followed by a washing period and the concentration response curve for the other drug.

All statistics were performed using Graph Pad Prism 5. Two tailed T-tests were run to test whether or not the average morphine to placebo ratio was significantly different from unity. One-way ANOVAs were run to test for the differences in the average ratios between time points. Results were considered significant at a p value of less than 0.05.

3.4 Experimental Results

The paw pressure test was intended to be a measure of tolerance in the whole animal. However, we were able to detect no difference between placebo and morphine animals at any time point measured (see figures 3.1-3.3). In the LM/MP, nicotine concentration response curves were generated and the EC_{50} and maximum contraction were calculated (see figures 3.4-3.7). No significant differences were detected at any time point for the EC_{50}. There was a

significant increase in the morphine to placebo ratio of the maximum response for 10 day – 2 day animals. DAMGO and 2-CADO concentration response curves were also generated in the LM/MP for each sample (see figures 3.8-3.10). There was a significant increase in the morphine to placebo ratio of the IC_{50}s for both drugs at the 4 day – 0 day time points and the 10 day – 0 day time points, indicating that the LM/MP was sub-sensitive to the inhibitory effects of both drugs at these time points. Although it was not significant, there was a similar trend present for the 7 day – 0 day animals. There was no significant difference in the morphine to placebo ratios of the IC_{50}s of DAMGO or 2-CADO between the 4 day – 0 day, 7 day – 0 day, or 10 day – 0 day time points.

3.5 Discussion

The paw pressure analgesic test was intended to be a measure of tolerance in the whole animal and has been used in this lab previously with reasonable success (Barrett, Maguma & Taylor, 2011; Maguma & Taylor, 2011). It was troubling that we obtained such poor results with the test. Upon examination of the data, it was discovered that the problem was not that the morphine treated animals were not becoming tolerant to the drug, but rather it was that the placebo animals were not responding as robustly as that observed previously to the test dose of morphine used. The dose used was 10 mg/kg; a standard dose that should have produced a measureable analgesic effect. However, it was discovered that the dose employed was actually a 10 mg/kg dose of morphine sulfate pentahydrate as opposed to a 10 mg/kg dose of morphine. Dosing of the animals was subject to the same error. The result was that the animals were receiving a dose of morphine ~ 25% lower than what was planned. This clearly had an impact on the paw pressure results. However, even with a reduced dose, the animals were still receiving enough morphine to become tolerant to the effects of DAMGO and 2-CADO as early as 4 days

of treatment. Although there was too much variability in the 7 day – 0 day LM/MP data to achieve statistical significance, there was no difference between the 4 day – 0day, 7 day – 0 day, and 10 day – 0 day morphine to placebo ratios of the IC_{50}s of DAMGO and 2-CADO which implies that the same magnitude of tolerance had developed independent of treatment length. There was not a statistically significant difference at either the 4 day – 1 day or the 7 day – 2 day and the 10 day – 2 day time points, but it does appear that the concentration response curves for DAMGO and 2-CADO appeared similar. Similarity also exists for the 4 day – 2 day, 7 day – 4 day, and 10 day – 4 day curves. These data may imply that despite a similar magnitude of tolerance, more extensive adaptations occurred in the 7 and 10 day treated animals that took longer to reverse.

Nicotine was examined because previous work has suggested that neurons adapt to chronic morphine by becoming partially depolarized to compensate for the hyperpolarizing effect of morphine (Fleming, 1999; Taylor & Fleming, 2001). In a partially depolarized state the neurons would be expected to be subsensitive to inhibitory agonists such as DAMGO and 2-CADO as well as supersensitive to excitatory agonists such as nicotine. Indeed, it has been shown previously in the guinea pig LM/MP that chronic morphine treatment does induce supersensitivity to nicotine as well as other excitatory agonists (Barrett, Maguma & Taylor, 2011; Johnson, Westfall, Howard & Fleming, 1978). That finding could not be replicated in this study. It may be worth pointing out that the method of administration in those studies in which supersensitivity to nicotine was observed was pellet implantation. The difference in the method of administration may be important because it has been shown that pellet implantation does not cause as much stress on the animals as injections. Both pellet implantation and subcutaneous injection of morphine acutely activate the hypothalamic-pituitary-adrenal (HPA) axis and

chronic exposure by either method results in tolerance to HPA axis effects (Sarnyai, Shaham & Heinrichs, 2001). However, the difference between the two is that pellet implantation is considered to be a continuous exposure whereas injections are not. It has been shown in rats that during the time between injections the animals undergo a partial withdrawal from the drug which, over the period of treatment, causes a state of constant stress (Houshyar, Gomez, Manalo, Bhargava & Dallman, 2003). There is a connection between chronic activation of the HPA axis and the function of nicotine receptors (Lutfy et al., 2006) and it may be that the chronic stress state caused by the injection method of administration suppresses the supersensitivity of nicotine that was observed in the pellet implanted animals. The lack of supersensitivity to nicotine does not necessarily imply that there is no generalized supersensitivity to excitatory stimuli in the LM/MP. Although nicotine was the only agonist tested here, chronic morphine treatment also leads to supersensitivity of the LM/MP to 5-HT and K^+ (Johnson, Westfall, Howard & Fleming, 1978).

This work was intended to elucidate the time course for the onset and decay of tolerance when using an IP injection administration protocol. We were able to show that after 4 days of treatment a significant level of heterologous tolerance develops as evidenced by the increase in the IC_{50}s values for DAMGO and 2-CADO in the LM/MP and that there is no difference between the magnitude of tolerance that develops between 4, 7, and 10 days of treatment. Despite there being no difference between the level of tolerance in these groups, the 7 and 10 day groups appear to take longer to return to baseline than the 4 day groups which implies that more extensive adaptations occurred in those groups. We were unable to demonstrate supersensitivity to nicotine in the LM/MP, but this may be due to the manner in which morphine was administered. Unfortunately due to the dosing error, the paw pressure testing revealed nothing in

the whole animal. Also, there appears to be greater variability in the data generated here than in the data obtained following either pellet implantation or sc injection which prevented statistical significance in some of the groups in which trends were observed. We believe the source of this variability to be the differential absorption of the drug from the mesenterium around the gut and hepatic metabolism. For this reason, these data suggest that IP injection may not be the best method of administration for a time course study.

Table 3.1 Injection Schedule

This injection schedule was adapted from previous work in this lab (Li, Maguma, Thayne, Davis & Taylor, 2010). Animals were treated with the doses of morphine sulfate pentahydrate or an equivalent volume of saline. Some animals followed this schedule for only 4 days, some for only 7, and some for all 10 days.

Injection Schedule	
Day	**Dose of Morphine Sulfate Pentahydrate**
1	**10 mg/kg**
2 and 3	**20 mg/kg**
4, 5, 6, and 7	**40 mg/kg**
8, 9, and 10	**80 mg/kg**

Figure 3.1 Paw Pressure Data for Animals Treated for 4 days

A) Average paw pressure data for 4 day – 0 day animals (n = 4). The placebo to morphine ratio of the area under the curve (AUC) = 1.308 and was not significantly different from 1 (p value = 0.0616).

B) Average paw pressure data for 4 day – 1 day animals (n = 4). The placebo to morphine ratio of the AUC = 1.160 and was not significantly different from 1 (p value = 0.1472).

C) Average paw pressure data for 4 day – 2 day animals (n = 4). The placebo to morphine ratio of the AUC = 1.181 and was not significantly different from 1 (p value = 0.3345).

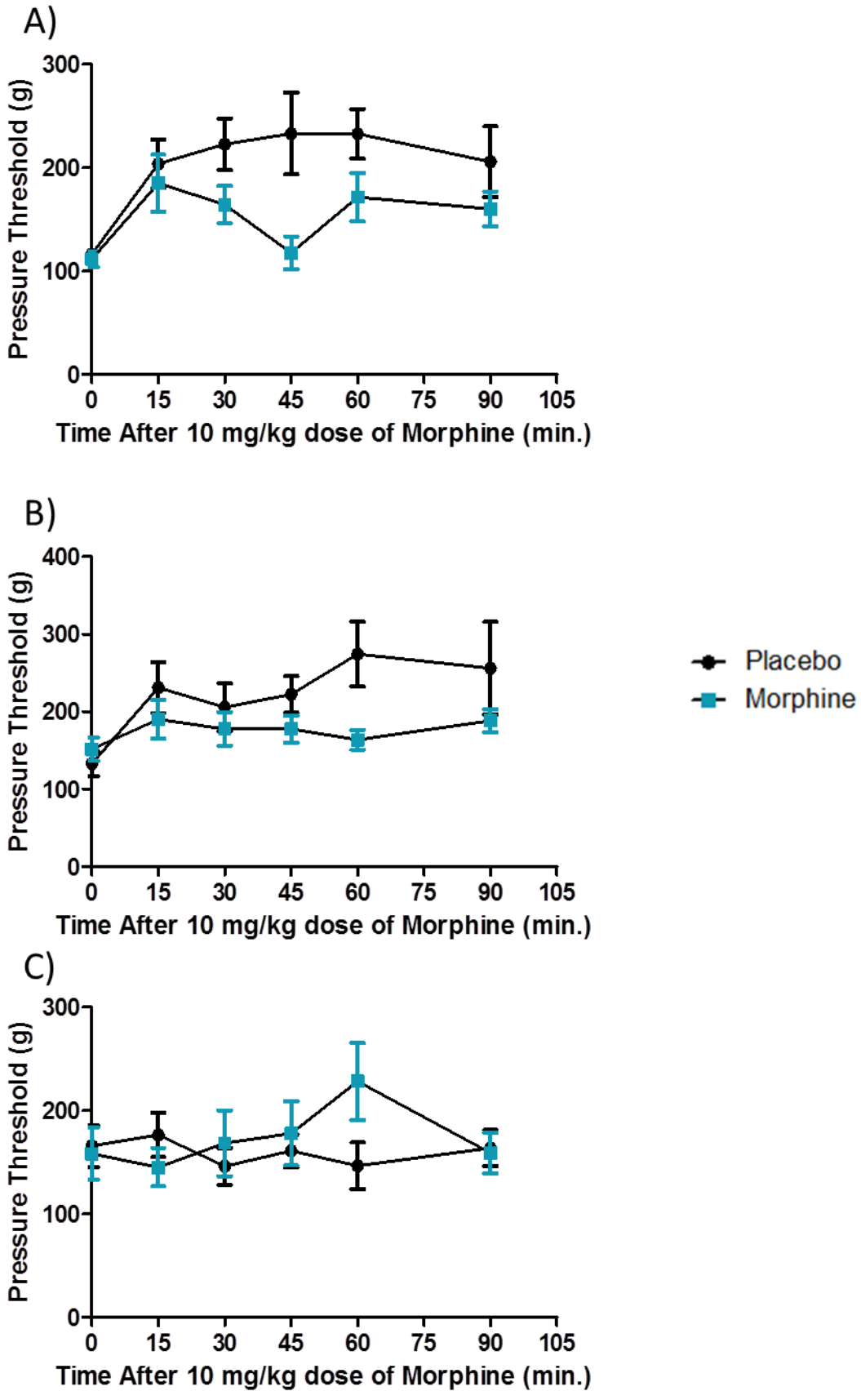
A)
Pressure Threshold (g)
300
200
100
0
0
15
30
45
60
75
90
105
Time After 10 mg/kg dose of Morphine (min.)
B)
Pressure Threshold (g)
400
300
200
100
0
0
15
30
45
60
75
90
105
Time After 10 mg/kg dose of Morphine (min.)
Placebo
Morphine
C)
Pressure Threshold (g)
300
200
100
0
0
15
30
45
60
75
90
105
Time After 10 mg/kg dose of Morphine (min.)

Figure 3.2 Paw Pressure Data for Animals Treated for 7 days

A) Average paw pressure data for 7 day – 0 day animals (n = 4). The placebo to morphine ratio of the area under the curve (AUC) = 1.145 and was not significantly different from 1 (p value = 0.2043).

B) Average paw pressure data for 7 day – 2 day animals (n = 4). The placebo to morphine ratio of the AUC = 0.994 and was not significantly different from 1 (p value = 0.9662).

C) Average paw pressure data for 7 day – 4 day animals (n = 4). The placebo to morphine ratio of the AUC = 0.990 and was not significantly different from 1 (p value = 0.9333).

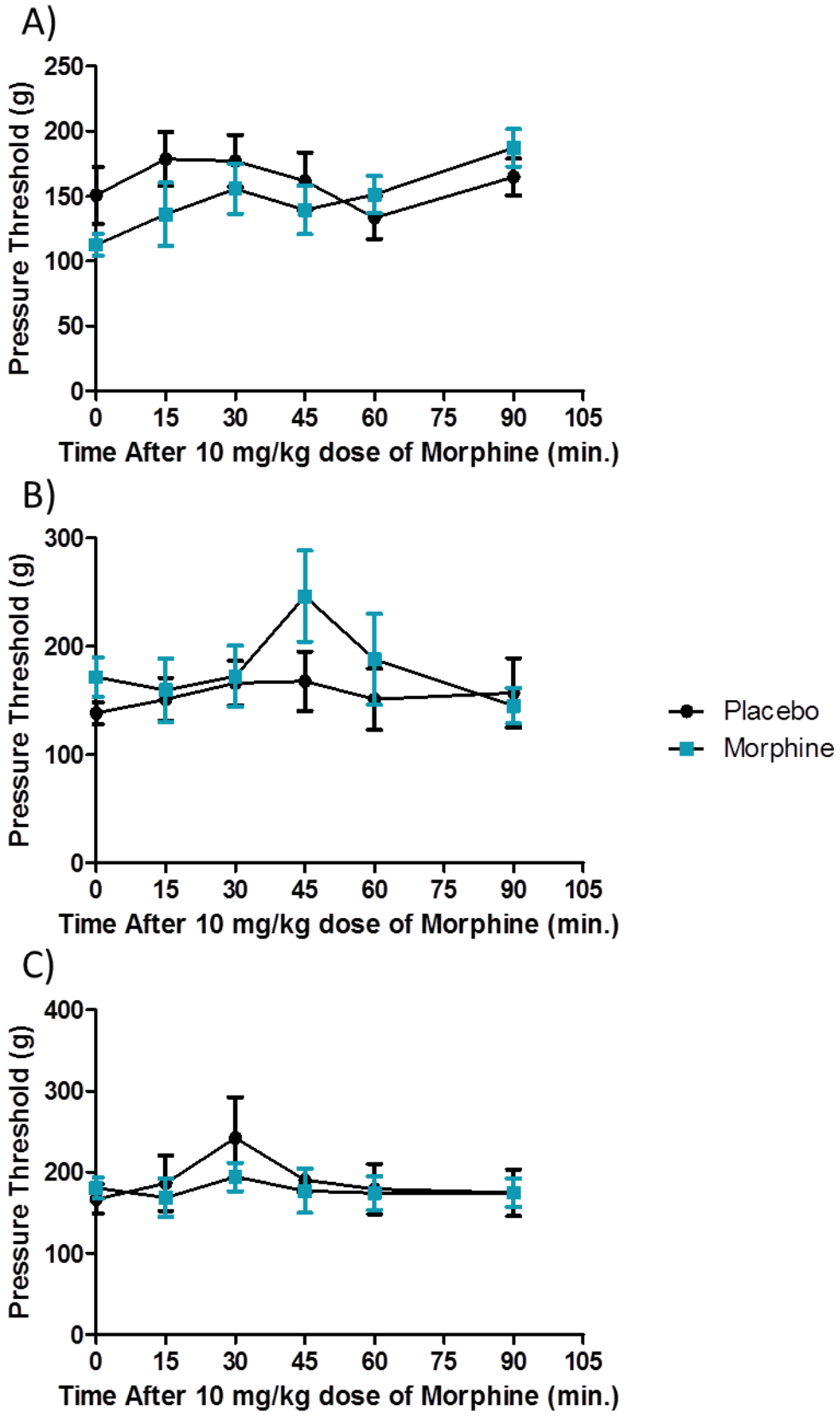
A)
Pressure Threshold (g)
250
200
150
100
50
0
0
15
30
45
60
75
90
105
Time After 10 mg/kg dose of Morphine (min.)
B)
Pressure Threshold (g)
300
200
100
0
0
15
30
45
60
75
90
105
Time After 10 mg/kg dose of Morphine (min.)
Placebo
Morphine
C)
Pressure Threshold (g)
400
300
200
100
0
0
15
30
45
60
75
90
105
Time After 10 mg/kg dose of Morphine (min.)

Figure 3.3 Paw Pressure Data for Animals Treated for 10 days

A) Average paw pressure data for 10 day – 0 day animals (n = 4). The placebo to morphine ratio of the area under the curve (AUC) = 1.228 and was not significantly different from 1 (p value = 0.1560).

B) Average paw pressure data for 10 day – 2 day animals (n = 3). The placebo to morphine ratio of the AUC = 1.291 and was not significantly different from 1 (p value = 0.1857).

C) Average paw pressure data for 10 day – 4 day animals (n = 4). The placebo to morphine ratio of the AUC = 0.931 and was not significantly different from 1 (p value = 0.1998).

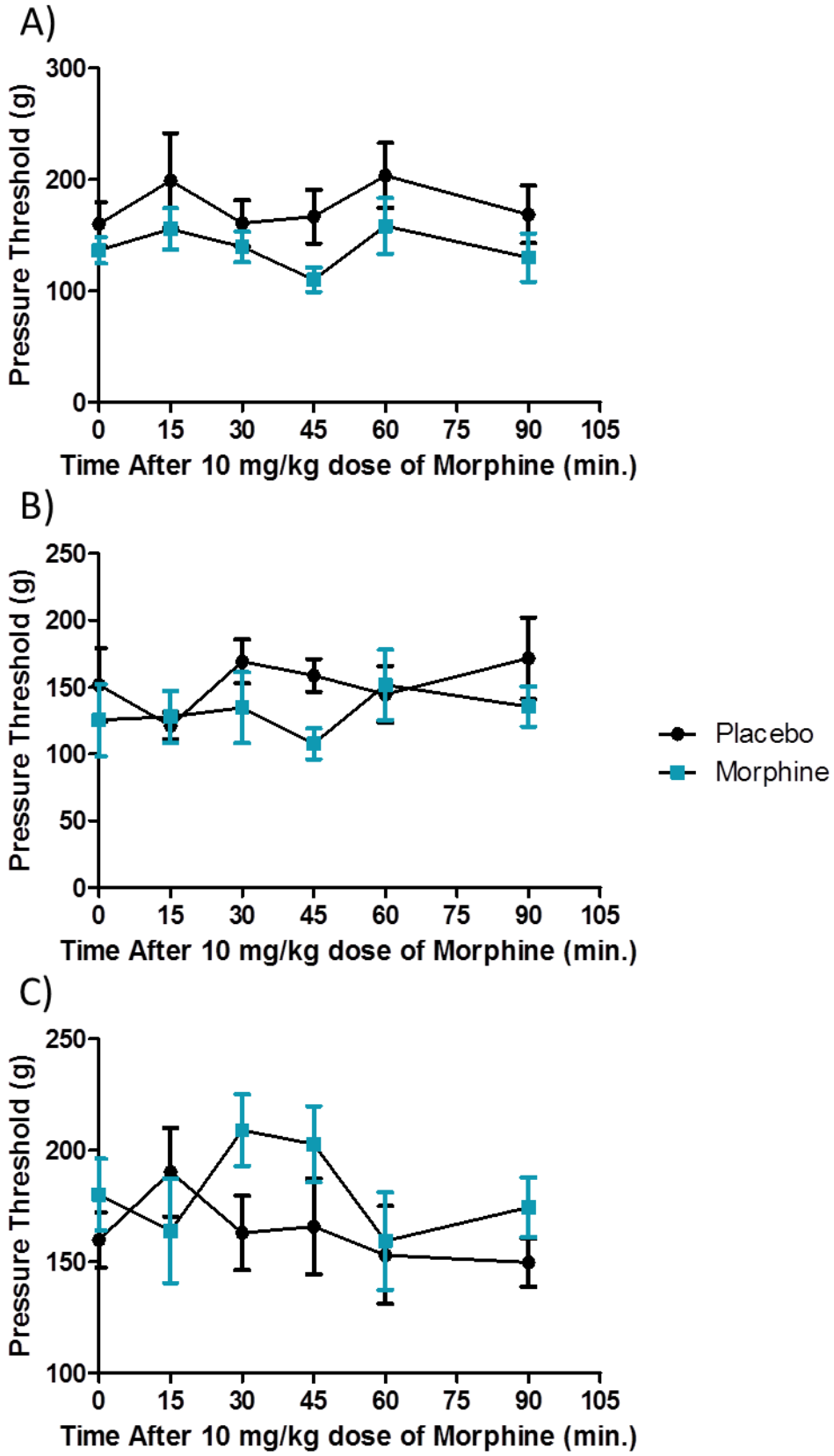
A)
Pressure Threshold (g)
300
200
100
0
0 15 30 45 60 75 90 105
Time After 10 mg/kg dose of Morphine (min.)
B)
Pressure Threshold (g)
250
200
150
100
50
0
0 15 30 45 60 75 90 105
Time After 10 mg/kg dose of Morphine (min.)
Placebo
Morphine
C)
Pressure Threshold (g)
250
200
150
100
0 15 30 45 60 75 90 105
Time After 10 mg/kg dose of Morphine (min.)

Figure 3.4 Nicotine Concentration Response Curves for Animals Treated for 4 days

A) Average nicotine concentration response curve for 4 days – 0 day animals (n = 4). The morphine to placebo ratio of the EC_{50} = 2.070 and was not significantly different from 1 (p value = 0.2459).

B) Average nicotine concentration response curve for 4 days – 1 day animals (n = 4). The morphine to placebo ratio of the EC_{50} = 1.175 and was not significantly different from 1 (p value = 0.2296).

C) Average nicotine concentration response curve for 4 days – 2 day animals (n = 4). The morphine to placebo ratio of the EC_{50} =1.888 and was not significantly different from 1 (p value = 0.3038).

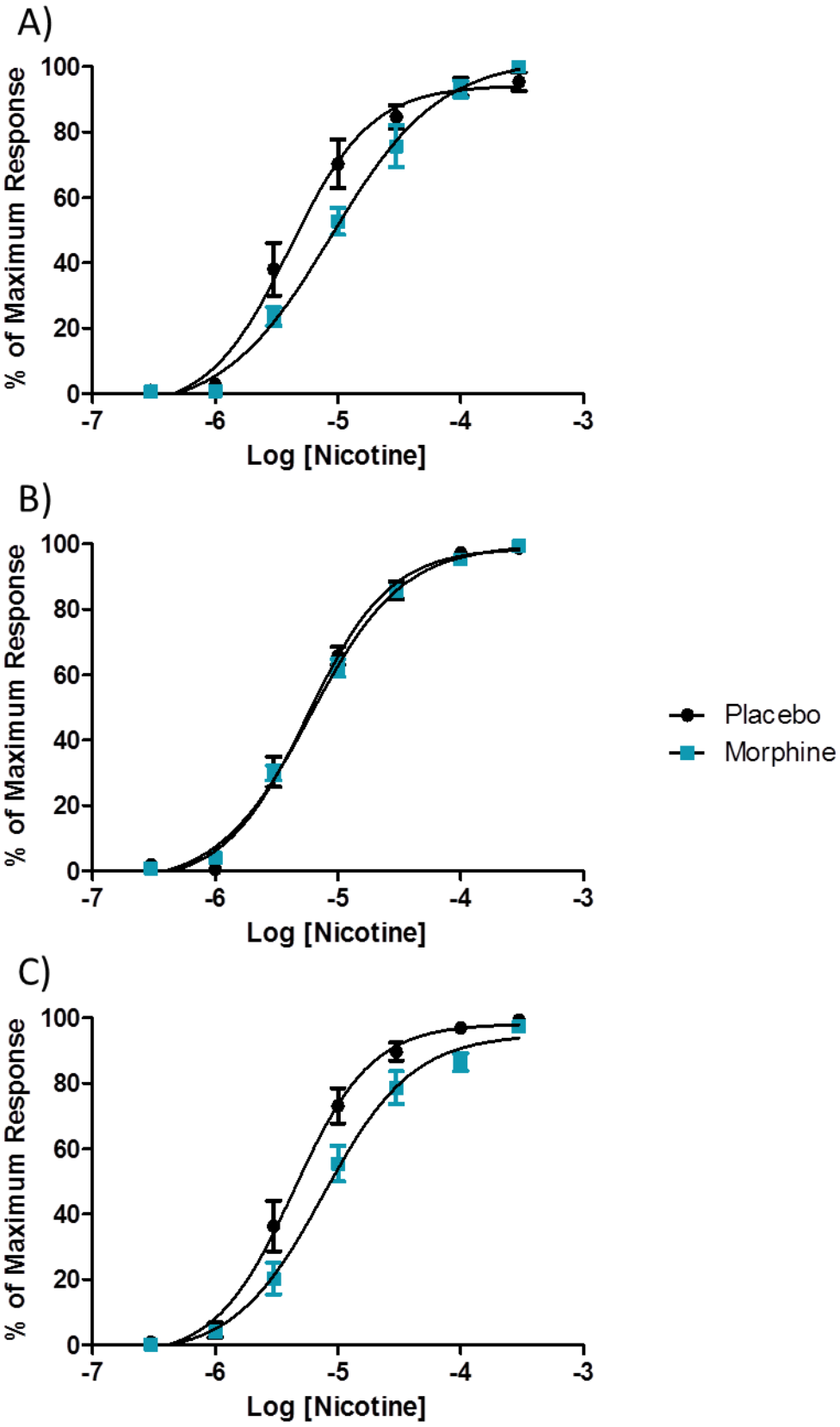
A)
% of Maximum Response
100
80
60
40
20
0
-7
-6
-5
-4
-3
Log [Nicotine]
B)
% of Maximum Response
100
80
60
40
20
0
-7
-6
-5
-4
-3
Log [Nicotine]
C)
% of Maximum Response
100
80
60
40
20
0
-7
-6
-5
-4
-3
Log [Nicotine]
Placebo
Morphine

Figure 3.5 Nicotine Concentration Response Curves for Animals Treated for 7 days

A) Average nicotine concentration response curve for 7 days – 0 day animals (n = 4). The morphine to placebo ratio of the EC_{50} = 1.279 and was not significantly different from 1 (p value = 0.4553).

B) Average nicotine concentration response curve for 7 days – 2 day animals (n = 4). The morphine to placebo ratio of the EC_{50} = 1.222 and was not significantly different from 1 (p value = 0.2895).

C) Average nicotine concentration response curve for 7 days – 4 day animals (n = 4). The morphine to placebo ratio of the EC_{50} = 1.327 and was not significantly different from 1 (p value = 0.1454).

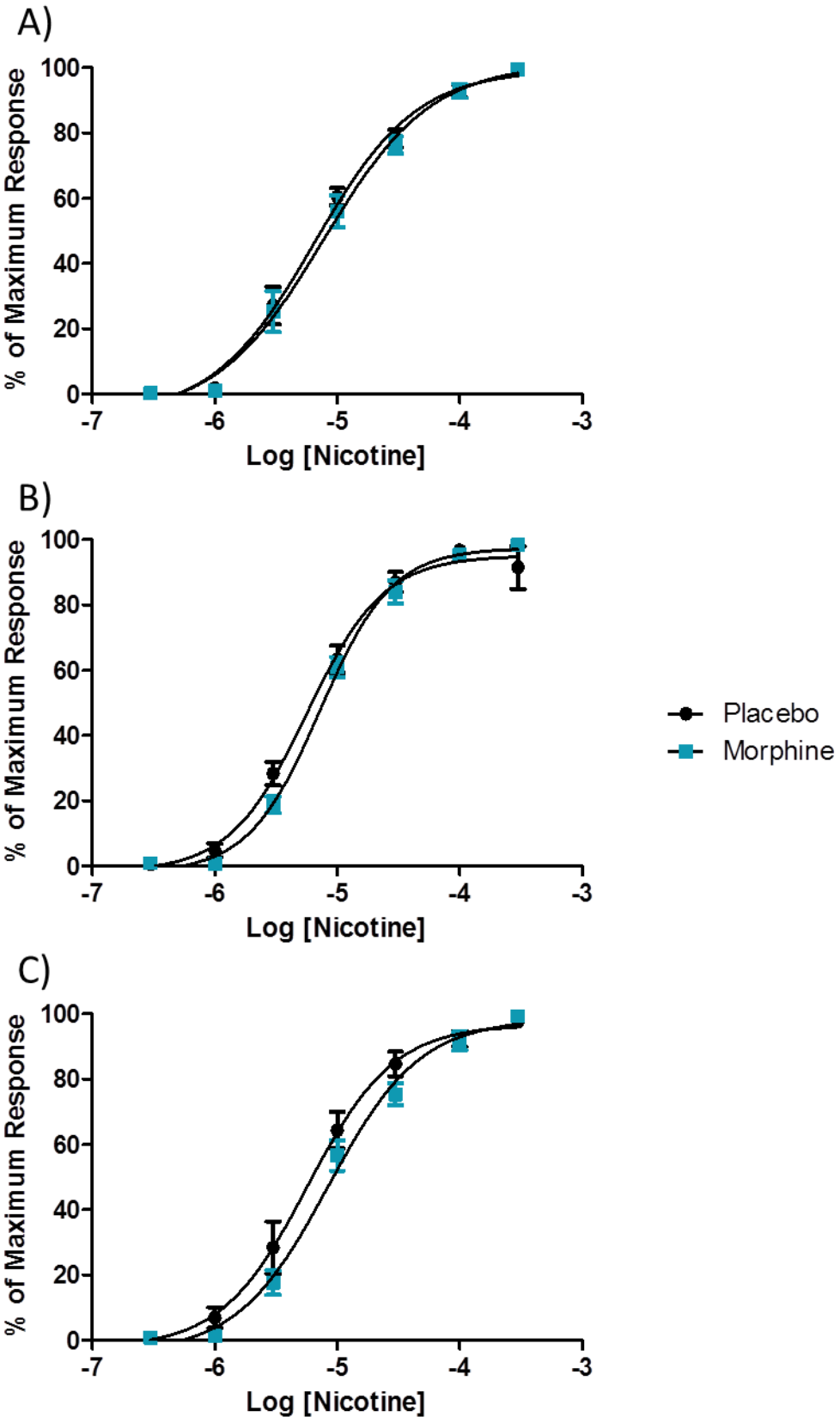
A)
% of Maximum Response
100
80
60
40
20
0
-7
-6
-5
-4
-3
Log [Nicotine]
B)
% of Maximum Response
100
80
60
40
20
0
-7
-6
-5
-4
-3
Log [Nicotine]
C)
% of Maximum Response
100
80
60
40
20
0
-7
-6
-5
-4
-3
Log [Nicotine]
Placebo
Morphine

Figure 3.6 Nicotine Concentration Response Curves for Animals Treated for 10 days

A) Average nicotine concentration response curve for 10 days – 0 day animals (n = 4). The morphine to placebo ratio of the EC_{50} = 1.155 and was not significantly different from 1 (p value = 0.3994).

B) Average nicotine concentration response curve for 10 days – 2 day animals (n = 3). The morphine to placebo ratio of the EC_{50} = 1.456 and was not significantly different from 1 (p value = 0.4275).

C) Average nicotine concentration response curve for 10 days – 4 day animals (n = 4). The morphine to placebo ratio of the EC_{50} = 1.233 and was not significantly different from 1 (p value = 0.4859).

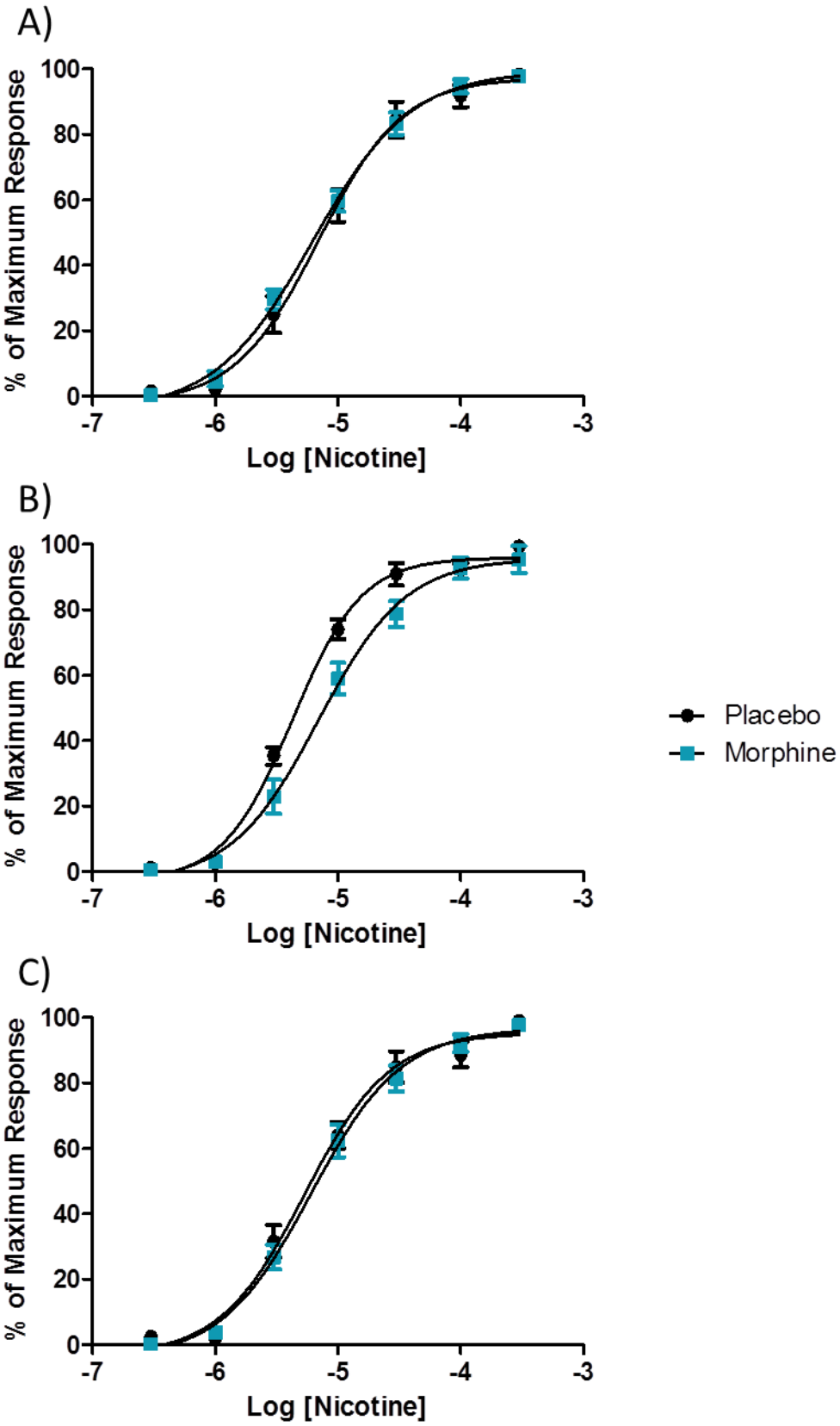
A)
% of Maximum Response
100
80
60
40
20
0
-7
-6
-5
-4
-3
Log [Nicotine]
B)
% of Maximum Response
100
80
60
40
20
0
-7
-6
-5
-4
-3
Log [Nicotine]
C)
% of Maximum Response
100
80
60
40
20
0
-7
-6
-5
-4
-3
Log [Nicotine]
Placebo
Morphine

Figure 3.7 Nicotine Maximum Response

A) Average morphine to placebo ratios of the nicotine maximum response in the LM/MP for animals treated for 4 days and assessed 0, 1, or 2 days after the last treatment day (n = 4 for each). The morphine to placebo ratios of the maximum response were 1.245, 1.584, and 0.886 for the 4 day – 0 day, 4 day – 1 day, and 4 day – 2 day groups respectively. None of these ratios were significantly different from 1 (p values = 0.1041, 0.6355, and 0.3902 respectively).

B) Average morphine to placebo ratios of the nicotine maximum response in the LM/MP for animals treated for 7 days and assessed 0, 2, or 4 days after the last treatment day (n = 4 for each). The morphine to placebo ratios of the maximum response were 0.772, 0.869, and 0.763 for the 7 day – 0 day, 7 day – 2 day, and 7 day – 4 day groups respectively. None of these ratios were significantly different from 1 (p values = 0.2762, 0.5668, 0.1518 respectively).

C) Average morphine to placebo ratios of the nicotine maximum response in the LM/MP for animals treated for 10 days and assessed 0, 2, or 4 days after the last treatment day (n = 4 for each except the 10 day – 2 day group for which n = 3). The morphine to placebo ratios of the maximum response were 0.872, 1.214, and 0.906 for the 10 day – 0 day, 10 day – 2 day, and 10 day – 4 day groups respectively. Only the 10 day – 2 day morphine to placebo ratio was significantly different from 1 (p value = 0.0473). The p values for the 10 day – 0 day and 10 day – 4 day groups were 0.3666 and 0.2091 respectively.

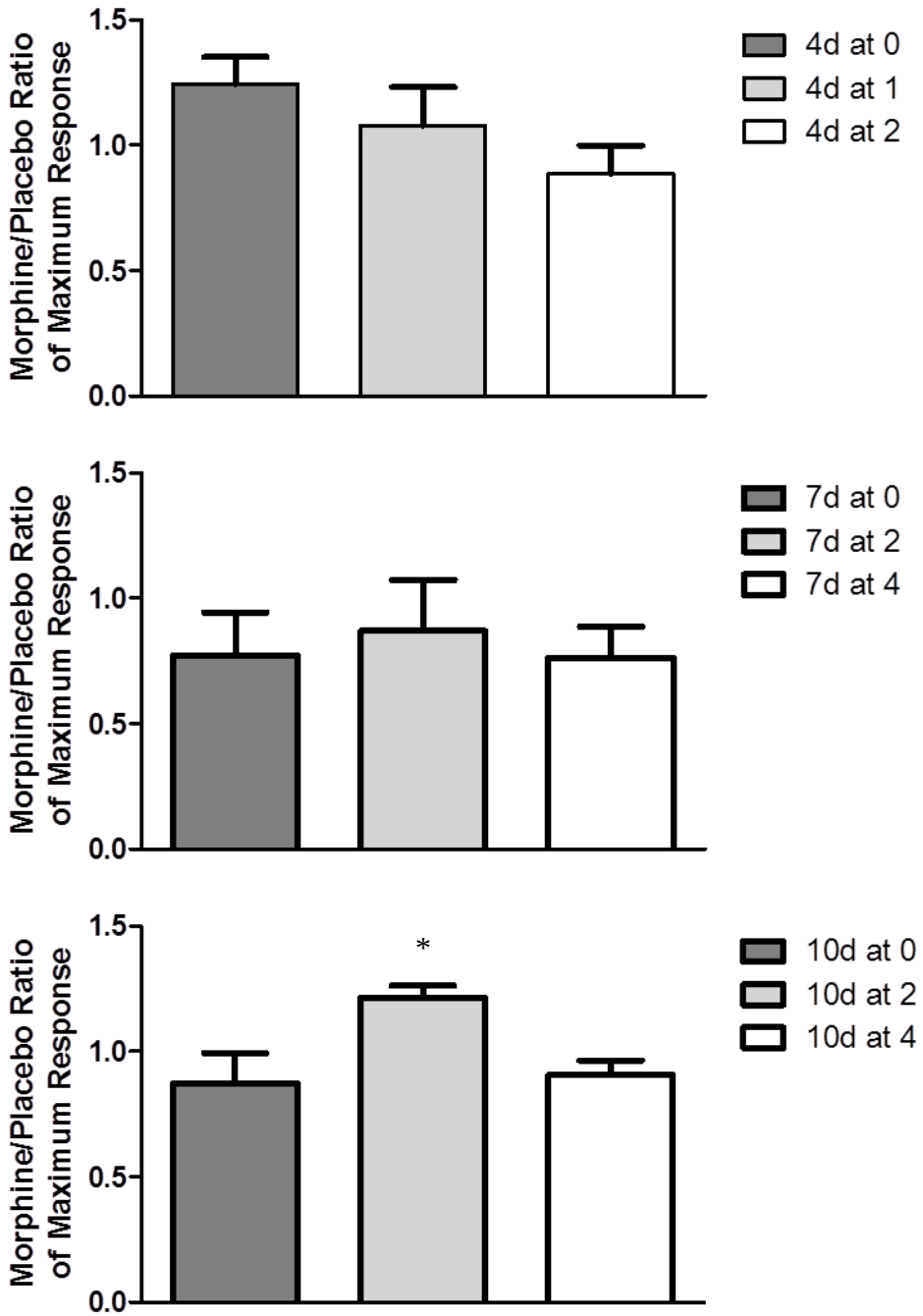
Morphine/Placebo Ratio of Maximum Response
1.5
1.0
0.5
0.0
4d at 0
4d at 1
4d at 2
Morphine/Placebo Ratio of Maximum Response
1.5
1.0
0.5
0.0
7d at 0
7d at 2
7d at 4
Morphine/Placebo Ratio of Maximum Response
1.5
1.0
0.5
0.0
*
10d at 0
10d at 2
10d at 4

Figure 3.8 DAMGO and 2-CADO Concentration Response Curves for Animals Treated for 4 days

A) Average DAMGO concentration response curve for 4 day – 0 day animals (n = 4). The morphine to placebo ratio of the IC_{50} = 4.578 and was significantly different from 1 (p value = 0.0199).

B) Average DAMGO concentration response curve for 4 day – 1 day animals (n = 4). The morphine to placebo ratio of the IC_{50} = 1.222 and was not significantly different from 1 (p value = 0.3378).

C) Average DAMGO concentration response curve for 4 day – 2 day animals (n = 4). The morphine to placebo ratio of the IC_{50} = 1.359 and was not significantly different from 1 (p value = 0.4520).

D) Average 2-CADO concentration response curve for 4 day – 0 day animals (n = 4). The morphine to placebo ratio of the IC_{50} = 4.186 and was significantly different from 1 (p value = <0.0001).

E) Average 2-CADO concentration response curve for 4 day – 1 day animals (n = 4). The morphine to placebo ratio of the IC_{50} = 1.080 and was not significantly different from 1 (p value = 0.7497).

F) Average 2-CADO concentration response curve for 4 day – 2 day animals (n = 4). The morphine to placebo ratio of the IC_{50} = 1.278 and was not significantly different from 1 (p value = 0.4322).

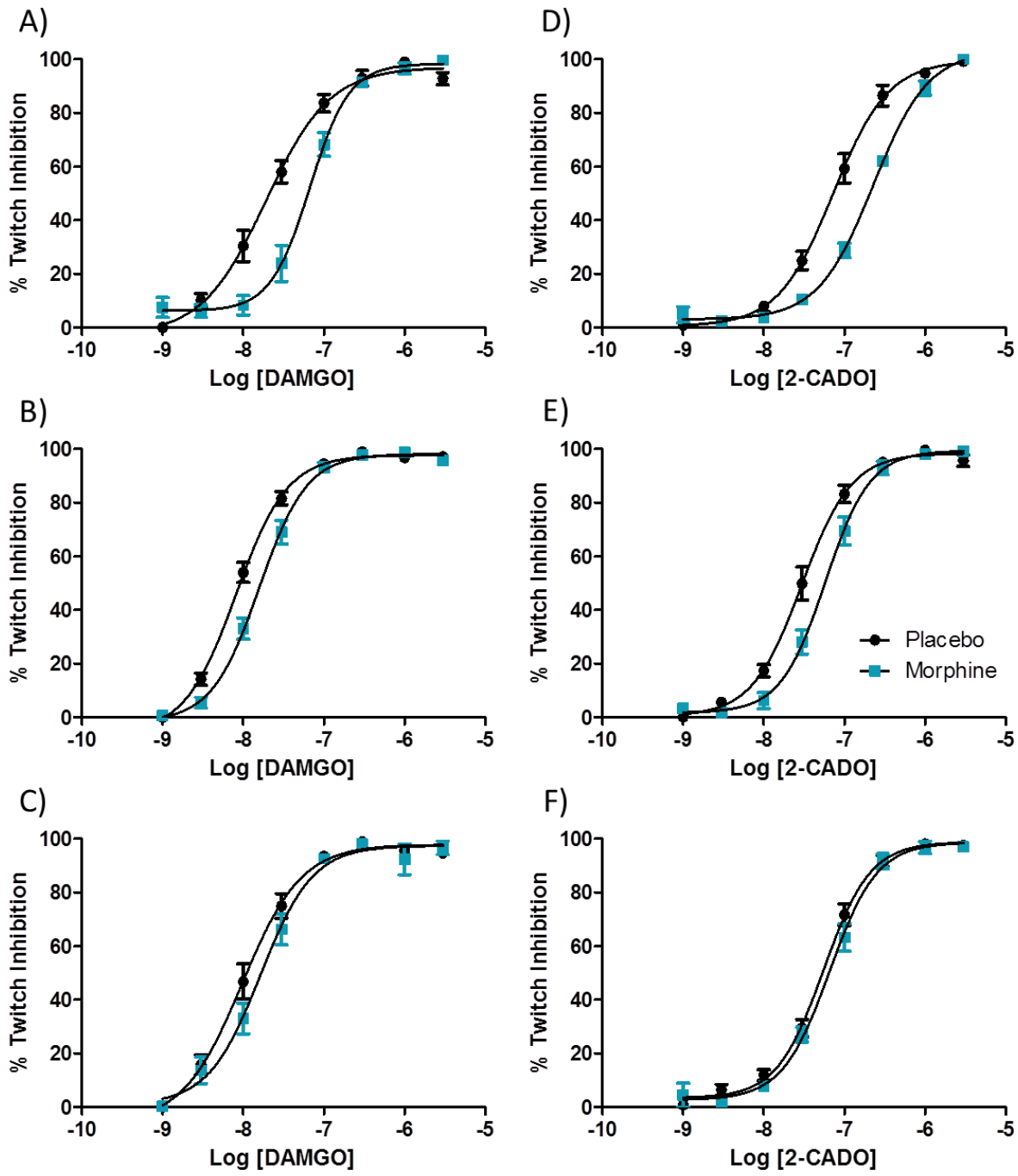
A)
D)
B)
E)
C)
F)
% Twitch Inhibition
Log [DAMGO]
Log [2-CADO]
Placebo
Morphine

Figure 3.9 DAMGO and 2-CADO Concentration Response Curves for Animals Treated for 7 days

A) Average DAMGO concentration response curve for 7 day – 0 day animals (n = 4). The morphine to placebo ratio of the IC_{50} = 3.160 and was not significantly different from 1 (p value = 0.0776).

B) Average DAMGO concentration response curve for 7 day – 2 day animals (n = 4). The morphine to placebo ratio of the IC_{50} = 1.857 and was not significantly different from 1 (p value = 0.0885).

C) Average DAMGO concentration response curve for 7 day – 4 day animals (n = 4). The morphine to placebo ratio of the IC_{50} = 0.964 and was not significantly different from 1 (p value = 0.8302).

D) Average 2-CADO concentration response curve for 7 day – 0 day animals (n = 4). The morphine to placebo ratio of the IC_{50} = 2.038 and was not significantly different from 1 (p value = 0.0754).

E) Average 2-CADO concentration response curve for 7 day – 2 day animals (n = 4). The morphine to placebo ratio of the IC_{50} = 1.466 and was not significantly different from 1 (p value = 0.4201).

F) Average 2-CADO concentration response curve for 7 day – 4 day animals (n = 4). The morphine to placebo ratio of the IC_{50} = 1.336 and was not significantly different from 1 (p value = 0.4956).

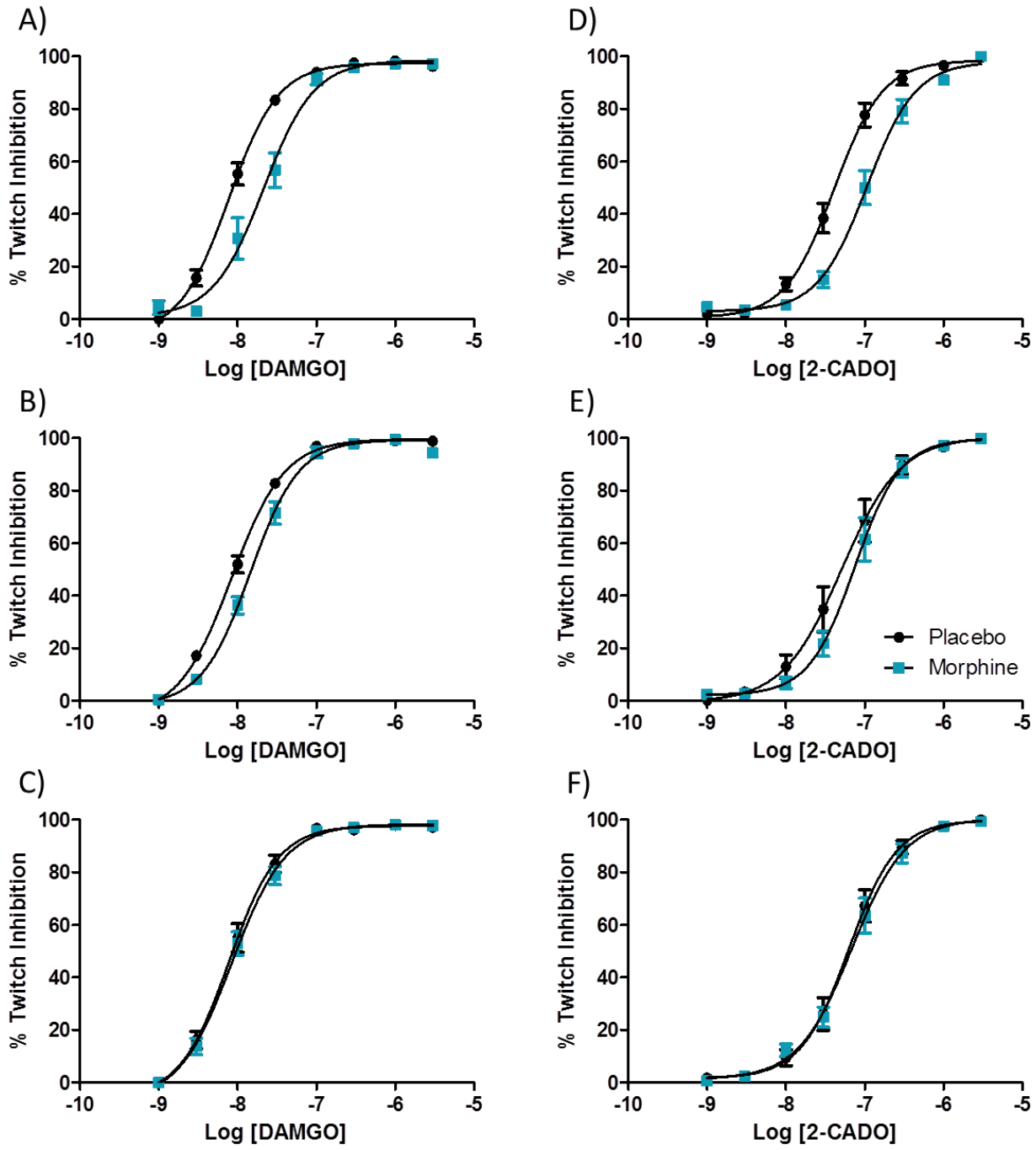
A)
% Twitch Inhibition
Log [DAMGO]
D)
Log [2-CADO]
B)
C)
E)
F)
Placebo
Morphine

Figure 3.10 DAMGO and 2-CADO Concentration Response Curves for Animals Treated for 10 days

A) Average DAMGO concentration response curve for 10 day – 0 day animals (n = 4). The morphine to placebo ratio of the IC_{50} = 3.806 and was significantly different from 1 (p value = 0.0402).

B) Average DAMGO concentration response curve for 10 day – 2 day animals (n = 3). The morphine to placebo ratio of the IC_{50} = 1.259 and was not significantly different from 1 (p value = 0.2898).

C) Average DAMGO concentration response curve for 10 day – 4 day animals (n = 4). The morphine to placebo ratio of the IC_{50} = 1.387 and was not significantly different from 1 (p value = 0.3807).

D) Average 2-CADO concentration response curve for 10 day – 0 day animals (n = 4). The morphine to placebo ratio of the IC_{50} = 1.920 and was significantly different from 1 (p value = <0.0348).

E) Average 2-CADO concentration response curve for 10 day – 2 day animals (n = 3). The morphine to placebo ratio of the IC_{50} = 0.752 and was not significantly different from 1 (p value = 0.3473).

F) Average 2-CADO concentration response curve for 10 day – 4 day animals (n = 4). The morphine to placebo ratio of the IC_{50} = 1.941 and was not significantly different from 1 (p value = 0.3843).

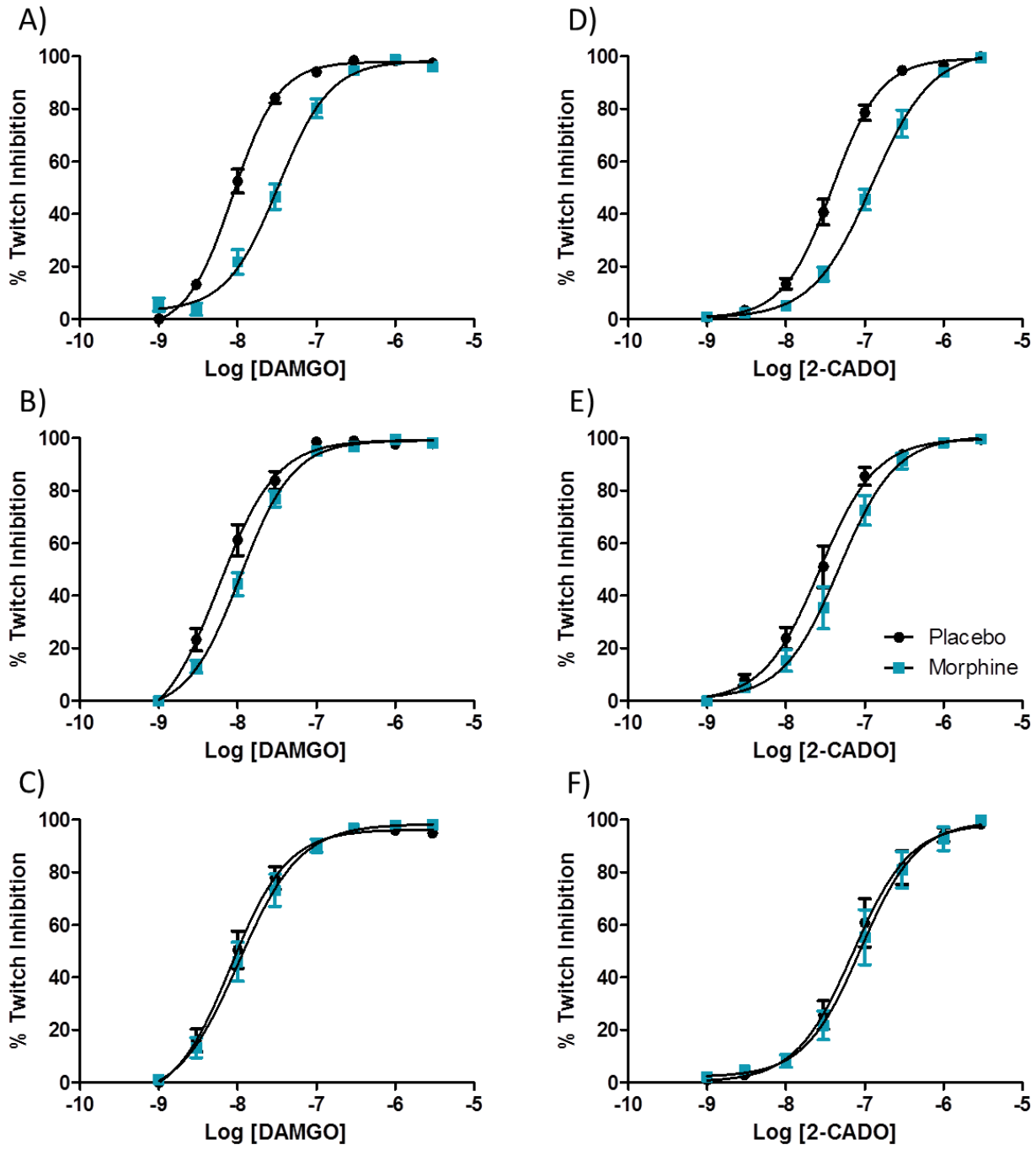
A)
% Twitch Inhibition
Log [DAMGO]
B)
% Twitch Inhibition
Log [DAMGO]
C)
% Twitch Inhibition
Log [DAMGO]
D)
% Twitch Inhibition
Log [2-CADO]
E)
% Twitch Inhibition
Log [2-CADO]
Placebo
Morphine
F)
% Twitch Inhibition
Log [2-CADO]

CHAPTER FOUR: TIME COURSE FOR THE ONSET AND DECAY OF HETEROLOGOUS TOLERANCE TO MORPHINE SUBCUTANEOUSLY INJECTED INTO GUINEA PIGS

4.1 Abstract

The development and decay of heterologous tolerance following chronic morphine exposure via pellet implantation is well documented in the guinea pig longitudinal muscle/myenteric plexus (LM/MP). However, this method of administration only permits a qualitative analysis of the decay phase of tolerance because the time at which morphine exposure is completed is unknown. IP administration of morphine was shown to be inadequate for time course studies due to variable absorption from the gut. Therefore, we assessed tolerance development in animals treated with twice daily subcutaneous injections of morphine for 1, 2, 4, 7, or 10 days. The analgesic effect of morphine was assessed using the paw pressure test and the heterologous nature of tolerance evaluated using the neurogenic twitch inhibition of DAMGO and 2-CADO in the LM/MP. Decay of tolerance was determined by evaluating animals or tissues from them 0, 1, 2, or 4 days after treatment cessation. A significant level of tolerance was generated by 2 days after treatment, which peaked at 4 days and was maintained through both 7 and 10 days of treatment. The data indicated that the time for return to baseline was correlated to the magnitude of tolerance in all animal groups and was not significantly different by 2 days after treatment stopped in animals that were treated for 4 days and by 4 days in animals that were treated for 7 or 10 days. The fact that the decay of tolerance is a function of both the length of treatment and magnitude of tolerance developed reinforces the idea that tolerance following chronic treatment with morphine is an adaptive process produced by alterations in at least one of several possible cellular signaling proteins.

4.2 Introduction

Tolerance to opioids remains a problem for clinicians who use them to treat patients with severe chronic pain. For decades researchers have sought to uncover the cellular mechanism(s) that underlie the development of tolerance to morphine. With a mechanism identified, it would then be possible to develop drugs that could circumvent tolerance to morphine in the clinic. It is widely believed that tolerance to opioids is the result of cellular adaptations to the prolonged exposure to the agonist. There were five criteria proposed by Taylor and Fleming for a given cellular adaptation to account for the altered responsiveness that is observed in the tolerant state. The second of these criteria states that "the proposed cellular change must follow a similar time course as the development of tolerance and/or dependence in that tissue (Taylor & Fleming, 2001)". The majority of work that exists in opioid research tends to focus on single time points, usually 7 days after treatment, when the animal is known to be tolerant to the drug used. While this approach can yield important information about whether or not an adaptation exists, no information about when this change occurred or when/if it reverses once treatment ends can be obtained. For a number of years this laboratory has focused on developing a time course for the onset and decay of tolerance to morphine. Previous work has yielded such a time course in pellet implanted animals (Barrett, Maguma & Taylor, 2011; Li, Maguma, Thayne, Davis & Taylor, 2010). However, pellet implantation is inadequate for precisely examining the decay of tolerance because it is unknown when all of the morphine has diffused from the pellet and therefore a time zero for evaluation of the decay of tolerance cannot be defined. Previous work had suggested that several different methods of inducing tolerance, pellet implantation and subcutaneous injection among others, produce a magnitude of tolerance that is indistinguishable from one another (Li, Maguma, Thayne, Davis & Taylor, 2010). Work in chapter 3 sought to

add IP injection to this list while defining a time course for the onset and decay of tolerance. However it was discovered that IP injection led to higher variability in the data than the other methods and therefore is not the best choice for a time course study. Because of the higher variability associated with IP injections, the time course study done in chapter 3 was repeated and expanded using subcutaneous injections. Subcutaneous injection has already been used by the laboratory and shown to induce a tolerance that is similar in magnitude and character to that observed with pellet implantation. Because animals that were treated for 4 days seemed to develop a magnitude of tolerance indistinguishable from animals treated for 7 or 10 days, animals that had been treated for 1 or 2 days and assessed immediately after the last treatment day were added to the study to better characterize the time of onset of tolerance. Because the results of chapter 3 indicated that decay of tolerance for the 7 and 10 day treated animals progressed faster than originally hypothesized, to better characterize the decay of tolerance animals that were treated for 7 or 10 days and assessed 1 day after the last treatment day were added.

4.3 Experimental Protocol

All of the methods used here are detailed in chapter 2. Dunkin-Hartley guinea pigs were treated via twice daily subcutaneous injections for 1, 2, 4, 7, or 10 days with either morphine (corrected for the free base) or saline. The dosing schedule employed (see table 3.1) was adapted from previous work in this laboratory (Li, Maguma, Thayne, Davis & Taylor, 2010). Some of the animals for each of the treatment lengths were allowed to remain in the animal facility for specified lengths of time after the last dose of morphine in order to assess the decay of the developed tolerance. Animals treated for 1 or 2 days were assessed immediately after the last treatment day (0 days after). Animals treated for 4 days were assessed at 0, 1, or 2 days after the

last treatment day. Because it was expected that a greater degree of tolerance would take longer to fade, the animals treated for 7 or 10 days were assessed at 0, 1, 2, or 4 days after the last treatment day. To help control for daily variations animals were dosed in pairs, a treated and a control, and a daily morphine to placebo ratio was calculated. All statistics were done on these ratios. For the sake of simplicity animals treated for 4 days and assessed 0 days after the last treatment day will be referred to as 4 day – 0 day animals while animals treated for 4 days and assessed 1 day after the last treatment day will be referred to as 4 day – 1 day animals and so forth.

Tolerance assessment consisted of paw pressure testing followed by euthanasia after isoflurane anesthesia. At this point tissues were collected and segments of the LM/MP were prepared for the organ bath apparatus (see figure 2.3). After a washing period electrical stimulation was applied and the tissue was allowed to acclimate. Cumulative concentration response curves for either DAMGO or 2-CADO (the order was randomized) were performed next, followed by a washing period and the concentration response curve for the other drug.

All statistics were performed using Graph Pad Prism 5. T-tests were run to test whether or not the average morphine to placebo ratio was significantly different from unity. Results were considered significant at a p value of less than 0.05.

4.4 Experimental Results

4.4.1 Onset of Heterologous Tolerance

Paw pressure testing in the whole animal revealed that the magnitude of tolerance that develops does indeed depend on the length of treatment (see figure 4.1; table 4.1). A significant difference in the AUC was observed by as early as 2 days of treatment with ~1.5 fold increase in the placebo to morphine ratio of the AUC. The magnitude of this shift increased with treatment

length, reaching a 2 fold increase in the AUC after 10 days of treatment. Although the average AUC ratios for 4, 7, or 10 days of treatment were not significantly different from each other, it does appear that the longer the treatment, the greater the average AUC ratio. These data were complemented by the organ bath data using LM/MP preparations obtained from these same animals. The DAMGO IC_{50} data (see figure 4.2; table 4.1) mirror what was seen in the whole animal with paw pressure testing. A 2 fold increase in the IC_{50} was observed after the second day of treatment. After 4 days of treatment the shift had increased to ~2.7 fold. A shift of similar magnitude was observed in the 7 and 10 day animals as well. The development of heterologous tolerance (tolerance to 2-CADO stimulation of the A_1 receptor) appears to lag behind tolerance to the μ receptor system and tolerance to the analgesic effect in the whole animal (see figure 4.3; table 4.1). By the second day of treatment there was a non-significant (~1.8 fold) shift in the IC_{50} of 2-CADO. A statistically significant shift in the 2-CADO IC50 was not observed until 4 days of treatment (~2.7 fold increase). A similar increase was also observed in the 7 and 10 day treated animals.

4.4.2 Decay of Heterologous Tolerance

Because heterologous tolerance was not observed in animals treated with morphine for 1 or 2 days, no study of the decay of tolerance was necessary for these animals. A significant level of tolerance was observed for all endpoints measured 1 day after treatment cessation in animals that had been treated for 4 days (see figures 4.4, 4.7, and 4.10; table 4.1). By 2 days after treatment cessation in 4 day treated animals the LM/MP responses to DAMGO and 2-CADO had returned to baseline but there was still a significant level of tolerance present to the analgesic effect of morphine based on the increased AUC from the paw pressure test. In animals that were treated for 7 days a significant level of tolerance exists to the inhibitory effects of DAMGO and 2-

CADO up to 2 days after treatment cessation (see figures 4.8 and 4.11; table 4.1). Although the paw pressure AUCs are not significantly increased at these time points (see figure 4.5; table 4.1), it is interesting to note that the magnitude of the change is the same as the 4 day post treatment AUC, which is significant. The response of the LM/MP to DAMGO and 2-CADO returned to baseline by 4 days after treatment. In animals that were treated for 10 days a significant level of tolerance to DAMGO in the LM/MP and to the analgesic effect of morphine, but not to 2-CADO, was observed by 1 day post treatment (see figures 4.6, 4.9, and 4.12; table 1). By 2 days after treatment cessation, only the analgesic effect of morphine in the paw pressure test demonstrated a significant level of tolerance which returned to baseline by 4 days after treatment.

4.5 Discussion

It is believed that heterologous tolerance results from adaptive changes in a number of intracellular proteins involved in regulating cell excitability. This change in responsiveness should take time to be fully expressed as well as to return to normal after treatment has ceased. The second of five criteria that have been suggested to be fulfilled for a proposed cellular mechanism to account for any observed changes in responsiveness states that the change must occur over a similar time course as the change in responsiveness (Taylor & Fleming, 2001). Previous work from this laboratory has defined a time course for the onset and decay of tolerance both in the whole animal and in the LM/MP model system with pellet implanted animals (Barrett, Maguma & Taylor, 2011; Li, Maguma, Thayne, Davis & Taylor, 2010). However, because of the nature of the pellet implantation method of administration, an accurate time course for the decay of tolerance back to baseline could not be established in those studies. This set of experiments are the first to attempt to examine the time course for the decay of tolerance in

detail. The hypothesis being tested by these studies was that the magnitude to tolerance that develops should increase with treatment length and that a greater magnitude of tolerance should take longer to return to baseline. In addition the time course for the development and decline of heterologous tolerance following chronic treatment with morphine should be similar in vivo and ex vivo. Although there were some issues with the work from chapter 3, it was shown that the magnitude of tolerance that develops in the LM/MP when morphine is administered IP does depend on the length of treatment and that the decay time was also related to the length of treatment based on the fact that it takes longer for animals treated for 7 or 10 days to return to baseline than animals that were treated for 4 days (see chapter 3). The same phenomenon was observed in these studies with subcutaneous administration of morphine. In addition, with the dosing issue corrected, tolerance could be examined and observed to occur in the whole animal via paw pressure testing. The data indicate that tolerance in the whole animal and in the LM/MP develops and decays over a similar time course.

An interesting observation is that there was not a significant difference between the magnitude of tolerance that developed in the LM/MP between the 4, 7, and 10 day treated animals. A similar relationship was observed in the IP treated animals as well and would imply that maximum tolerance in the LM/MP was achieved after only 4 days of treatment. However, like the IP treated animals, it took longer for the observed tolerance in the 7 and 10 day animals to fade than in the 4 day animals (>2 days in the 7 and 10 day treated animals vs. 1 in the 4 day treated animals). This would imply that despite the same magnitude of tolerance, more extensive cellular adaptations occurred in the animals treated for 7 or 10 days than in the 4 day treated animals. This is consistent with data from many other laboratories that suggest that maximum tolerance in the LM/MP occurs after 7 days of treatment (Barrett, Maguma & Taylor, 2011;

Goldstein & Schulz, 1973; Leedham, Doak, Taylor & Fleming, 1989; Li, Maguma, Thayne, Davis & Taylor, 2010). A similar phenomenon was observed in the paw pressure AUC ratios. However, despite the lack of a significant difference in the paw pressure AUC ratios of the 4, 7, and 10 day treated animals, a trend was present for an incremental increase as treatment length increased. A greater increase in the AUC ratio may be more difficult to obtain using the 10 mg/kg test dose of morphine in the paw pressure test in animals treated for longer than 10 days because that dose had almost no effect in the animals treated for 10 days (see figure 4.6).

There are a few observations in the current experiments that could be improved upon. The first is the fact that blood was not collected from any of the animals for measurement of morphine levels. Morphine has a half-life of about 120 minutes (Trescot, Datta, Lee & Hansen, 2008) but it has been reported that morphine levels could still be detected in urine 1 to 1.5 days after a dose is given (Vandevenne, Vandenbussche & Verstraete, 2000). The latest that we still observed tolerance was 2 days after treatment cessation. Plasma levels of morphine were not measured in these animals because there was no feasible way to do so at the time of these experiments. As a result we cannot be certain that some of the observed effects of tolerance at 0 or 1 day after treatment cessation were not simply due to the continued presence of morphine, especially with animals treated for 7 or 10 days, given our escalating dose schedule. The fact that we still have a significant level of tolerance at 2 days after treatment cessation, a time when detectable levels of morphine should not be present in the plasma, in animals treated for 7 days would seem to indicate that tolerance has developed in these animals. Another issue, which was actually raised concerning pellet implanted animals, is inflammation. With pellet implanted animals there was some concern that the pellet implantation surgery produced inflammation around the surgery site that may have interfered with some of the measured endpoints and it was

suggested that an injection would reduce inflammation (Li, Maguma, Thayne, Davis & Taylor, 2010). To further minimize the impact of this potential confounding influences we injected at a different site, though still at nape of the neck, each time. However, since some animals received injections 20 times in roughly the same area over 10 days, it is possible that there is still some influence of inflammation. The IC_{50} data for DAMGO and 2-CADO and the paw pressure test were comparable to previous work in the laboratory, so we believe that there was, at most, the same level of inflammation if not less.

With the time course for the development and decay of tolerance to morphine known, it is possible to correlate changes in protein expression to the observed changes in function. Because receptor down-regulation could account for tolerance, one obvious choice for protein analysis is the μ receptor. Other proteins such as the Na^+/K^+ ATPase and PKC have been suggested to play a role in the development of tolerance to morphine. Tissues from the same animals that the functional responses were obtained in were used to examine the concentration of these and other proteins in chapter 5.

Table 4.1 Summary of Onset and Decay of Tolerance Data

For ease of comparison between time points, this table contains all of the placebo/morphine ratios of the AUC from the paw pressure experiments and the morphine/placebo ratios of the IC_{50}s of DAMGO and 2-CADO in the LM/MP from all time points. See figures 4.1-4.12 for more details.

Length of Treatment	Time After Treatment	In vivo Response: Paw Pressure AUC Placebo/Morphine Ratio	Ex vivo Responses: DAMGO IC_{50} Morphine/Placebo Ratio	Ex vivo Responses: 2-CADO IC_{50} Morphine/Placebo Ratio	n =
1 day	0 days	1.28 (0.097)	1.50 (0.231)	1.33 (0.200)	4
2 days	0 days	1.44 (0.114)*	2.03 (0.310)*	1.75 (0.322)	6
4 days	0 days	1.70 (0.181)*	2.71 (0.403)*	2.66 (0.496)*	4
	1 day	1.30 (0.092)*	2.60 (0.430)*	1.73 (0.141)*	5
	2 days	1.33 (0.098)*	0.83 (0.164)	0.89 (0.204)	4
7 days	0 days	1.92 (0.229)*	3.27 (0.452)*	2.98 (0.612)*	4
	1 day	1.39 (0.139)	1.95 (0.348)	2.67 (0.652)	4
	2 days	1.52 (0.220)	1.56 (0.163)*	1.66 (0.435)	5
	4 days	1.45 (0.106)*	0.96 (0.301)	0.90 (0.320)	4
10 days	0 days	2.18 (0.054)*	2.70 (0.327)*	2.97 (0.407)*	4
	1 day	1.43 (0.121)*	1.69 (0.118)*	2.22 (0.881)	5
	2 days	2.02 (0.245)*	1.48 (0.430)	1.21 (0.252)	5
	4 days	1.24 (0.134)	0.74 (0.099)	0.774 (0.136)	4

Figure 4.1 Onset of Analgesic Tolerance in the Guinea Pig

For all graphs, the green line represents the morphine treated group, while the black line is the placebo treated group

A) Average paw pressure data for 1 day – 0 day animals (n = 4). The placebo to morphine ratio of the area under the curve (AUC) = 1.279 and was not significantly different from 1 (p value = 0.0639).

B) Average paw pressure data for 2 day – 0 day animals (n = 6). The placebo to morphine ratio of the area under the curve (AUC) = 1.440 and was significantly different from 1 (p value = 0.0141).

C) Average paw pressure data for 4 day – 0 day animals (n = 4). The placebo to morphine ratio of the area under the curve (AUC) = 1.695 and was significantly different from 1 (p value = 0.0313).

D) Average paw pressure data for 7 day – 0 day animals (n = 4). The placebo to morphine ratio of the area under the curve (AUC) = 1.918 and was significantly different from 1 (p value = 0.0279).

E) Average paw pressure data for 10 day – 0 day animals (n = 4). The placebo to morphine ratio of the area under the curve (AUC) = 2.180 and was significantly different from 1 (p value = 0.0002).

F) Summary bar graph of the placebo to morphine ratio of the AUC from the data presented in A-E.

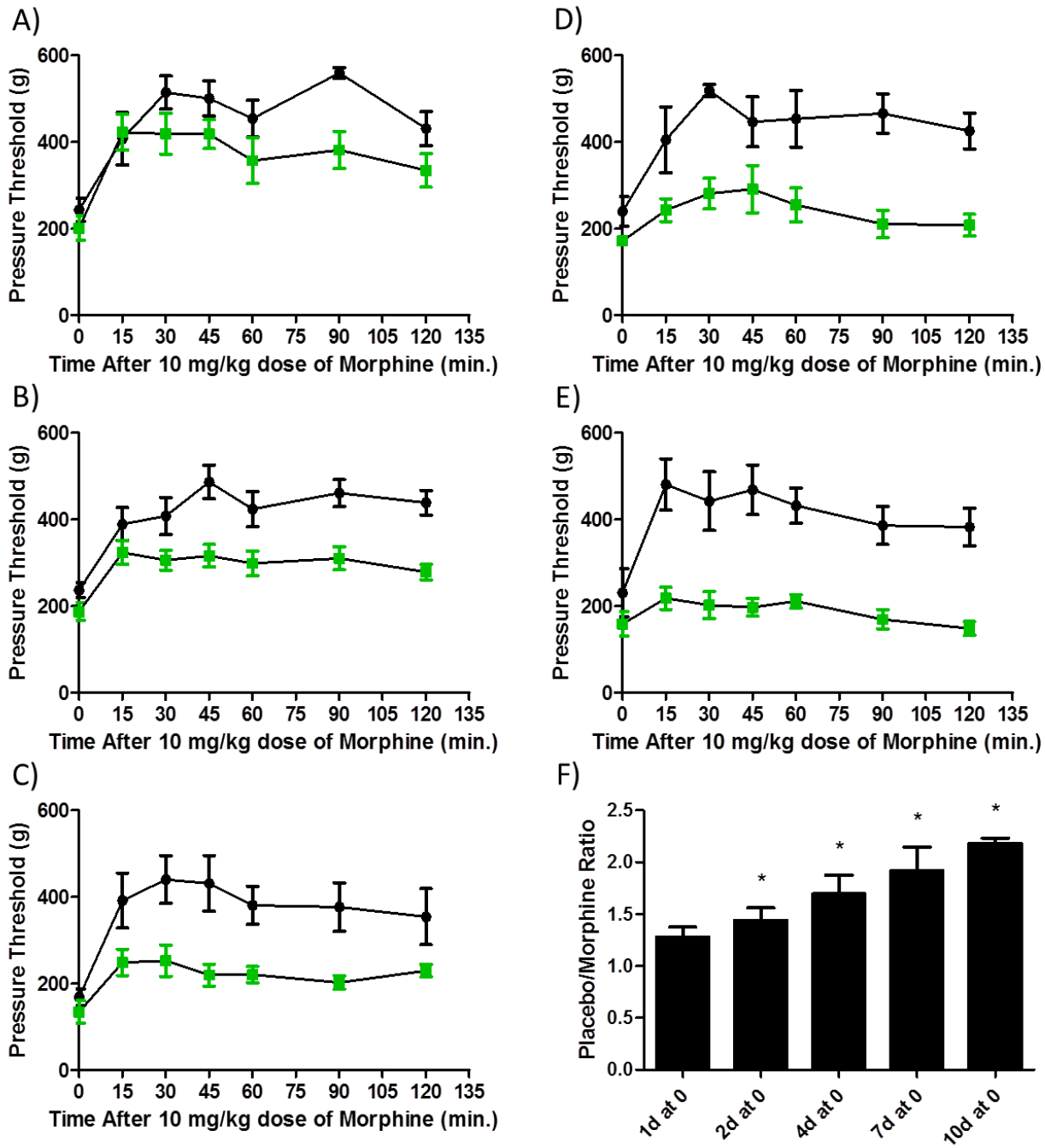
A)
Pressure Threshold (g)
600
400
200
0
0 15 30 45 60 75 90 105 120 135
Time After 10 mg/kg dose of Morphine (min.)
D)
Pressure Threshold (g)
600
400
200
0
0 15 30 45 60 75 90 105 120 135
Time After 10 mg/kg dose of Morphine (min.)
B)
Pressure Threshold (g)
600
400
200
0
0 15 30 45 60 75 90 105 120 135
Time After 10 mg/kg dose of Morphine (min.)
E)
Pressure Threshold (g)
600
400
200
0
0 15 30 45 60 75 90 105 120 135
Time After 10 mg/kg dose of Morphine (min.)
C)
Pressure Threshold (g)
600
400
200
0
0 15 30 45 60 75 90 105 120 135
Time After 10 mg/kg dose of Morphine (min.)
F)
Placebo/Morphine Ratio
2.5
2.0
1.5
1.0
0.5
0.0
*
*
*
*
1d at 0
2d at 0
4d at 0
7d at 0
10d at 0

Figure 4.2 Onset of Tolerance to DAMGO in the LM/MP

For all concentration response curves: green line = morphine treated group, black line = placebo treated group.

A) Average DAMGO concentration response curve for 1 day – 0 day animals (n = 6). The morphine to placebo ratio of the IC_{50} = 1.503 and was not significantly different from 1 (p value = 0.0816).

B) Average DAMGO concentration response curve for 2 day – 0 day animals (n = 6). The morphine to placebo ratio of the IC_{50} = 2.027 and was significantly different from 1 (p value = 0.0211).

C) Average DAMGO concentration response curve for 4 day – 0 day animals (n = 6). The morphine to placebo ratio of the IC_{50} = 2.708 and was significantly different from 1 (p value = 0.0080).

D) Average DAMGO concentration response curve for 7 day – 0 day animals (n = 5). The morphine to placebo ratio of the IC_{50} = 3.266 and was significantly different from 1 (p value = 0.0074).

E) Average DAMGO concentration response curve for 10 day – 0 day animals (n = 4). The morphine to placebo ratio of the IC_{50} = 2.698 and was significantly different from 1 (p value = 0.0138).

F) Summary bar graph of the morphine to placebo ratios of the IC_{50}s from the concentration response curves presented in A-E.

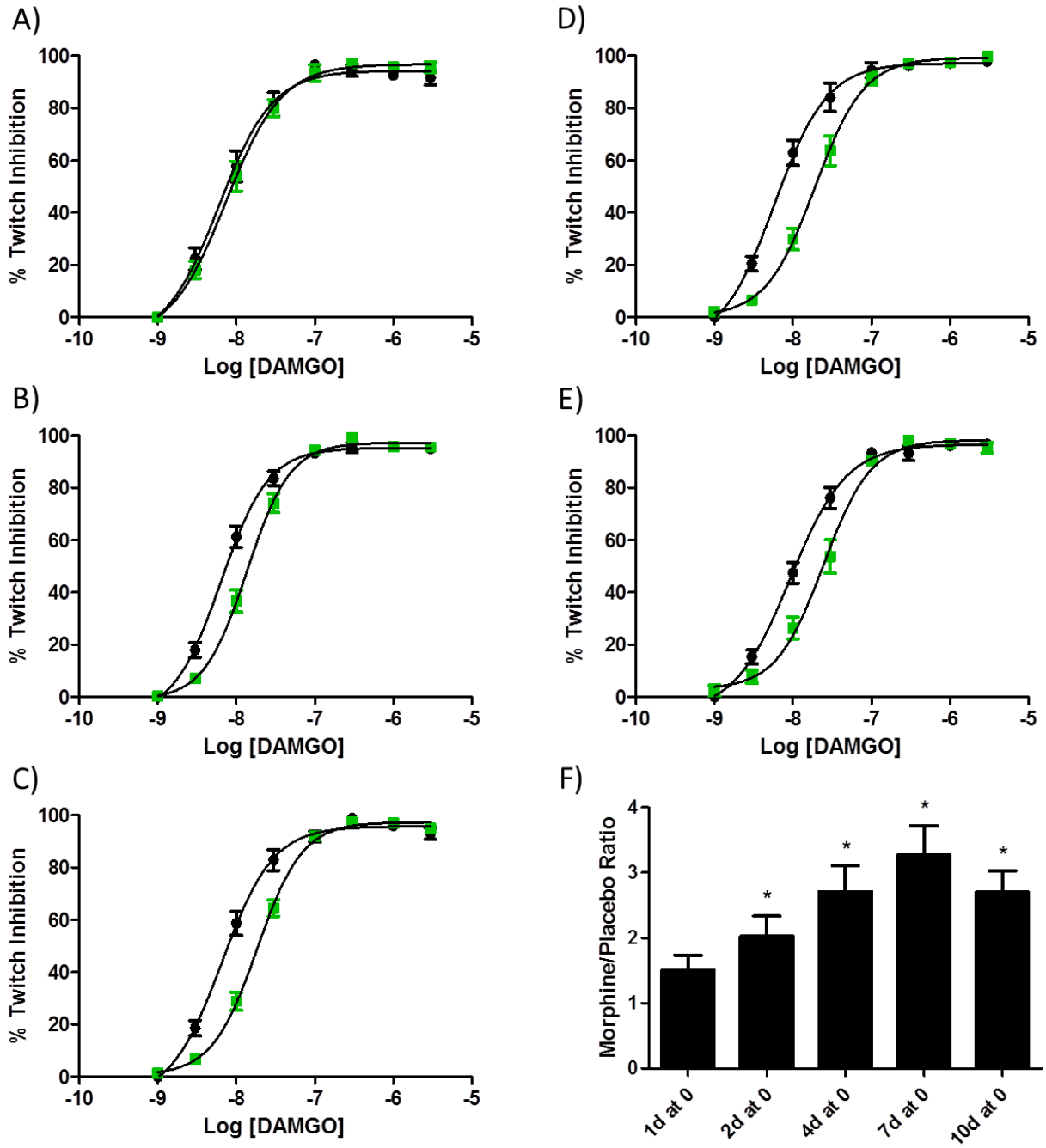
A)
% Twitch Inhibition
Log [DAMGO]
B)
% Twitch Inhibition
Log [DAMGO]
C)
% Twitch Inhibition
Log [DAMGO]
D)
% Twitch Inhibition
Log [DAMGO]
E)
% Twitch Inhibition
Log [DAMGO]
F)
Morphine/Placebo Ratio
1d at 0
2d at 0
4d at 0
7d at 0
10d at 0

Figure 4.3 Onset of Tolerance to 2-CADO in the LM/MP

For all concentration response curves: green line = morphine treated group, black line = placebo treated group.

A) Average 2-CADO concentration response curve for 1 day – 0 day animals (n = 6). The morphine to placebo ratio of the IC_{50} = 1.328 and was not significantly different from 1 (p value = 0.1608).

B) Average 2-CADO concentration response curve for 2 day – 0 day animals (n = 6). The morphine to placebo ratio of the IC_{50} = 1.752 and was not significantly different from 1 (p value = 0.0669).

C) Average 2-CADO concentration response curve for 4 day – 0 day animals (n = 6). The morphine to placebo ratio of the IC_{50} = 2.657 and was significantly different from 1 (p value = 0.0206).

D) Average 2-CADO concentration response curve for 7 day – 0 day animals (n = 5). The morphine to placebo ratio of the IC_{50} = 2.976 and was significantly different from 1 (p value = 0.0319).

E) Average 2-CADO concentration response curve for 10 day – 0 day animals (n = 4). The morphine to placebo ratio of the IC_{50} = 2.965 and was significantly different from 1 (p value = 0.0170).

F) Summary bar graph of the morphine to placebo ratios of the IC_{50}s from the concentration response curves presented in A-E.

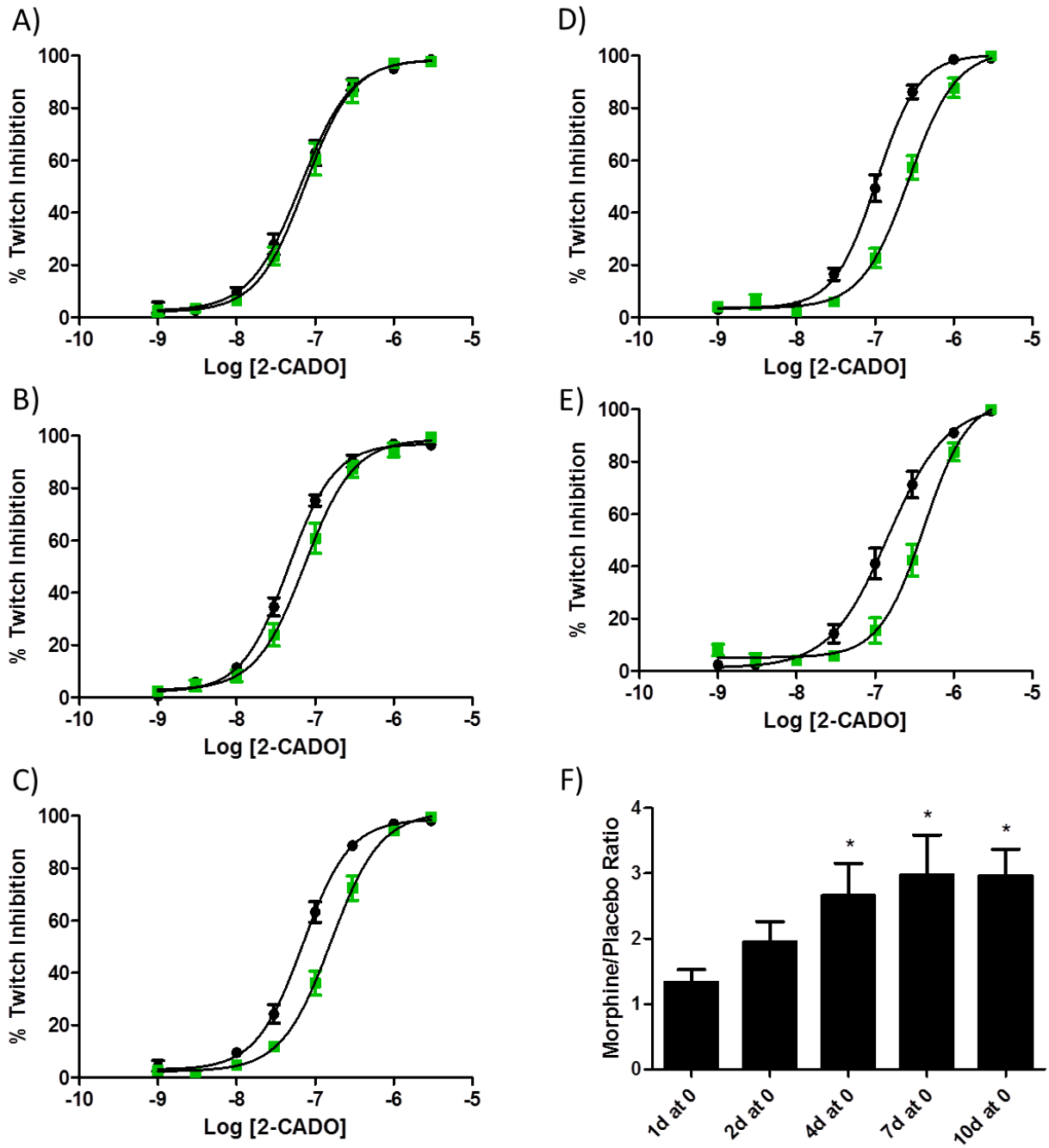
A)
% Twitch Inhibition
Log [2-CADO]
B)
% Twitch Inhibition
Log [2-CADO]
C)
% Twitch Inhibition
Log [2-CADO]
D)
% Twitch Inhibition
Log [2-CADO]
E)
% Twitch Inhibition
Log [2-CADO]
F)
Morphine/Placebo Ratio
1d at 0
2d at 0
4d at 0
7d at 0
10d at 0

Figure 4.4 Decay of Analgesic Tolerance in Guinea Pigs Treated for 4 Days

For all graphs: green line = morphine treated group, black line = placebo treated group.

A) Average paw pressure data for 4 day – 0 day animals (n = 4). The placebo to morphine ratio of the area under the curve (AUC) = 1.695 and was significantly different from 1 (p value = 0.0313).

B) Average paw pressure data for 4 day – 1 day animals (n = 6). The placebo to morphine ratio of the area under the curve (AUC) = 1.293 and was significantly different from 1 (p value = 0.0118).

C) Average paw pressure data for 4 day – 2 day animals (n = 4). The placebo to morphine ratio of the area under the curve (AUC) = 1.330 and was significantly different from 1 (p value = 0.0436).

D) Summary bar graph of the placebo to morphine ratio of the AUC from the data presented in A-C.

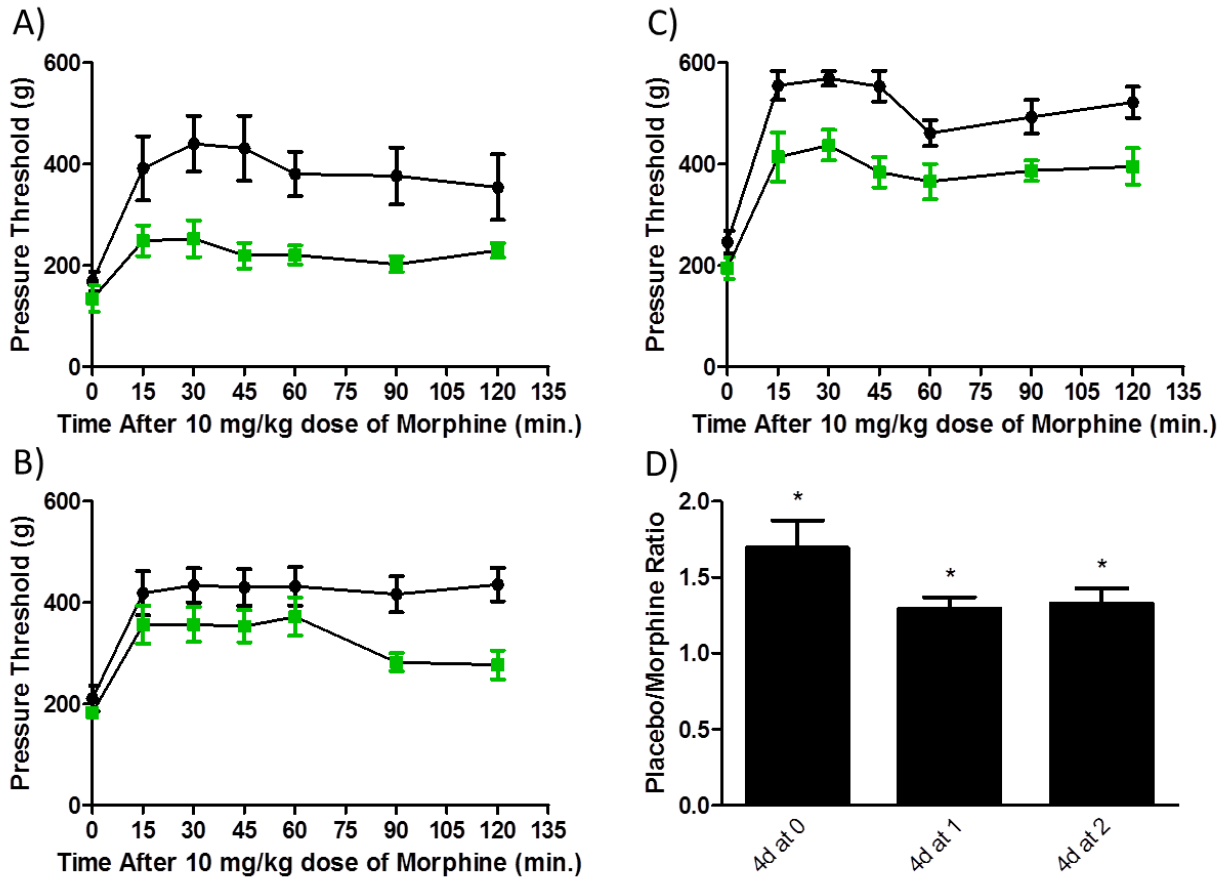
A)
Pressure Threshold (g)
600
400
200
0
0 15 30 45 60 75 90 105 120 135
Time After 10 mg/kg dose of Morphine (min.)
C)
Pressure Threshold (g)
600
400
200
0
0 15 30 45 60 75 90 105 120 135
Time After 10 mg/kg dose of Morphine (min.)
B)
Pressure Threshold (g)
600
400
200
0
0 15 30 45 60 75 90 105 120 135
Time After 10 mg/kg dose of Morphine (min.)
D)
Placebo/Morphine Ratio
2.0
1.5
1.0
0.5
0.0
*
*
*
4d at 0
4d at 1
4d at 2

Figure 4.5 Decay of Analgesic Tolerance in Guinea Pigs Treated for 7 Days

For all graphs: green line = morphine treated group, black line = placebo treated group.

A) Average paw pressure data for 7 day – 0 day animals (n = 4). The placebo to morphine ratio of the area under the curve (AUC) = 1.918 and was significantly different from 1 (p value = 0.0279).

B) Average paw pressure data for 7 day – 1 day animals (n = 4). The placebo to morphine ratio of the area under the curve (AUC) = 1.388 and was not significantly different from 1 (p value = 0.0).

C) Average paw pressure data for 7 day – 2 day animals (n = 4). The placebo to morphine ratio of the area under the curve (AUC) = 1.520 and was not significantly different from 1 (p value = 0.0777).

D) Average paw pressure data for 7 day – 4 day animals (n = 4). The placebo to morphine ratio of the area under the curve (AUC) = 1.453 and was significantly different from 1 (p value = 0.0233).

E) Summary bar graph of the placebo to morphine ratio of the AUC from the data presented in A-D.

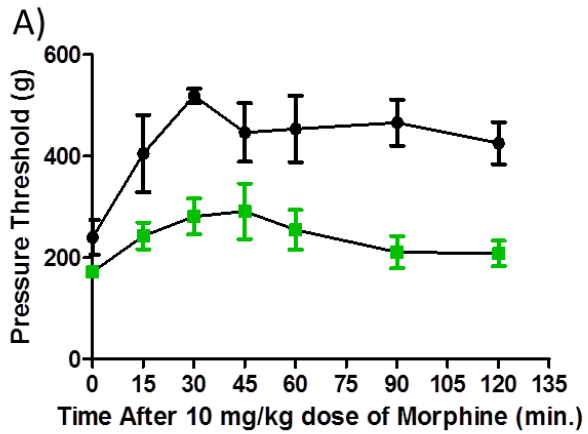
A)
Pressure Threshold (g)
600
400
200
0
0 15 30 45 60 75 90 105 120 135
Time After 10 mg/kg dose of Morphine (min.)

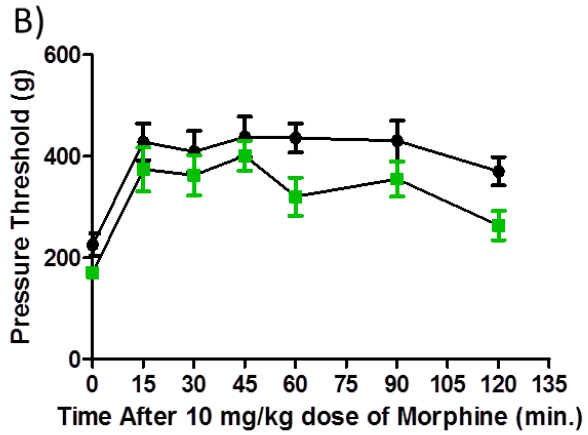
B)
Pressure Threshold (g)
600
400
200
0
0 15 30 45 60 75 90 105 120 135
Time After 10 mg/kg dose of Morphine (min.)

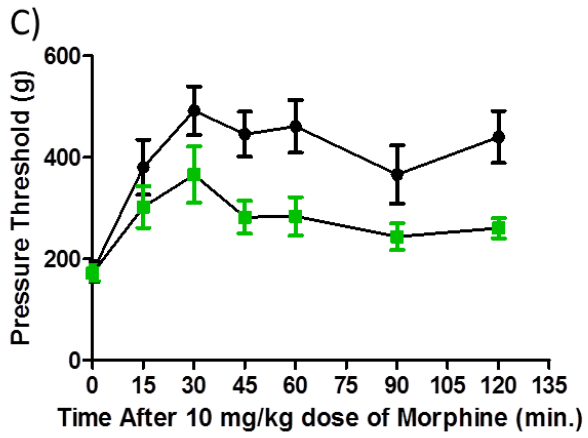
C)
Pressure Threshold (g)
600
400
200
0
0 15 30 45 60 75 90 105 120 135
Time After 10 mg/kg dose of Morphine (min.)

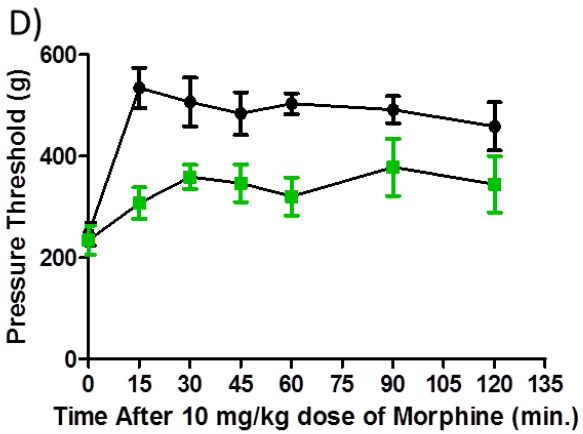
D)
Pressure Threshold (g)
600
400
200
0
0 15 30 45 60 75 90 105 120 135
Time After 10 mg/kg dose of Morphine (min.)

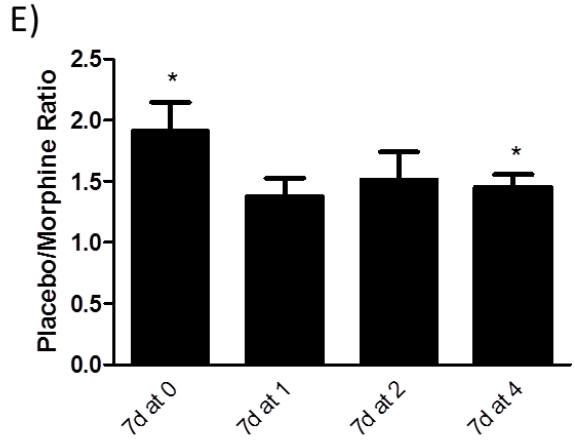
E)
Placebo/Morphine Ratio
2.5
2.0
1.5
1.0
0.5
0.0
*
*
7d at 0
7d at 1
7d at 2
7d at 4

Figure 4.6 Decay of Analgesic Tolerance in Guinea Pigs Treated for 10 Days

For all graphs: green line = morphine treated group, black line = placebo treated group.

A) Average paw pressure data for 10 day – 0 day animals (n = 4). The placebo to morphine ratio of the area under the curve (AUC) = 2.180 and was significantly different from 1 (p value = 0.0002).

B) Average paw pressure data for 10 day – 1 day animals (n = 5). The placebo to morphine ratio of the area under the curve (AUC) = 1.434 and was significantly different from 1 (p value = 0.0233).

C) Average paw pressure data for 10 day – 2 day animals (n = 5). The placebo to morphine ratio of the area under the curve (AUC) = 2.022 and was significantly different from 1 (p value = 0.0141).

D) Average paw pressure data for 10 day – 4 day animals (n = 4). The placebo to morphine ratio of the area under the curve (AUC) = 1.238 and was not significantly different from 1 (p value = 0.1737).

E) Summary bar graph of the placebo to morphine ratio of the AUC from the data presented in A-D.

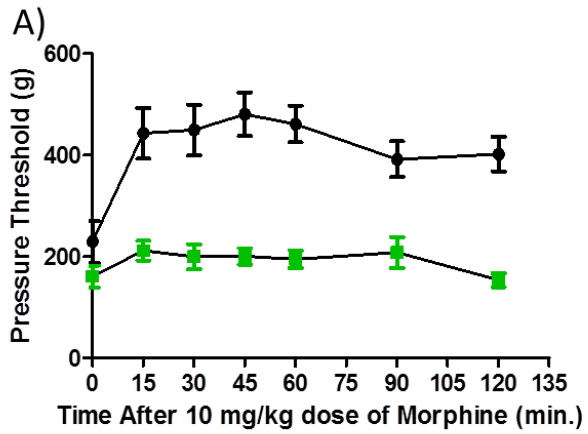
A)
Pressure Threshold (g)
600
400
200
0
0 15 30 45 60 75 90 105 120 135
Time After 10 mg/kg dose of Morphine (min.)

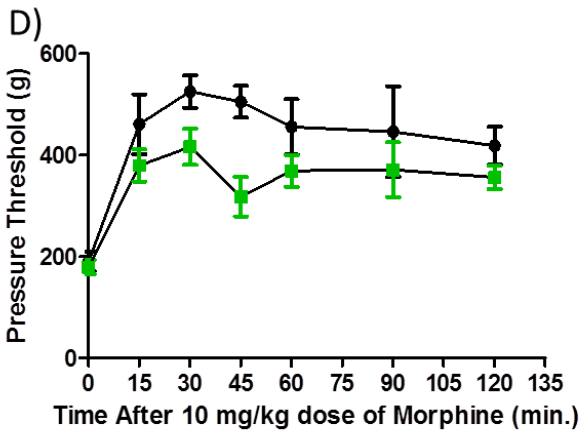
D)
Pressure Threshold (g)
600
400
200
0
0 15 30 45 60 75 90 105 120 135
Time After 10 mg/kg dose of Morphine (min.)

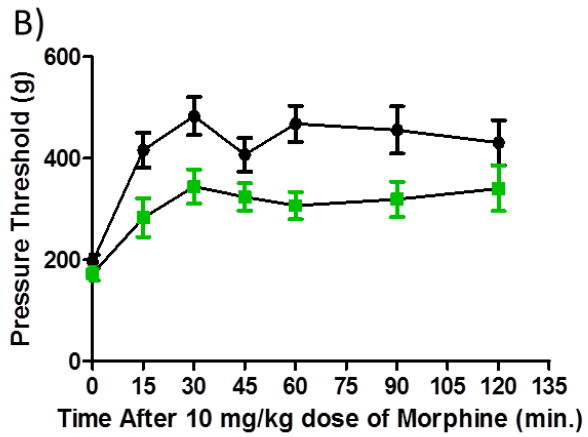
B)
Pressure Threshold (g)
600
400
200
0
0 15 30 45 60 75 90 105 120 135
Time After 10 mg/kg dose of Morphine (min.)

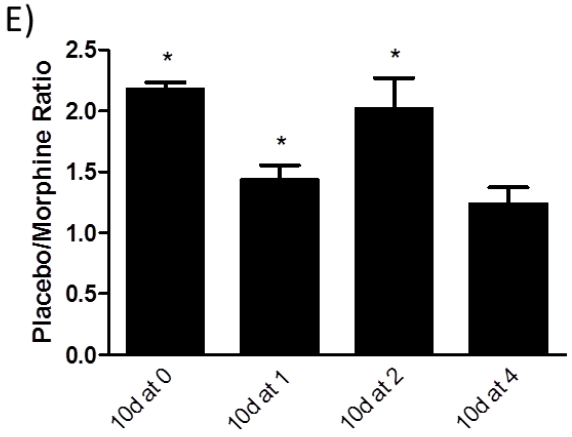
E)
Placebo/Morphine Ratio
2.5
2.0
1.5
1.0
0.5
0.0
*
*
*
10d at 0
10d at 1
10d at 2
10d at 4

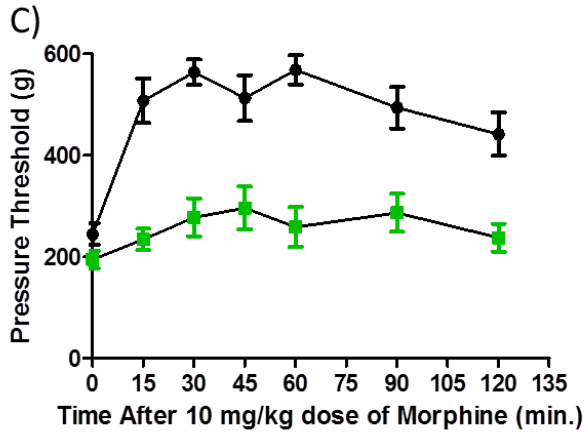
C)
Pressure Threshold (g)
600
400
200
0
0 15 30 45 60 75 90 105 120 135
Time After 10 mg/kg dose of Morphine (min.)

Figure 4.7 Decay of Tolerance to DAMGO in the LM/MP of Guinea Pigs Treated for 4 Days

For all concentration response curves: green line = morphine treated group, black line = placebo treated group.

A) Average DAMGO concentration response curve for 4 day – 0 day animals (n = 6). The morphine to placebo ratio of the IC_{50} = 2.708 and was significantly different from 1 (p value = 0.0080).

B) Average DAMGO concentration response curve for 4 day – 1 day animals (n = 6). The morphine to placebo ratio of the IC_{50} = 2.597 and was significantly different from 1 (p value = 0.0138).

C) Average DAMGO concentration response curve for 4 day – 2 day animals (n = 5). The morphine to placebo ratio of the IC_{50} = 0.830 and was not significantly different from 1 (p value = 0.3594).

D) Summary bar graph of the morphine to placebo ratios of the IC_{50}s from the concentration response curves presented in A-C.

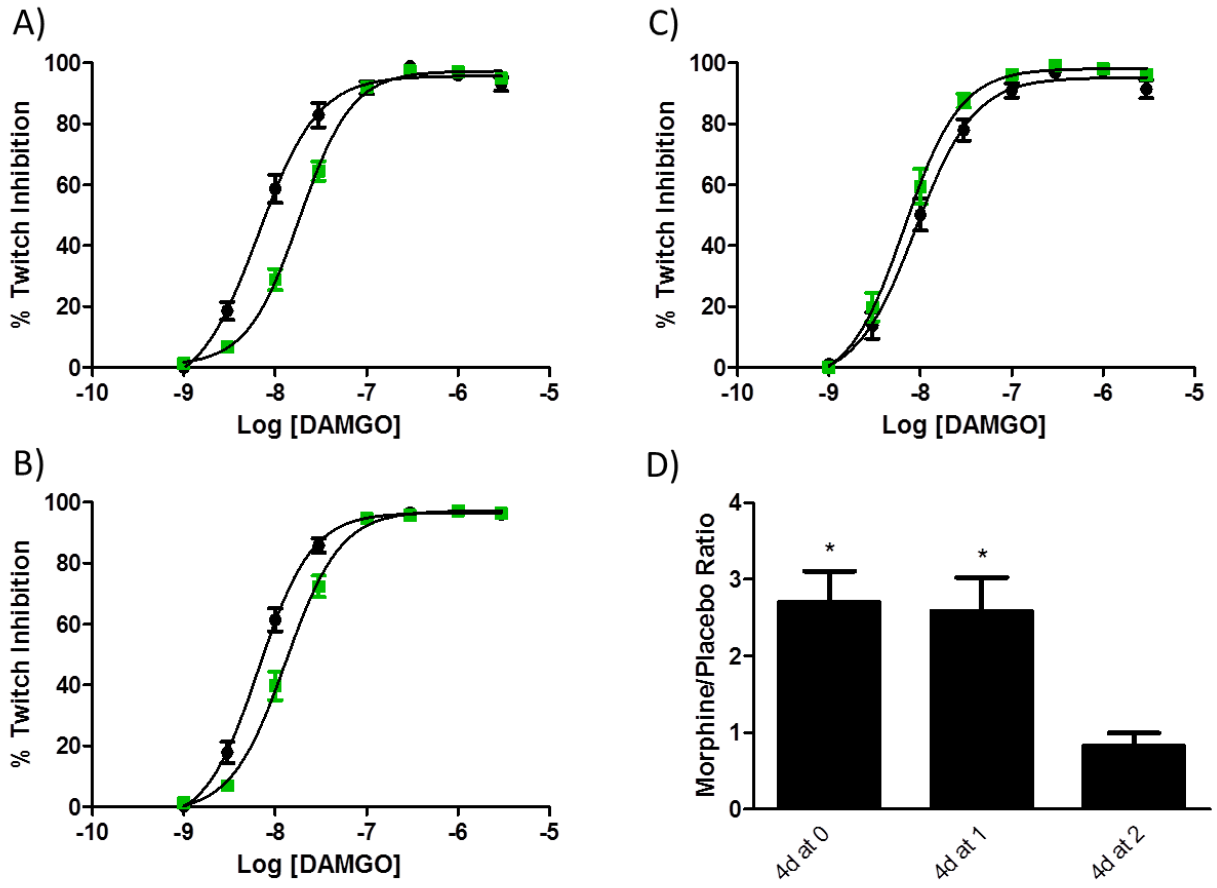
A)
% Twitch Inhibition
Log [DAMGO]
B)
% Twitch Inhibition
Log [DAMGO]
C)
% Twitch Inhibition
Log [DAMGO]
D)
Morphine/Placebo Ratio
4d at 0
4d at 1
4d at 2

Figure 4.8 Decay of Tolerance to DAMGO in the LM/MP of Guinea Pigs Treated for 7 Days

For all concentration response curves: green line = morphine treated group, black line = placebo treated group.

A) Average DAMGO concentration response curve for 7 day – 0 day animals (n = 5). The morphine to placebo ratio of the IC_{50} = 3.266 and was significantly different from 1 (p value = 0.0074).

B) Average DAMGO concentration response curve for 7 day – 1 day animals (n = 5). The morphine to placebo ratio of the IC_{50} = 1.952 and was not significantly different from 1 (p value = 0.0523).

C) Average DAMGO concentration response curve for 7 day – 2 day animals (n = 6). The morphine to placebo ratio of the IC_{50} = 1.563 and was significantly different from 1 (p value = 0.0179).

D) Average DAMGO concentration response curve for 7 day – 4 day animals (n = 5). The morphine to placebo ratio of the IC_{50} = 0.964 and was not significantly different from 1 (p value = 0.9104).

E) Summary bar graph of the morphine to placebo ratios of the IC_{50}s from the concentration response curves presented in A-D.

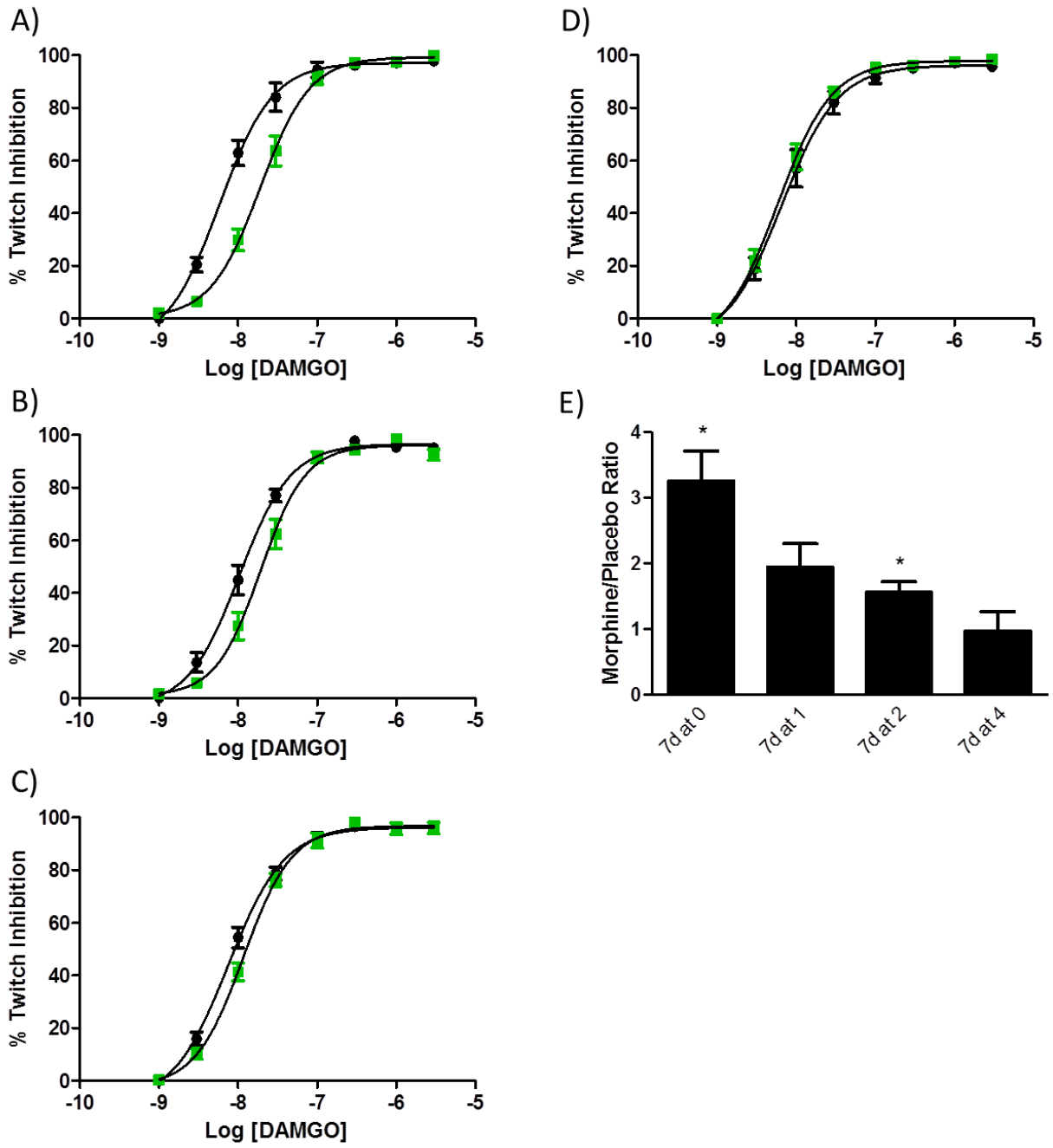
A)
% Twitch Inhibition
Log [DAMGO]
B)
% Twitch Inhibition
Log [DAMGO]
C)
% Twitch Inhibition
Log [DAMGO]
D)
% Twitch Inhibition
Log [DAMGO]
E)
Morphine/Placebo Ratio
7d at 0
7d at 1
7d at 2
7d at 4

Figure 4.9 Decay of Tolerance to DAMGO in the LM/MP of Guinea Pigs Treated for 10 Days

For all concentration response curves: green line = morphine treated group, black line = placebo treated group.

A) Average DAMGO concentration response curve for 10 day – 0 day animals (n = 4). The morphine to placebo ratio of the IC_{50} = 2.698 and was significantly different from 1 (p value = 0.0138).

B) Average DAMGO concentration response curve for 10 day – 1 day animals (n = 4). The morphine to placebo ratio of the IC_{50} = 1.693 and was significantly different from 1 (p value = 0.0098).

C) Average DAMGO concentration response curve for 10 day – 2 day animals (n = 5). The morphine to placebo ratio of the IC_{50} = 1.478 and was not significantly different from 1 (p value = 0.3284).

D) Average DAMGO concentration response curve for 10 day – 4 day animals (n = 5). The morphine to placebo ratio of the IC_{50} = 0.736 and was not significantly different from 1 (p value = 0.0559).

E) Summary bar graph of the morphine to placebo ratios of the IC_{50}s from the concentration response curves presented in A-D.

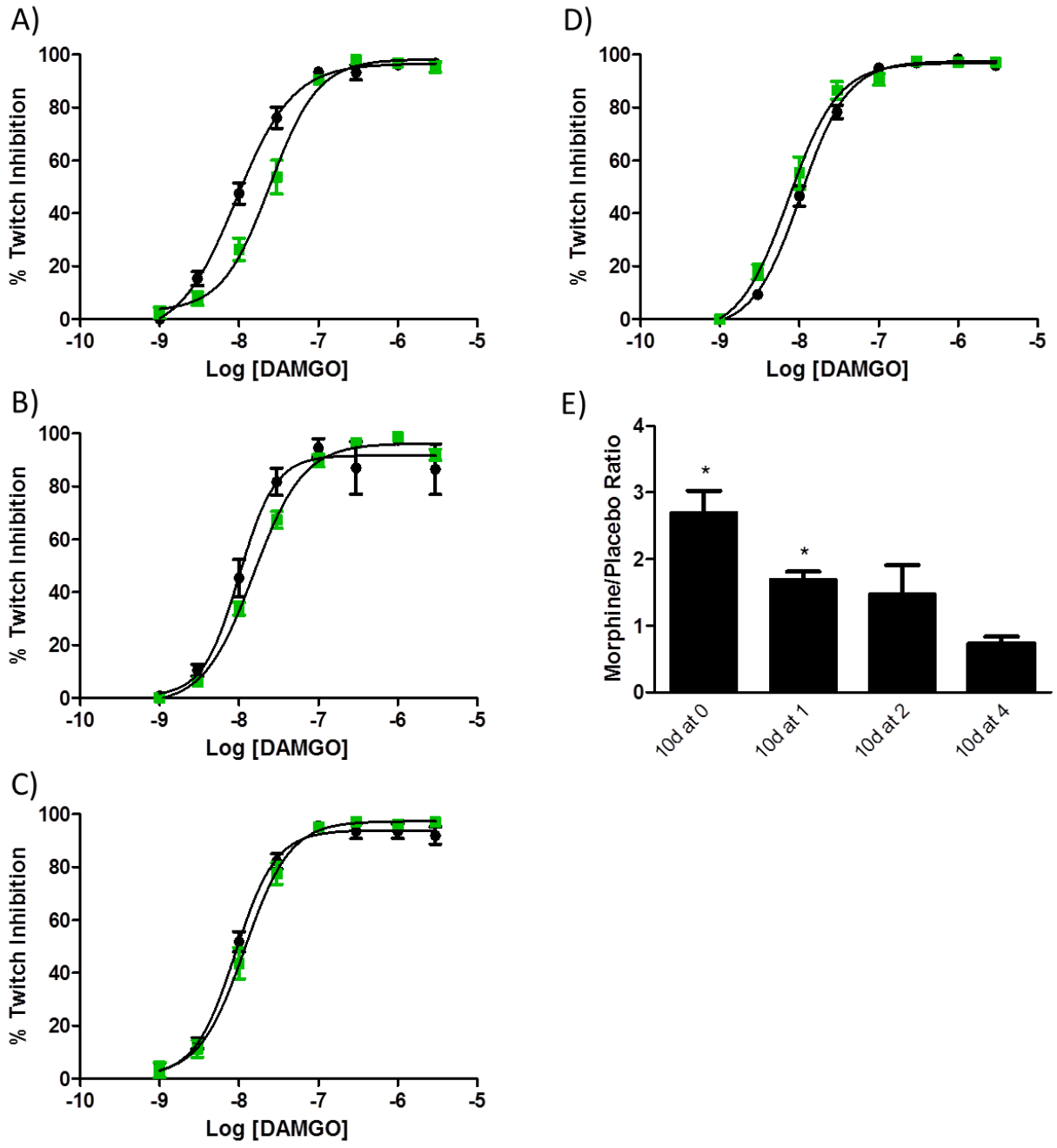
A)
% Twitch Inhibition
Log [DAMGO]
B)
% Twitch Inhibition
Log [DAMGO]
C)
% Twitch Inhibition
Log [DAMGO]
D)
% Twitch Inhibition
Log [DAMGO]
E)
Morphine/Placebo Ratio
10d at 0
10d at 1
10d at 2
10d at 4

Figure 4.10 Decay of Tolerance to 2-CADO in the LM/MP of Guinea Pigs Treated for 4 Days

For all concentration response curves: green line = morphine treated group, black line = placebo treated group.

A) Average 2-CADO concentration response curve for 4 day – 0 day animals (n = 6). The morphine to placebo ratio of the IC_{50} = 2.657 and was significantly different from 1 (p value = 0.0206).

B) Average 2-CADO concentration response curve for 4 day – 1 day animals (n = 6). The morphine to placebo ratio of the IC_{50} = 1.728 and was significantly different from 1 (p value = 0.0035).

C) Average 2-CADO concentration response curve for 4 day – 2 day animals (n = 5). The morphine to placebo ratio of the IC_{50} = 0.888 and was not significantly different from 1 (p value = 0.6116).

D) Summary bar graph of the morphine to placebo ratios of the IC_{50}s from the concentration response curves presented in A-C.

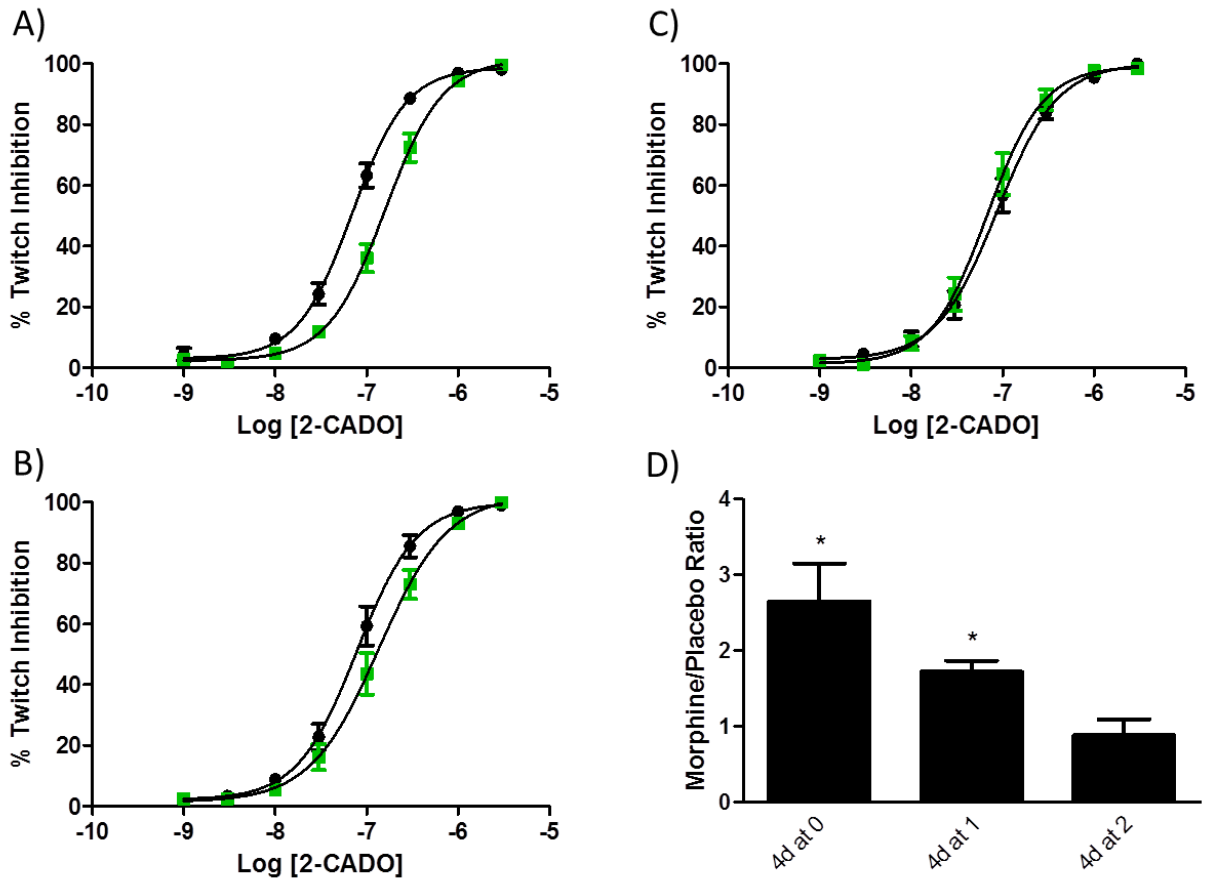
A)
% Twitch Inhibition
Log [2-CADO]
B)
% Twitch Inhibition
Log [2-CADO]
C)
% Twitch Inhibition
Log [2-CADO]
D)
Morphine/Placebo Ratio
4d at 0
4d at 1
4d at 2

Figure 4.11 Decay of Tolerance to 2-CADO in the LM/MP of Guinea Pigs Treated for 7 Days

For all concentration response curves: green line = morphine treated group, black line = placebo treated group.

A) Average 2-CADO concentration response curve for 7 day – 0 day animals (n = 5). The morphine to placebo ratio of the IC_{50} = 2.976 and was significantly different from 1 (p value = 0.0319).

B) Average 2-CADO concentration response curve for 7 day – 1 day animals (n = 5). The morphine to placebo ratio of the IC_{50} = 2.670 and was not significantly different from 1 (p value = 0.0627).

C) Average 2-CADO concentration response curve for 7 day – 2 day animals (n = 6). The morphine to placebo ratio of the IC_{50} = 1.662 and was not significantly different from 1 (p value = 0.1885).

D) Average 2-CADO concentration response curve for 7 day – 4 day animals (n = 5). The morphine to placebo ratio of the IC_{50} = 0.902 and was not significantly different from 1 (p value = 0.7748).

E) Summary bar graph of the morphine to placebo ratios of the IC_{50}s from the concentration response curves presented in A-D.

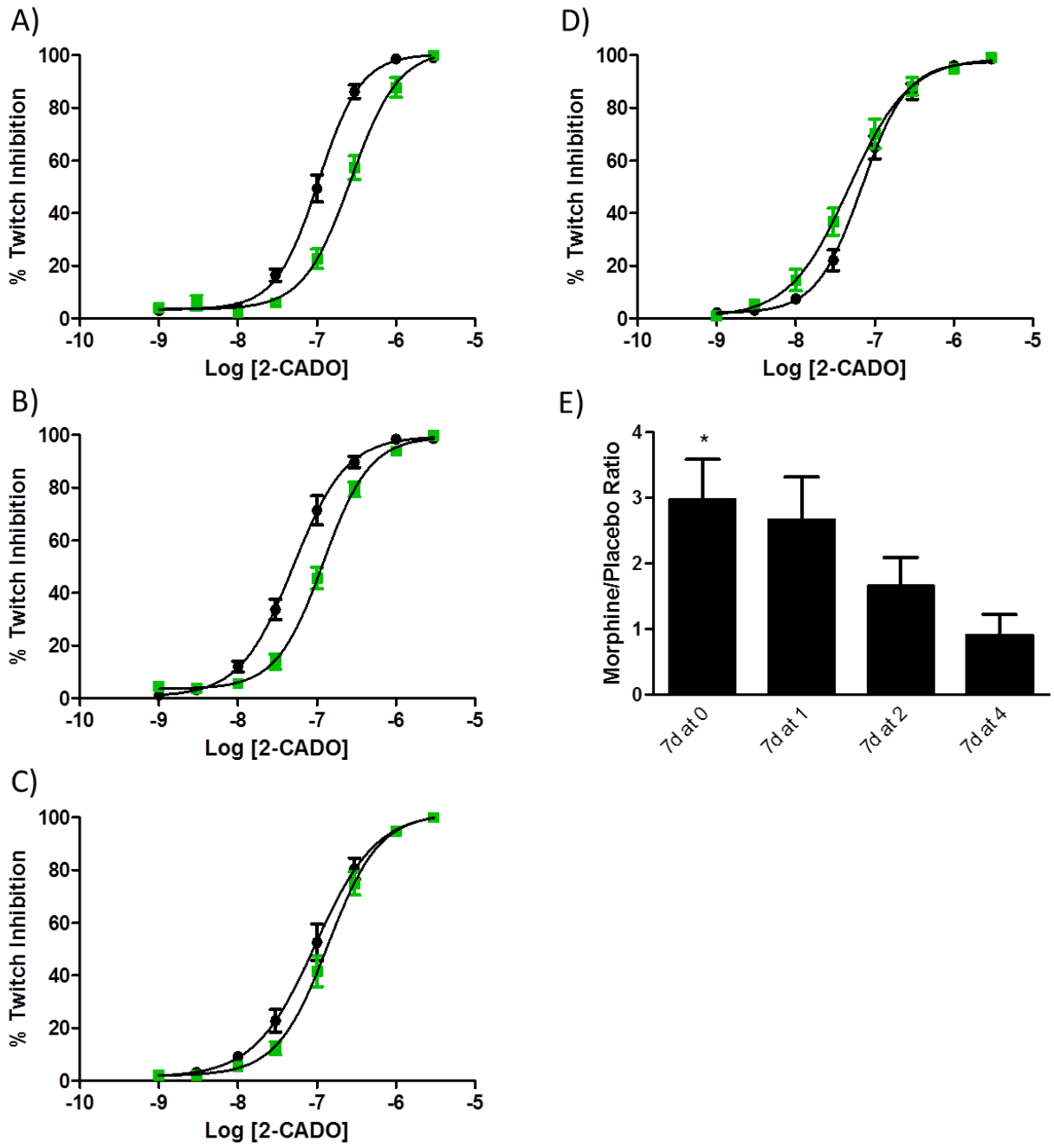
A)
% Twitch Inhibition
Log [2-CADO]
B)
% Twitch Inhibition
Log [2-CADO]
C)
% Twitch Inhibition
Log [2-CADO]
D)
% Twitch Inhibition
Log [2-CADO]
E)
Morphine/Placebo Ratio
*
7d at 0
7d at 1
7d at 2
7d at 4

Figure 4.12 Decay of Tolerance to 2-CADO in the LM/MP of Guinea Pigs Treated for 10 Days

For all concentration response curves: green line = morphine treated group, black line = placebo treated group.

A) Average 2-CADO concentration response curve for 10 day – 0 day animals (n = 4). The morphine to placebo ratio of the IC_{50} = 2.965 and was significantly different from 1 (p value = 0.0170).

B) Average 2-CADO concentration response curve for 10 day – 1 day animals (n = 4). The morphine to placebo ratio of the IC_{50} = 2.223 and was not significantly different from 1 (p value = 0.2595).

C) Average 2-CADO concentration response curve for 10 day – 2 day animals (n = 5). The morphine to placebo ratio of the IC_{50} = 1.210 and was not significantly different from 1 (p value = 0.4513).

D) Average 2-CADO concentration response curve for 10 day – 4 day animals (n = 5). The morphine to placebo ratio of the IC_{50} = 0.774 and was not significantly different from 1 (p value = 0.1709).

E) Summary bar graph of the morphine to placebo ratios of the IC_{50}s from the concentration response curves presented in A-D.

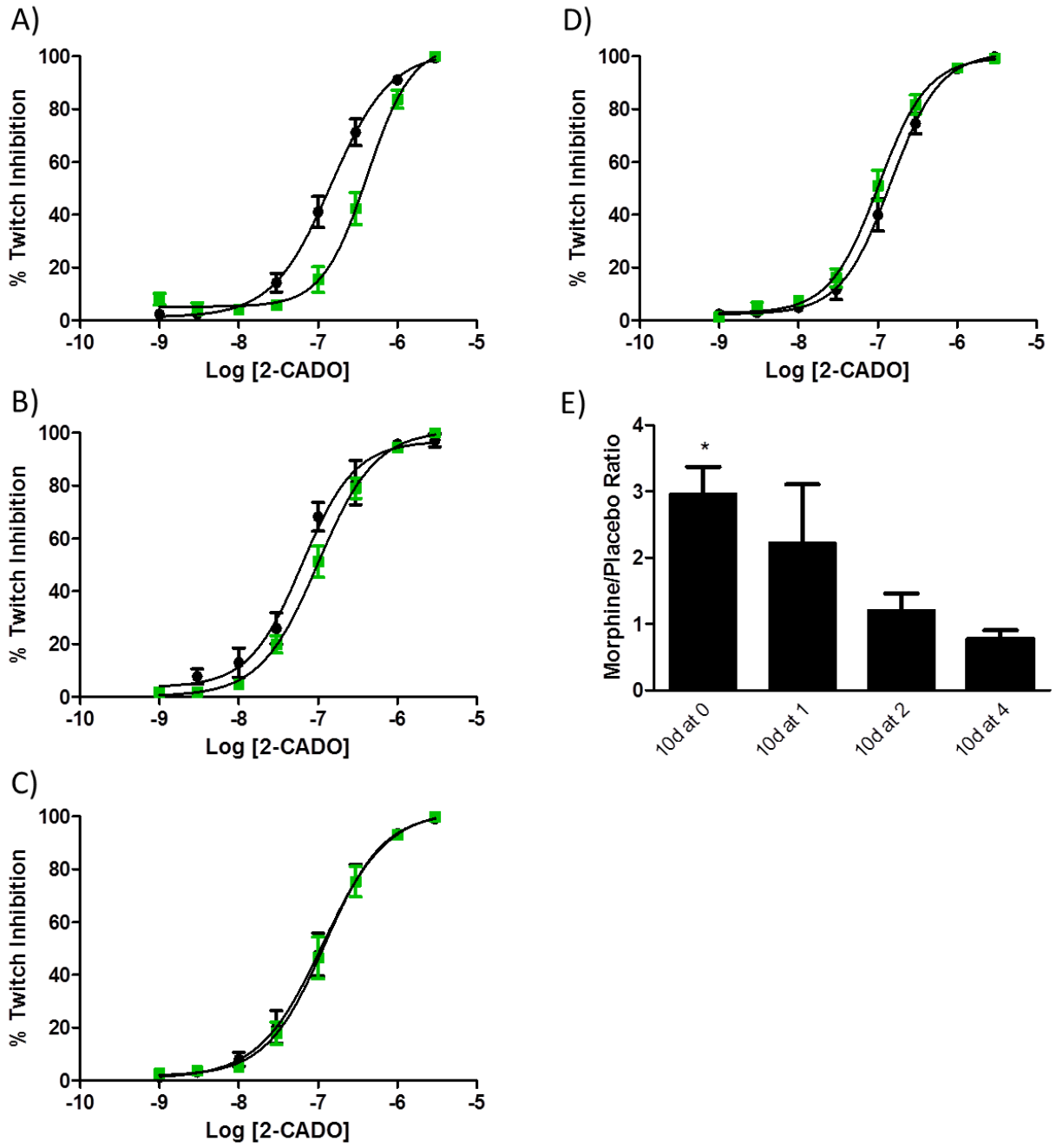
A)
% Twitch Inhibition
Log [2-CADO]
B)
% Twitch Inhibition
Log [2-CADO]
C)
% Twitch Inhibition
Log [2-CADO]
D)
% Twitch Inhibition
Log [2-CADO]
E)
Morphine/Placebo Ratio
*
10d at 0
10d at 1
10d at 2
10d at 4

CHAPTER FIVE: WESTERN BLOT ANALYSIS OF FACTORS ASSOCIATED WITH THE DEVELOPMENT AND DECAY OF TOLERANCE TO MORPHINE IN THE LM/MP AND BRAINSTEM

5.1 Abstract

The development of tolerance to morphine is thought to be a homeostatic response in the expression of one or more cellular signaling proteins produced by chronic activation of the receptor-activated signaling pathway. Any adaptive change should occur as tolerance to morphine develops and this change should reverse as tolerance decays. Previous work has developed a time course over which tolerance to morphine develops and decays in guinea pigs subcutaneously injected with escalating doses of morphine. Western blot analysis of LM/MP and brainstem homogenates from those animals was performed to assess the concentration of several receptors, subunits of the Na^+/K^+ ATPase, and two isoforms of PKC. This analysis revealed that the expression of the μ receptor, adenosine A_1 and A_{2a} receptors, and the α_{2b} adernergic receptor were unchanged by the development of tolerance in those tissues. This indicates that the heterologous tolerance that was observed in the LM/MP in chapter 4 is not simply due to receptor downregulation. The α_1 and β_1 subunits of the Na^+/K^+ ATPase were also unchanged in the brainstem as tolerance to morphine developed. Although not statistically significant, there was a trend for a decrease in the α_3 subunit of the Na^+/K^+ ATPase in the LM/MP, but not in the brainstem. This difference in adaptation may be due to the mechanisms by which those tissues develop tolerance or simply the fact that there are more neurons present in the brainstem that are not expected to respond to morphine than are present in the LM/MP. PKC_γ is not expressed by cells in the LM/MP, but it is present in the brainstem where there appears to be a trend for a decrease in expression as tolerance develops. PKC_ε follows a similar

trend in the brainstem, but not in the LM/MP. These data suggest that the mechanism(s) by which tolerance to morphine develops may be tissue dependent.

5.2 Introduction

The development of tolerance to opioids is thought to be a homeostatic adaptive response in one or more cellular signaling elements due to the continued presence of opioid agonist. It has been suggested that for any adaptive change to account for the observed changes in responsiveness there are five criteria that must be fulfilled (Taylor & Fleming, 2001). The second of these criteria states that the change must occur over a similar time course as the altered responsiveness. This second criteria has been the focus of work in this laboratory for the past several years. Results described in chapters 3 and 4 have provided a time course over which tolerance to morphine develops and decays to baseline as measured in the whole animal with paw pressure testing and ex vivo by measuring the responsiveness of the LM/MP to DAMGO and 2-CADO. Tissues collected from these animals were used to examine the concentration of several of the proteins that are thought to serve an integral role in the development of tolerance to morphine.

The μ receptor is an obvious protein of interest as it is the receptor that morphine acts on. Receptor down-regulation is one possible mechanism by which tolerance could develop upon chronic exposure to an agent. Indeed, such a mechanism has been described for other types of GPCRs (i.e. β adrenergic receptors). There are conflicting reports regarding the alteration in the number of μ receptors during the development of tolerance. Some authors report no change in receptor abundance during tolerance (De Vries, Tjon Tien Ril, Van der Laan, Mulder & Schoffelmeer, 1993; Klee & Streaty, 1974) while others have observed a down-regulation (Bernstein & Welch, 1998; Yoburn, Billings & Duttaroy, 1993). In contrast, other investigators

have reported an up-regulation (Fábián, Bozó, Szikszay, Horváth, Coscia & Szücs, 2002; Rothman et al., 1991). To evaluate whether or not the tolerance observed in the animals used for studies described in the previous chapters is due to a change in the receptor number or some other mechanism, western blot analysis was carried out on homogenates of the LM/MP and the brainstem.

This laboratory has used 2-CADO, an adenosine receptor agonist, as a marker of heterologous tolerance in the past. Like morphine and DAMGO, it causes inhibition of neurogenic twitches in the LM/MP by hyperpolarizing myenteric 'S' neurons (Meng, Malanga, Kong, Taylor & Fleming, 1997). However, unlike morphine it does not cause a change in input resistance, which would suggest that the mechanism by which this agent hyperpolarizes myenteric neurons is fundamentally different than that of morphine (Meng, Malanga, Kong, Taylor & Fleming, 1997). Of the adenosine receptors, 2-CADO has the highest affinity for the A_{2a} and the A_1 receptors (Mathoôt, Soudijn, Breimer, Ijzerman & Danhof, 1996). As mentioned previously, one potential mechanism to explain tolerance to an agonist is a down-regulation of the receptors for that agonist. As such, the adenosine A_1 and A_{2a} receptors were proteins of interest. Although they were not used in any of the experiments here, clonidine and xylazine, α_2 adrenergic receptor agonists, have been used in the past to demonstrate heterologous tolerance (Taylor, Leedham, Doak & Fleming, 1988). Therefore α_2 adrenergic receptors were also of interest.

There is evidence that suggests tolerance in the LM/MP is due to a partial depolarization of the resting membrane potential of myenteric neurons caused by a reduction in the electrogenic contribution of the Na^+/K^+ ATPase (see chapter 1.6.6). There is also evidence that suggests that there is a reduction of the expression of the Na^+/K^+ ATPase α_3 subunit that correlates to the onset

of tolerance in pellet implanted animals (Li, Maguma, Thayne, Davis & Taylor, 2010). There are two subunits to the pump with multiple isoforms of each subunit. The catalytic subunit is the α subunit while the β subunit is responsible for trafficking and insertion in the membrane. A reduction in either of these subunits could cause a reduction in the concentration and/or activity of the Na^+/K^+ ATPase. Because the α_1 and α_3 subunits were examined previously in pellet implanted animals and the α_3 subunit was shown to decrease, they were measured here following subcutaneous treatment (Li, Maguma, Thayne, Davis & Taylor, 2010). The β_1 subunit is most often paired with these two α subunits (Crambert et al., 2000), making it a protein of interest as well.

PKC is another protein that was suggested to play an integral role in opioid tolerance (see chapter 1.6.4). There are several isoforms of PKC, but only three were associated with morphine tolerance. PKC_γ is present only in neurons and is thought to mediate central nociception, while PKC_α and PKC_ε are found in the periphery and thought to mediate nociception there. Due to the limited amount of sample and that PKC_γ and PKC_ε were more heavily implicated in the literature as playing a role in the development of tolerance to morphine, these two isoforms were chosen for western blot analysis as well.

5.3 Experimental Protocol

All of the methods used here are detailed in chapter 2. Dunkin-Hartley guinea pigs were treated by subcutaneous injection with either morphine or saline on an escalating dose schedule for either 1, 2, 4, 7, or 10 days and then assessed for tolerance either 0, 1, 2, or 4 days after treatment as described in chapter 4.3. After paw pressure testing, the animals were euthanized and their tissues harvested and frozen in liquid nitrogen until western blot analysis could be performed. Thus, all tissues to be examined came from animals in which we had previously

obtained functional responses in the whole animal and in the LM/MP. All western blots were done with whole tissue homogenates of either LM/MP or brainstem. Homogenates were prepared by suspending the tissue in an appropriate amount of protease inhibitor buffer (see chapter 2.6.1) and homogenizing in a ground glass homogenizer until no visible chunks of tissue remained. The homogenate was then spun in a centrifuge for 5 seconds at maximum speed (14000 rpms). The supernatant was drawn off and spun again for 10 min at maximum speed at 4°C. The supernatant was then drawn off and aliquoted into microcentrifuge tubes. The samples were then stored at -20°C until they were used for western blot analysis.

Before each western blot, a BCA protein assay was performed to determine the amount of protein in each sample (see chapter 2.6.2). Briefly, serial dilutions of a standard protein (BSA) were loaded into a 96 well plate with a blank and the samples and then incubated with the BCA dye reagent for 15 minutes at 37°C. After this period the absorbance of each well was read at a wavelength of 562 nM using an Infinite M200 PRO plate reader (Tecan US, Research Triangle Park, NC). After this, calculation of the standard curve and interpolation of the concentration of protein in the samples was performed using Graph Pad Prism 5 software.

Following the BCA protein assay, the tissue homogenates were diluted 1:1 with working sample buffer (see chapter 2.7; Appendix D). The samples were then separated by gel electrophoresis, transferred to PVDF membranes, and probed for the housekeeper protein, GAPDH, and one of the following proteins: μ receptor, A_1 receptor, A_{2a} receptor, α_{2b} receptor, Na^+/K^+ ATPase α_1, Na^+/K^+ ATPase α_3, Na^+/K^+ ATPase β_1, PKC_γ, and PKC_ε (see Appendix E for antibody specifications and dilutions). The Odyssey CLX® near-infrared imaging system (Li-Cor Biosciences, Lincoln, NE) was used to visualize the proteins and the Image Studio 5.2 software was used to perform densitometry.

5.4 Experimental Results

The μ receptor, A_1 receptor, A_{2a} receptor, and α_{2b} receptors remained largely unchanged at any time point measured in either the LM/MP or the brainstem (see figures 5.1-5.7). These data indicate that the heterologous tolerance observed in these animals was not the result of receptor down-regulation in those tissues. To examine the possibility that changes in the expression of the Na^+/K^+ ATPase subunits may play a role in the development of tolerance to morphine the expression of the α_1, α_3, and β_1 subunits were measured in the brainstem and the α_3 subunit in the LM/MP. Consistent with previous studies from this laboratory (Li, Maguma, Thayne, Davis & Taylor, 2010), the α_1 subunit did not change in response to morphine treatment at any time point measured in the brainstem (see figure 5.8). Although the variability was too great to achieve statistical significance, there was approximately a 30% decrease in the amount of the α_3 subunit in the LM/MP after 7 days of treatment (see figure 5.9). This decrease in expression was not observed in the brainstem of those same animals (see figure 5.10). The β_1 subunit was also unaffected by morphine treatment of any duration in the brainstem (see figure 5.11). Since PKC_γ was not present in the LM/MP, the expression of this protein could not be measured. However, in the brainstem the protein was present and there was a general trend for a decrease in the expression of this protein (see figure 5.12). PKC_ε followed a similar trend in the brainstem. In contrast, in the LM/MP, the expression of this protein appeared to trend toward an increase in expression as treatment length increases (see figures 5.13 and 5.14).

5.5 Discussion

One of the more common mechanisms that could account for the development of tolerance to an agonist is down-regulation of its receptor. This has been described for a number of other GPCRs and because there were conflicting results in the literature regarding changes in the

number of μ receptors during the development of tolerance, we measured the receptor population using western blot analysis in both the LM/MP, a tissue in which we had functional data to indicate tolerance, and in the brainstem, a brain structure that contains circuits that mediate the antinociceptive effect of morphine. The data show that not only was there no change in the μ receptor in those tissues obtained from tolerant animals, there was also no change in adenosine A_1 and A_{2a} receptors or in the α_{2b} receptor populations. The adenosine agonist 2-CADO has been used previously in this laboratory to demonstrate the development of heterologous tolerance (Barrett, Maguma & Taylor, 2011; Li, Maguma, Thayne, Davis & Taylor, 2010; Meng, Malanga, Kong, Taylor & Fleming, 1997). Although activation of μ, A_1, and α_2 receptors hyperpolarize myenteric neurons, their mechanisms of action differ. For example, this laboratory has previously shown that the hyperpolarizing effect of 2-CADO, unlike that of morphine, occurs without a change in input resistance, which would suggest that the mechanism by which 2-CADO changes membrane potential does not involve activation of ion channels (Meng, Malanga, Kong, Taylor & Fleming, 1997). The fact that the change in responsiveness to DAMGO and 2-CADO was nearly equivalent in magnitude without any change in the receptor populations would suggest that the cellular mechanism responsible for the change in responsiveness must involve some factor that has the capacity to affect the overall responsiveness of the cell and/or tissue to multiple stimuli rather than a change in the receptor populations.

It was observed in the 1970s that the LM/MP from morphine tolerant guinea pigs were subsensitive to inhibitory stimuli and supersensitive to excitatory stimuli (Schulz & Goldstein, 1973). This observation was proposed to be due to an adaptive partial depolarization of the myenteric neurons that were acted upon by morphine (Fleming, 1999). Such a depolarization

has since been observed in myenteric 'S' neurons that were activated by morphine but not those that were unaffected by the agonist. Furthermore, no change in the threshold for action potential generation or in the magnitude of the hyperpolarizing effects of morphine and 2-CADO were observed (Leedham, Kong, Taylor, Johnson & Fleming, 1992; Meng, Malanga, Kong, Taylor & Fleming, 1997). A decrease in the electrogenic contribution of the Na^+/K^+ ATPase to membrane potential has been previously reported by this laboratory to coincide with those changes (Kong, Leedham, Taylor & Fleming, 1997). This decrease in Na^+/K^+ ATPase activity was reported to be due to a decrease in the abundance of the α_3 subunit of this protein (Biser, Thayne, Fleming & Taylor, 2002). Because these observations were made in pellet implanted animals, we examined the expression of several subunits of the Na^+/K^+ ATPase in homogenates of LM/MP and brainstem of subcutaneously injected animals. Consistent with previous observations in the LM/MP, the α_1 subunit did not change in abundance as tolerance developed (Li, Maguma, Thayne, Davis & Taylor, 2010). Although we did not see a statistically significant change in the abundance of the α_3 subunit, we did see an approximate 30% decrease in the expression in the LM/MP, which is consistent with the magnitude of the reduction observed in previous studies from both this laboratory and others (Gonzalez et al., 2012; Li, Maguma, Thayne, Davis & Taylor, 2010). Interestingly, this decrease was not observed in the brainstem. This could be due to some difference in the way that the brainstem develops tolerance when compared to the LM/MP. Since the α_3 subunit is specifically expressed in neurons and there is a much larger population of neurons in the brainstem, not all of which respond to morphine, a decrease in the abundance of this subunit could be masked simply because there is a comparatively larger proportion of neurons that are expected to not respond to morphine treatment in the brainstem. This analysis was performed in whole brainstem homogenates, thus a more precise examination

of specific brainstem nuclei (i.e. periaqueductal gray, etc.) that are involved with nociception may yield a result more consistent with the LM/MP data. A decrease in Na^+/K^+ ATPase activity could also be due to changes in the number of β subunits as well as α subunits. Because the α_3 subunit most often pairs with the β_1 subunit (Crambert et al., 2000), the β_1 subunit was examined in the brainstem. There was no change in the level of β_1 subunit in the brainstem, a result that suggests the development of tolerance to morphine does not induce a change in membrane trafficking of the Na^+/K^+ ATPase in the brainstem.

PKC_γ and PKC_ε have been reported to increase following chronic morphine treatment (see chapter 1.6.4). Additionally, inhibition of either isoform of PKC prior to prolonged morphine treatment results in the mitigation of tolerance and administering inhibitors after treatment reverses the tolerance that has developed. Consistent with previous reports in the literature, PKC_γ was not detected in the LM/MP (Aley & Levine, 1997). However, PKC_ε was detected in both the LM/MP and the brainstem. Although not statistically significant, there did appear to be a trend for an increase in PKC_ε levels in the LM/MP. There was not a significant change detected for several time points in the brainstem. However, a general trend for a decrease in the expression of PKC_γ and PKC_ε in the brainstem as tolerance to morphine develops was observed. These data are not consistent with most of the literature that reports an increase in these two proteins with the development of tolerance to morphine. Similar to what was observed with the α_3 subunit of the Na^+/K^+ ATPase in the brainstem, this observation may be due to the fact that the homogenate was obtained from the entire brainstem as opposed to specific neuronal areas which were used by many of the other authors. It may be the case that in specific areas associated with nociception PKC is increased with morphine treatment, but in other regions a

different set of adaptations is occurring that results in a decrease in PKC levels. Despite the contradiction with the literature, the data indicate that PKC may be worth further investigation.

This study examined the expression of several proteins that were thought to be involved in the development of tolerance. Based on this protein analysis, we confirmed that the heterologous tolerance observed in the LM/MP is not due to receptor downregulation as none of the receptors measured changed significantly at any time point. The α_3 subunit of the Na^+/K^+ ATPase trended towards a decrease in the LM/MP, but not the brainstem, as tolerance to morphine develops whereas the α_1 and β_1 subunits were unchanged. PKC_γ and PKC_ε trended towards a decrease as tolerance develops in the brainstem, but not in the LM/MP. As such, the role of both, the Na^+/K^+ ATPase and PKC, should be further explored in the context of opioid tolerance.

Figure 5.1 μ Receptor Abundance in LM/MP Homogenates

A) This table contains the average morphine to placebo ratio of the densitometric units (normalized to GAPDH) of the μ receptor in the LM/MP. It also contains the p and n values for each group. The only statistically significant change was observed in the 4 day – 1 day animals, but it may have little biological significance.

B) This presents the average morphine to placebo ratio of densitometric units (normalized to GAPDH) of the μ receptor in the LM/MP expressed in a bar graph.

A)

Length of Treatment	Time After Treatment	μ Receptor in the LM/MP M/P Ratios (Std. Error)	P values	n=
1 day	0 days	0.95 (0.101)	0.6713	4
2 days	0 days	0.93 (0.082)	0.4481	4
4 days	0 days	1.21 (0.119)	0.1695	4
	1 day	0.84 (0.037)*	0.0219	4
	2 days	0.82 (0.111)	0.2126	4
7 days	0 days	1.31 (0.250)	0.2974	4
	1 day	0.97 (0.111)	0.8050	4
	2 days	1.08 (0.400)	0.8600	3
	4 days	1.11 (0.105)	0.3692	4
10 days	0 days	1.01 (0.134)	0.9658	3
	1 day	0.92 (0.098)	0.4928	4
	2 days	0.87 (0.086)	0.2313	4
	4 days	1.22 (0.118)	0.1629	4

B)

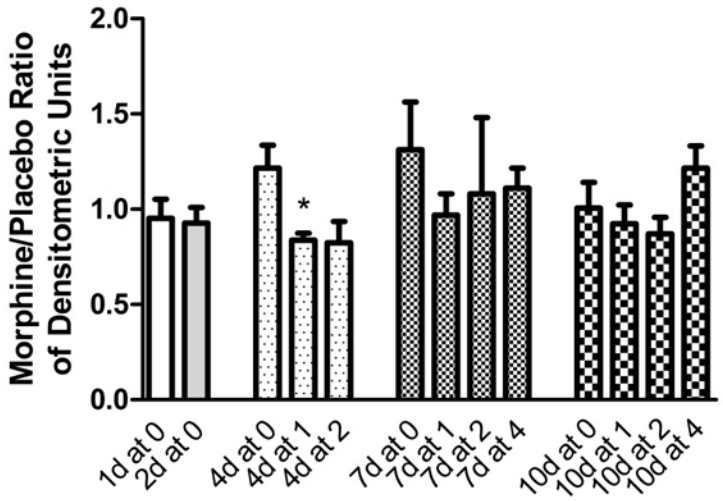

Figure 5.2 μ Receptor Abundance in Brainstem Homogenates

A) This table contains the average morphine to placebo ratio of the densitometric units (normalized to GAPDH) of the μ receptor in the brainstem. It also contains the p and n values for each group. No ratio was statistically significantly different from unity.

B) This presents the average morphine to placebo ratio of densitometric units (normalized to GAPDH) of the μ receptor in the brainstem expressed in a bar graph.

A)

Length of Treatment	Time After Treatment	μ Receptor in the Brainstem M/P Ratios (Std. Error)	P values	n=
1 day	0 days	0.96 (0.789)	0.6910	3
2 days	0 days	0.97 (0.131)	0.8198	3
4 days	0 days	0.84 (0.081)	0.1960	3
	1 day	0.90 (0.103)	0.4441	3
	2 days	0.85 (0.145)	0.3989	3
7 days	0 days	1.27 (0.158)	0.2359	3
	1 day	0.96 (0.147)	0.8069	3
	2 days	0.99 (0.070)	0.8584	3
	4 days	0.90 (0.045)	0.1515	3
10 days	0 days	1.32 (0.229)	0.4026	3
	1 day	0.92 (0.048)	0.2561	3
	2 days	0.86 (0.048)	0.1010	3
	4 days	0.78 (0.189)	0.3653	3

B)

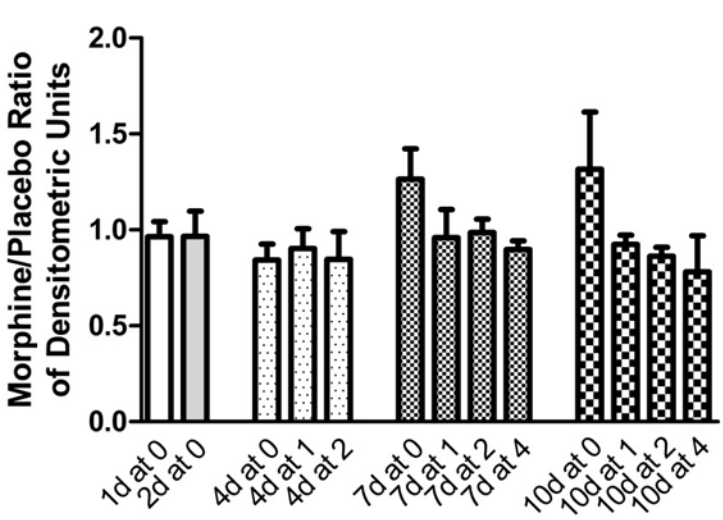

Figure 5.3 A_1 Receptor Abundance in LM/MP Homogenates

A) This table contains the average morphine to placebo ratio of the densitometric units (normalized to GAPDH) of the A_1 receptor in the LM/MP. It also contains the p and n values for each group. The only statistically significant change was observed in the 4 day – 0 day animals, but it may have little biological significance.

B) This presents the average morphine to placebo ratio of densitometric units (normalized to GAPDH) of the A_1 receptor in the LM/MP expressed in a bar graph.

A)

Length of Treatment	Time After Treatment	A_1 Receptor in the LM/MP M/P Ratios (Std. Error)	P values	n=
1 day	0 days	1.12 (0.204)	0.6001	5
2 days	0 days	1.47 (0.223)	0.1046	5
4 days	0 days	1.42 (0.099)*	0.0082	6
	1 day	1.48 (0.187)	0.0520	6
	2 days	1.01 (0.199)	0.9599	5
7 days	0 days	1.63 (0.221)	0.0646	4
	1 day	1.03 (0.234)	0.9128	5
	2 days	1.08 (0.221)	0.7459	4
	4 days	1.10 (0.284)	0.7443	5
10 days	0 days	1.72 (0.283)	0.0643	5
	1 day	1.15 (0.136)	0.3438	5
	2 days	1.25 (0.274)	0.4063	5
	4 days	1.09 (0.180)	0.6300	5

B)

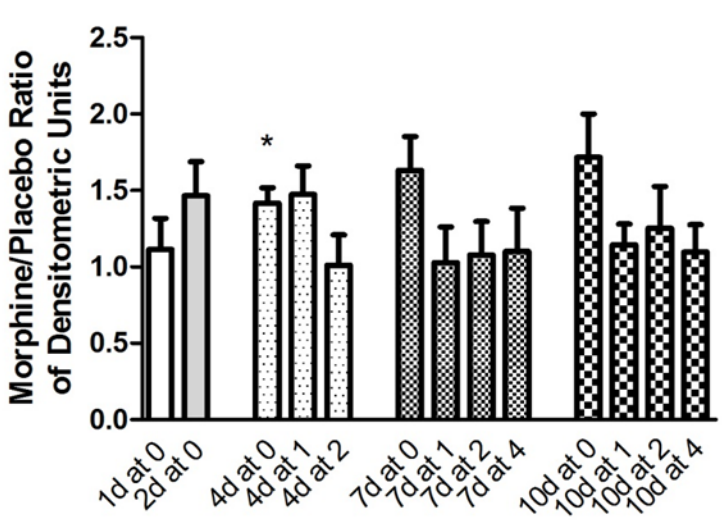

Figure 5.4 A_1 Receptor Abundance in Brainstem Homogenates

A) This table contains the average morphine to placebo ratio of the densitometric units (normalized to GAPDH) of the A_1 receptor in the brainstem. It also contains the p and n values for each group. The only statistically significant change was observed in the 10 day – 4 day animals, but it may have little biological significance.

B) This presents the average morphine to placebo ratio of densitometric units (normalized to GAPDH) of the A_1 receptor in the brainstem expressed in a bar graph.

A)

Length of Treatment	Time After Treatment	A_1 Receptor in the Brainstem M/P Ratios (Std. Error)	P values	n=
1 day	0 days	0.86 (0.093)	0.2831	3
2 days	0 days	0.84 (0.200)	0.4966	3
4 days	0 days	0.86 (0.230)	0.6083	3
	1 day	0.88 (0.067)	0.2062	3
	2 days	0.79 (0.060)	0.0717	3
7 days	0 days	0.89 (0.259)	0.7087	3
	1 day	1.07 (0.113)	0.5817	3
	2 days	1.18 (0.366)	0.6723	3
	4 days	0.92 (0.076)	0.3884	3
10 days	0 days	0.80 (0.081)	0.1288	3
	1 day	0.97 (0.107)	0.7947	3
	2 days	0.82 (0.109)	0.2350	3
	4 days	0.80 (0.045)*	0.0473	3

B)

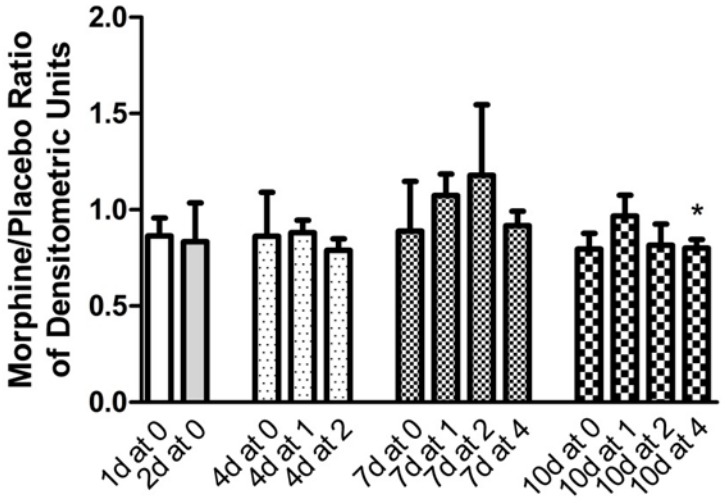

Figure 5.5 A_{2a} Receptor Abundance in LM/MP Homogenates

A) This table contains the average morphine to placebo ratio of the densitometric units (normalized to GAPDH) of the A_{2a} receptor in the LM/MP. It also contains the p and n values for each group. The only statistically significant change was observed in the 10 day – 0 day animals, but it may have little biological significance.

B) This presents the average morphine to placebo ratio of densitometric units (normalized to GAPDH) of the A_{2a} receptor in the LM/MP expressed in a bar graph.

A)

Length of Treatment	Time After Treatment	A_{2a} Receptor in the LM/MP M/P Ratios (Std. Error)	P values	n=
1 day	0 days	1.00 (0.100)	0.9816	4
2 days	0 days	0.91 (0.134)	0.5521	4
4 days	0 days	1.17 (0.191)	0.4412	4
	1 day	0.88 (0.068)	0.1960	4
	2 days	0.94 (0.146)	0.7231	4
7 days	0 days	0.95 (0.133)	0.7086	4
	1 day	1.41 (0.436)	0.4217	4
	2 days	1.10 (0.275)	0.7546	3
	4 days	1.02 (0.151)	0.9191	4
10 days	0 days	0.69 (0.090)*	0.0404	4
	1 day	0.90 (0.119)	0.4801	4
	2 days	0.94 (0.095)	0.5533	4
	4 days	2.15 (0.379)	0.0565	4

B)

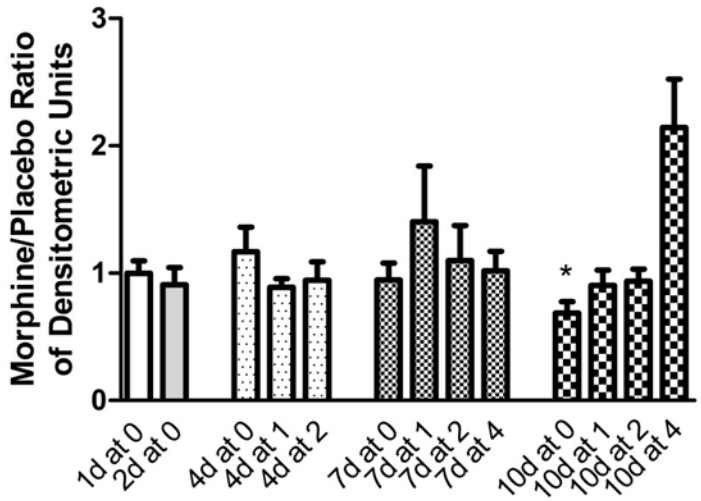

Figure 5.6 A_{2a} Receptor Abundance in Brainstem Homogenates

A) This table contains the average morphine to placebo ratio of the densitometric units (normalized to GAPDH) of the A_{2a} receptor in the brainstem. It also contains the p and n values for each group. The only statistically significant changes were observed in the 1 day – 0 day and 2 day – 0 day animals, but those changes may have little biological significance.

B) This presents the average morphine to placebo ratio of densitometric units (normalized to GAPDH) of the A_{2a} receptor in the brainstem expressed in a bar graph.

A)

Length of Treatment	Time After Treatment	A_{2a} Receptor in the Brainstem M/P Ratios (Std. Error)	P values	n=
1 day	0 days	1.15 (0.010)*	0.0438	2
2 days	0 days	0.94 (0.003)*	0.0277	2
4 days	0 days	1.43 (0.000)	-	1
	1 day	0.91 (0.050)	0.3228	2
	2 days	0.75 (0.115)	0.2697	2
7 days	0 days	1.05 (0.195)	0.8556	2
	1 day	1.20 (0.140)	0.3888	2
	2 days	1.01 (0.195)	0.9837	2
	4 days	0.94 (0.015)	0.1444	2
10 days	0 days	1.23 (0.108)	0.2757	2
	1 day	1.21 (0.250)	0.5552	2
	2 days	0.95 (0.020)	0.2422	2
	4 days	1.25 (0.050)	0.1257	2

B)

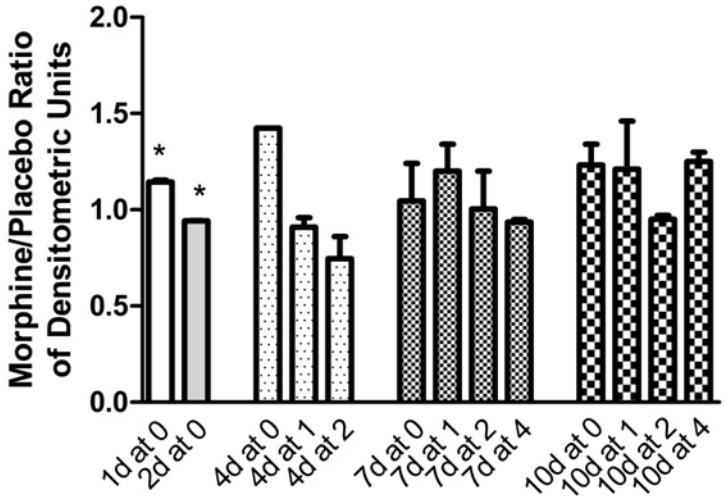

Figure 5.7 α_{2b} Receptor Abundance in Brainstem Homogenates

A) This table contains the average morphine to placebo ratio of the densitometric units (normalized to GAPDH) of the α_{2b} receptor in the brainstem. It also contains the p and n values for each group. The only statistically significant change was observed in the 4 day – 0 day but that change may have little biological significance.

B) This presents the average morphine to placebo ratio of densitometric units (normalized to GAPDH) of the α_{2b} receptor in the brainstem expressed in a bar graph.

A)

Length of Treatment	Time After Treatment	α_{2b} Receptor in the Brainstem M/P Ratios (Std. Error)	P values	n=
1 day	0 days	0.82 (0.167)	0.4005	3
2 days	0 days	0.77 (0.077)	0.1005	3
4 days	0 days	0.78 (0.030)*	0.0185	3
	1 day	1.05 (0.199)	0.8197	3
	2 days	0.97 (0.118)	0.8223	3
7 days	0 days	1.07 (0.146)	0.6837	3
	1 day	1.25 (0.186)	0.3084	3
	2 days	0.85 (0.078)	0.1940	3
	4 days	0.91 (0.073)	0.3643	3
10 days	0 days	1.04 (0.160)	0.8254	3
	1 day	1.21 (0.260)	0.5047	3
	2 days	0.63 (0.087)	0.0513	3
	4 days	0.95 (0.111)	0.6872	3

B)

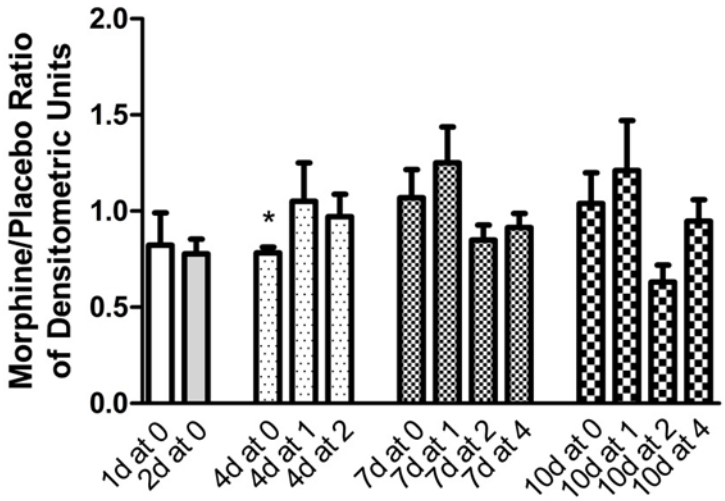

Figure 5.8 Na^+/K^+ ATPase α_1 Subunit Abundance in Brainstem Homogenates

A) This table contains the average morphine to placebo ratio of the densitometric units (normalized to GAPDH) of the Na^+/K^+ ATPase α_1 subunit in the brainstem. It also contains the p and n values for each group.

B) This presents the average morphine to placebo ratio of densitometric units (normalized to GAPDH) of the Na^+/K^+ ATPase α_1 subunit in the brainstem expressed in a bar graph.

A)

Length of Treatment	Time After Treatment	Na^+/K^+ ATPase α_1 in the Brainstem M/P Ratios (Std. Error)	P values	n=
1 day	0 days	1.38 (0.287)	0.3183	3
2 days	0 days	0.65 (0.215)	0.2418	3
4 days	0 days	1.26 (0.220)	0.3578	3
	1 day	0.80 (0.166)	0.3502	3
	2 days	0.87 (0.316)	0.7227	3
7 days	0 days	0.98 (0.167)	0.9106	3
	1 day	1.60 (0.505)	0.3599	3
	2 days	1.41 (0.310)	0.3138	3
	4 days	0.95 (0.119)	0.7244	3
10 days	0 days	1.25 (0.080)	0.0891	3
	1 day	2.20 (0.982)	0.3451	3
	2 days	1.34 (0.261)	0.3207	3
	4 days	1.10 (0.150)	0.5774	3

B)

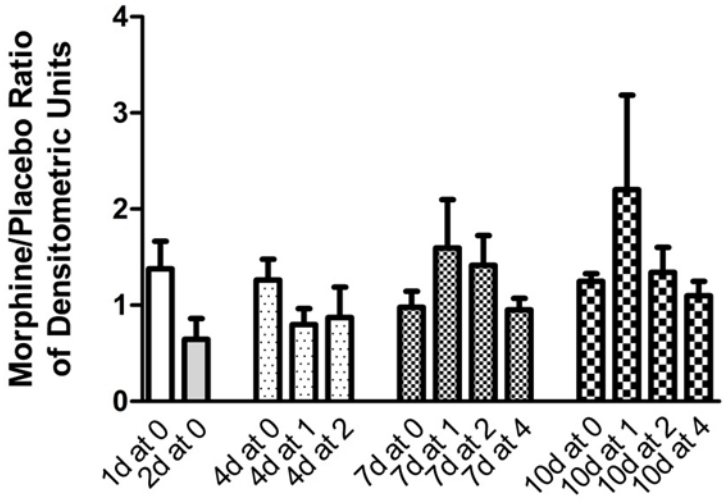

Figure 5.9 Na^+/K^+ ATPase α_3 Subunit Abundance in LM/MP Homogenates

A) This table contains the average morphine to placebo ratio of the densitometric units (normalized to GAPDH) of the Na^+/K^+ ATPase α_3 subunit in the LM/MP. It also contains the p and n values for each group. Only the 4 day – 2 day animals displayed a significant decrease in the abundance of this protein.

B) This presents the average morphine to placebo ratio of densitometric units (normalized to GAPDH) of the Na^+/K^+ ATPase α_3 subunit in the LM/MP expressed in a bar graph.

A)

Length of Treatment	Time After Treatment	Na^+/K^+ ATPase α_3 in the LM/MP M/P Ratios (Std. Error)	P values	n=
1 day	0 days	1.07 (0.111)	0.5629	6
2 days	0 days	1.07 (0.104)	0.5121	6
4 days	0 days	0.95 (0.068)	0.5055	6
	1 day	0.86 (0.067)	0.0985	6
	2 days	0.59 (0.097)*	0.0128	5
7 days	0 days	0.71 (0.133)	0.0944	5
	1 day	1.14 (0.450)	0.7661	5
	2 days	0.73 (0.103)	0.0570	5
	4 days	0.90 (0.215)	0.6804	5
10 days	0 days	0.99 (0.257)	0.9618	5
	1 day	0.85 (0.152)	0.3698	5
	2 days	1.29 (0.178)	0.1810	5
	4 days	1.04 (0.174)	0.8319	5

B)

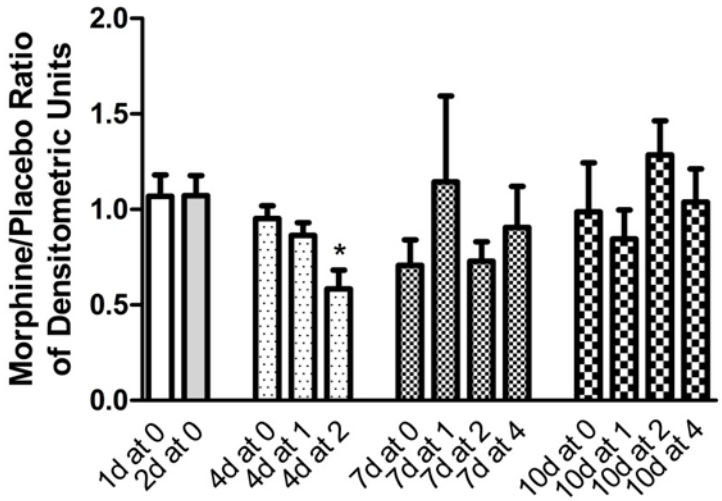

Figure 5.10 Na^+/K^+ ATPase α_3 Subunit Abundance in Brainstem Homogenates

A) This table contains the average morphine to placebo ratio of the densitometric units (normalized to GAPDH) of the Na^+/K^+ ATPase α_3 subunit in the brainstem. It also contains the p and n values for each group. The 2 day – 0 day and 4 day – 1 day animals displayed a significant decrease in the abundance of this protein.

B) This presents the average morphine to placebo ratio of densitometric units (normalized to GAPDH) of the Na^+/K^+ ATPase α_3 subunit in the brainstem expressed in a bar graph.

A)

Length of Treatment	Time After Treatment	Na^+/K^+ ATPase α_3 in the Brainstem M/P Ratios (Std. Error)	P values	n=
1 day	0 days	1.15 (0.169)	0.4629	3
2 days	0 days	0.81 (0.032)*	0.0289	3
4 days	0 days	1.08 (0.124)	0.5953	3
	1 day	0.91 (0.018)*	0.0421	3
	2 days	0.88 (0.074)	0.2601	3
7 days	0 days	1.02 (0.009)	0.1549	3
	1 day	1.12 (0.045)	0.1203	3
	2 days	1.17 (0.139)	0.3471	3
	4 days	0.93 (0.076)	0.4563	3
10 days	0 days	0.88 (0.152)	0.5021	3
	1 day	1.06 (0.140)	0.6899	3
	2 days	1.14 (0.087)	0.2421	3
	4 days	1.03 (0.094)	0.7608	3

B)

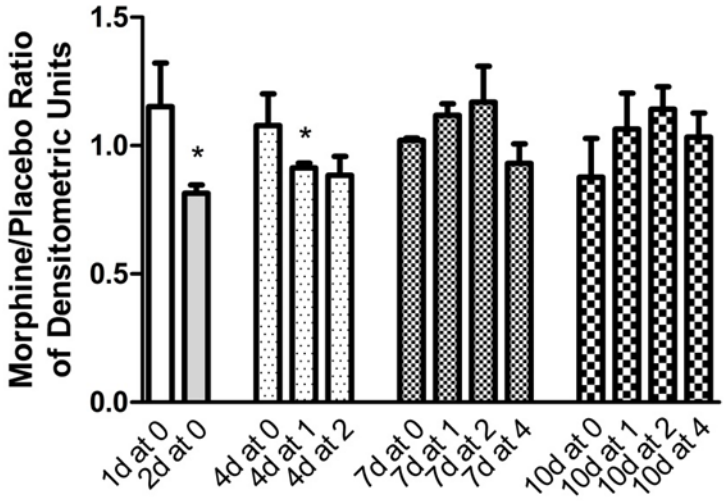

Figure 5.11 Na^+/K^+ ATPase β_1 Subunit Abundance in Brainstem Homogenates

A) This table contains the average morphine to placebo ratio of the densitometric units (normalized to GAPDH) of the Na^+/K^+ ATPase β_1 subunit in the brainstem. It also contains the p and n values for each group. There were statistically significant increases in the abundance of this protein in the 4 day – 0 day and 10 day – 0 day animals.

B) This presents the average morphine to placebo ratio of densitometric units (normalized to GAPDH) of the Na^+/K^+ ATPase β_1 subunit in the brainstem expressed in a bar graph.

A)

Length of Treatment	Time After Treatment	Na^+/K^+ ATPase β_1 in the Brainstem M/P Ratios (Std. Error)	P values	n=
1 day	0 days	0.98 (0.031)	0.5799	3
2 days	0 days	1.00 (0.032)	0.9634	3
4 days	0 days	1.13 (0.020)*	0.0215	3
	1 day	0.90 (0.040)	0.1226	3
	2 days	0.99 (0.778)	0.9254	3
7 days	0 days	0.96 (0.025)	0.2510	3
	1 day	1.04 (0.043)	0.4601	3
	2 days	0.96 (0.078)	0.6692	3
	4 days	1.08 (0.102)	0.5131	3
10 days	0 days	1.14 (0.029)*	0.0420	3
	1 day	1.02 (0.080)	0.8269	3
	2 days	0.80 (0.053)	0.0655	3
	4 days	1.06 (0.078)	0.5011	3

B)

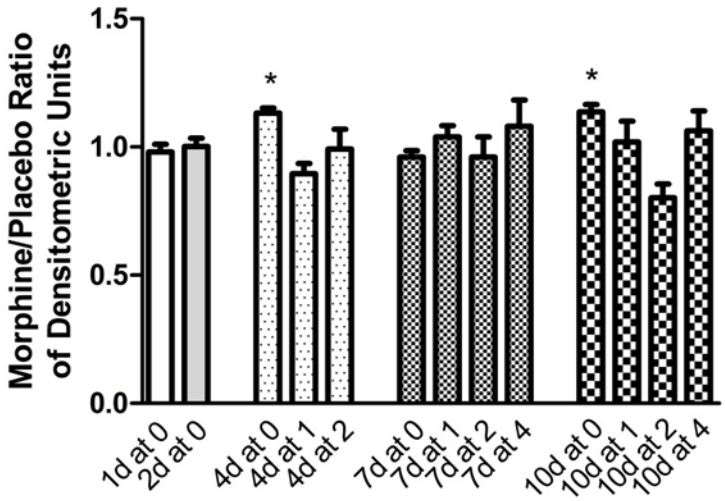

Figure 5.12 PKC_{γ} Abundance in Brainstem Homogenates

A) This table contains the average morphine to placebo ratio of the densitometric units (normalized to GAPDH) of PKC_{γ} in the brainstem. It also contains the p and n values for each group. There were statistically significant decreases in the abundance of this protein in the 1 day – 0 day, 7 day – 2 day, and 7 day – 4 day animals. There is also a general trend for a decrease across all time points.

B) This presents the average morphine to placebo ratio of densitometric units (normalized to GAPDH) of PKC_{γ} in the brainstem expressed in a bar graph.

A)

Length of Treatment	Time After Treatment	PKC$_\gamma$ in the Brainstem M/P Ratios (Std. Error)	P values	n=
1 day	0 days	0.55 (0.085)*	0.0129	4
2 days	0 days	0.88 (0.136)	0.4433	4
4 days	0 days	0.85 (0.129)	0.3005	5
	1 day	0.76 (0.116)	0.1076	5
	2 days	0.97 (0.248)	0.8998	5
7 days	0 days	0.74 (0.181)	0.2219	5
	1 day	0.66 (0.275)	0.2876	4
	2 days	0.64 (0.092)*	0.0299	4
	4 days	0.63 (0.028)*	0.0009	4
10 days	0 days	0.60 (0.201)	0.1426	4
	1 day	1.21 (0.326)	0.5515	5
	2 days	1.07 (0.330)	0.8380	5
	4 days	0.96 (0.188)	0.8562	5

B)

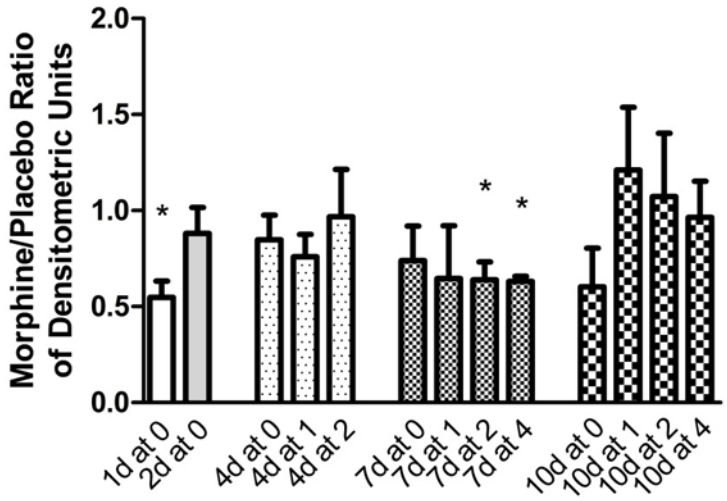

Figure 5.13 PKC_{ε} Abundance in LM/MP Homogenates

A) This table contains the average morphine to placebo ratio of the densitometric units (normalized to GAPDH) of PKC_{ε} in the LM/MP. It also contains the p and n values for each group.

B) This presents the average morphine to placebo ratio of densitometric units (normalized to GAPDH) of PKC_{ε} in the LM/MP expressed in a bar graph.

A)

Length of Treatment	Time After Treatment	PKC$_\varepsilon$ in the LM/MP M/P Ratios (Std. Error)	P values	n=
1 day	0 days	1.47 (0.317)	0.2362	4
2 days	0 days	1.19 (0.124)	0.2260	4
4 days	0 days	0.93 (0.054)	0.2691	4
	1 day	1.17 (0.250)	0.5519	4
	2 days	0.90 (0.129)	0.5040	3
7 days	0 days	1.31 (0.140)	0.1168	4
	1 day	1.06 (0.155)	0.7207	4
	2 days	1.00 (0.179)	0.9897	4
	4 days	1.01 (0.147)	0.9419	4
10 days	0 days	1.68 (0.243)	0.0689	4
	1 day	1.09 (0.170)	0.6468	4
	2 days	1.20 (0.117)	0.1857	4
	4 days	1.26 (0.280)	0.4195	4

B)

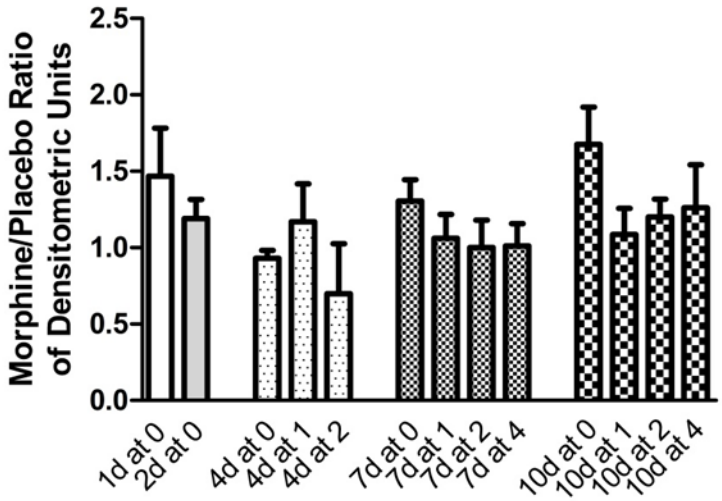

Figure 5.14 PKC_{ε} Abundance in Brainstem Homogenates

A) This table contains the average morphine to placebo ratio of the densitometric units (normalized to GAPDH) of PKC_{ε} in the brainstem. It also contains the p and n values for each group. There were statistically significant decreases in the abundance of this protein in the 4 day – 2 day, 10 day – 0 day, 10 day – 2 day, and 10 day – 4 day animals. There is also a general trend for a decrease across all time points.

B) This presents the average morphine to placebo ratio of densitometric units (normalized to GAPDH) of PKC_{ε} in the brainstem expressed in a bar graph.

A)

Length of Treatment	Time After Treatment	PKC$_\varepsilon$ in the Brainstem M/P Ratios (Std. Error)	P values	n=
1 day	0 days	0.80 (0.101)	0.1389	4
2 days	0 days	0.97 (0.156)	0.8792	4
4 days	0 days	0.85 (0.139)	0.3538	5
	1 day	0.93 (0.093)	0.5028	5
	2 days	0.83 (0.041)*	0.0131	5
7 days	0 days	0.82 (0.120)	0.2122	5
	1 day	0.83 (0.074)	0.0990	4
	2 days	0.90 (0.088)	0.3495	4
	4 days	0.89 (0.094)	0.3182	4
10 days	0 days	0.82 (0.049)*	0.0341	4
	1 day	0.77 (0.101)	0.0823	5
	2 days	0.82 (0.031)*	0.0105	4
	4 days	0.81 (0.054)*	0.0414	4

B)

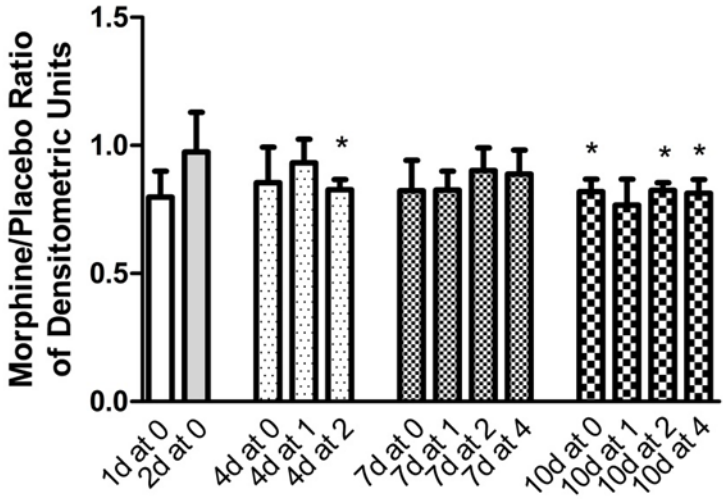

CHAPTER SIX: CONCLUSIONS AND FUTURE DIRECTIONS

6.1 Conclusions

The development of tolerance to morphine, and opioids in general, presents a serious obstacle to the effective management of pain in patients who suffer from severe, chronic pain. Tolerance to opioids occurs as a result of prolonged and repeated exposure to an opioid agonist such as morphine. It is believed that tolerance to morphine is the result of homeostatic adaptive changes in one or more of the cellular signaling elements involved in mediating the acute actions of the agonist. However, despite nearly a century of research, the precise cellular mechanism(s) that is/are responsible for the development of tolerance to morphine remain elusive. There are five criteria that have been proposed that must be fulfilled in order for any proposed cellular mechanism to be identified as accounting for an observed change in responsiveness. "The proposed cellular change must: 1) be induced by experimental procedures identical to those that induce tolerance and/or dependence; 2) follow a similar time course as the tolerance and/or dependence in that tissue; 3) quantitatively account for the tolerance and/or dependence; 4) account for the qualitative characteristics of the tolerance and/or dependence; and 5) occur in the very cells upon which the opioid is acting (Taylor & Fleming, 2001)". There are a number of hypotheses that have been put forth to explain the development of tolerance to morphine (see chapter 1.6). However, not all of these hypotheses have fulfilled all five criteria at the present time. Work from this laboratory has focused on the decrease in the abundance of the α_3 subunit of Na^+/K^+ ATPase as a possible mechanism for the development of tolerance and has generated data that satisfies all but the second criteria in the guinea pig LM/MP preparation (see (Taylor & Fleming, 2001)). Many laboratories tend to use single time points (usually 4 or 7 days after treatment) for their studies and thus cannot satisfy the second criterion. Previous work from this

laboratory has attempted to fulfill criterion two and has demonstrated that the expression of the α_3 subunit of the Na^+/K^+ ATPase does decrease over a similar time course as that for tolerance to develop and this change in protein expression reverses as tolerance fades (Li, Maguma, Thayne, Davis & Taylor, 2010). However, the actual time course for decay of tolerance back to baseline could not be accurately characterized because of the nature of the pellet implantation method of administration of morphine. With pellet implantation there is uncertainty as to when all of the morphine has left the pellet and thus a time zero from which to evaluate the return cannot be defined. Therefore, this project has focused on accurately developing a time course for the onset and decay of tolerance in guinea pigs treated with morphine using a parenteral method of administration which allows definition for the cessation of treatment in order to fulfill the second criterion.

The guinea pig was chosen as a model animal to study the cellular mechanisms of tolerance to morphine over some of the more commonly used animals for a number of reasons. Firstly, the distribution of opioid receptors in the guinea pig brain is more similar to that of humans than that of mice or rats (Mansour, Khachaturian, Lewis, Akil & Watson, 1988). Guinea pigs also have a pharmacological response to morphine that is more similar to that of humans than that observed in mice and rats. Mice and rats also display a locomotor response to morphine whereas humans and guinea pigs do not (Bot, Chahl, Brent & Johnston, 1992). Furthermore, the guinea pig LM/MP has been employed as an ex-vivo model system to demonstrate and study tolerance to opioids since the 1970s (Goldstein & Schulz, 1973).

This project had two specific aims; the first was to generate a time course for the onset and offset of tolerance to morphine in the guinea pig using injections as the method of administration. The second hypothesis was to perform an analysis of the expression of several

proteins that were thought to be intimately involved in the development of tolerance to morphine using the tissues from which functional data had been gathered in the first aim. Previous work in the laboratory had shown that various methods of inducing tolerance all produced a tolerance that is qualitatively and quantitatively similar (Li, Maguma, Thayne, Davis & Taylor, 2010). Intraperitoneal injections had not been used as a method of administration in that study so this method of administration was employed so as to compare the magnitude and characteristics of the tolerance generated with that of the other methods. Because of the dosing issue present in that study (see chapter 3), we were not able to obtain any paw pressure data in the whole animal. The absence of an antinociceptive response was likely due to the fact that the dose of morphine was insufficient to provide significant analgesia. Despite this, we were able to obtain dose-response curves in the LM/MP for DAMGO and 2-CADO indicating that we were able to generate tolerance in these animals. Unfortunately there was considerable variability in those data that was likely due to the variable absorption of the drug using that method of administration. We were not able to achieve a statistical difference with the DAMGO IC_{50} placebo to morphine ratios after 7 days of treatment, a time point at which virtually all of the previous studies and the literature reports the presence of tolerance to morphine. We believe that intraperitoneal injections resulted in variable absorption of morphine from the gut and thus generated higher variability in the data. Unfortunately, this effect seems to predominate in animals that were treated for 7 days but not other times. However, for the animals that did display tolerance, the magnitude of the IC_{50} shift for both DAMGO and 2-CADO were comparable to what was observed with subcutaneous injection and pellet implantation previously (Li, Maguma, Thayne, Davis & Taylor, 2010).

Because it was expected that the LM/MP should be supersensitive to excitatory stimuli, nicotine concentration response curves were also generated in these same LM/MP preparationss. Although supersensitivity was observed previously in pellet implanted animals (Barrett, Maguma & Taylor, 2011; Johnson, Westfall, Howard & Fleming, 1978), the results were highly variable such that a trend was not observable in this study. The method of administration may be the cause of the lack of supersensitivity to nicotine. Pellet implantation is a form of constant dosage in which high concentrations are immediately released and decline over time whereas injections are episodic. It has been shown in rats that during the time between injections the animals undergo a partial withdrawal from morphine and over the period of treatment, this puts the animal in a state of constant stress (Houshyar, Gomez, Manalo, Bhargava & Dallman, 2003). There is known to be a connection between chronic activation of the HPA axis and the function of nicotinic receptors (Lutfy et al., 2006) and it may be that the chronic stress state induced by the injections suppresses the supersensitivity that was observed in pellet implanted animals. The fact that we saw no supersensitivity to nicotine does not exclude the possibility that generalized supersensitivity may still exist in the LM/MP. Previous work has demonstrated supersensitivity in the LM/MP to 5-HT and to K^+ (Johnson, Westfall, Howard & Fleming, 1978).

Based on the work in chapter 3, we determined that IP injections may not be the best method of administration to use for a time course study because of the greater variability in the data when compared to other methods of administration. Because injections were necessary to more appropriately characterize the decay of tolerance to morphine, we chose to use subcutaneous injections to induce tolerance. Subcutaneous injections have been shown previously to successfully induce tolerance that was indistinguishable from the tolerance induced by pellet implantation (Li, Maguma, Thayne, Davis & Taylor, 2010). Although IP injections were not

optimal for studying tolerance, certain observations were made that led to changes in the experimental design of the work described in chapter 4. Significant tolerance was observed after only 4 days of treatment. Therefore, we added groups of animals that were treated for 1 or 2 days in order to more accurately characterize the time course for the onset of tolerance. No other studies have evaluated the characteristics of the response after 2 days of treatment. Because we did not see a significant difference in the return of the DAMGO and 2-CADO IC_{50} ratios to normal 2 days after treatment in animals that were treated for 7 or 10 days, we added groups of animals that were assessed for tolerance 1 day after both 7 and 10 days of treatment. The dosing issue present in chapter 3 was also corrected, allowing successful assessment of development of tolerance with paw pressure testing.

With the modified design, the experiments performed that are presented in chapter 4 were able to provide a more complete time course for the onset and offset of tolerance to morphine. Based on paw pressure AUCs and the morphine to placebo ratios of DAMGO and 2-CADO it appears that significant tolerance began to develop within 2 days of treatment. After 4 days of treatment, the magnitude of tolerance had reached a peak that was indistinguishable from the level of tolerance obtained from animals treated for 7 or 10 days. Despite this apparent peak in tolerance by 4 days that remained constant throughout the treatment period, the animals treated for 7 or 10 days were still tolerant, or close to it, 2 days after the cessation of treatment, whereas animals treated for only 4 days returned to baseline levels of sensitivity at this time point. This suggests that more extensive changes occurred in the animals treated for longer periods of time than in the animals treated for shorter periods of time. These data are consistent with our hypothesis that the magnitude of the changes responsible for the development of tolerance depends on the length of treatment. Tissues from these animals were collected so that a western

blot analysis of several different cellular proteins could be performed on the same tissues in which the functional data were obtained.

Because the development of tolerance to morphine is thought to be due to adaptive changes in protein expression or function, we measured the expression of several proteins that have been previously implicated as playing a role in the development of the phenomenon. Receptor downregulation is a common mechanism by which tolerance or reduced responsiveness could develop in a variety of GPCRs. There also have been some conflicting reports as to the direction and number of receptors present during the development of a tolerant state. Therefore, the μ receptor was considered to be a protein of interest. Experiments performed in chapter 5 demonstrated that in both LM/MP and brainstem homogenates the expression of the μ receptor does not change at any time point that was measured. In fact, none of the receptors examined changed significantly as a result morphine treatment. These data suggest that receptor down-regulation is unlikely to be the mechanism driving the appearance of the heterologous tolerance observed in experiments in animals and ex vivo tissue described in chapter 4.

There are data that satisfy all but the second criteria in order to establish that a potential mechanism that could explain the heterologous tolerance observed in the LM/MP is a decrease in the electrogenic contribution of the Na^+/K^+ ATPase to resting membrane potential (Taylor & Fleming, 2001). The Na^+/K^+ ATPase is composed of catalytic α subunits and β subunits responsible for membrane trafficking and insertion. A possible explanation for the observed decrease in the electrogenic contribution of the Na^+/K^+ ATPase would be a decrease in the abundance of either the α or the β subunits of the Na^+/K^+ ATPase, leading to a reduction in the total number of functional Na^+/K^+ ATPase units. A previous study from this laboratory had demonstrated that chronic morphine treatment results in a decrease in the level of the α_3 subunit

in the guinea pig LM/MP using dot blots analysis (Li, Maguma, Thayne, Davis & Taylor, 2010) and another laboratory has observed a decrease of a similar magnitude in the plasma membrane fraction of the rat forebrain in an α subunit they believe to be the α_3 subunit using mass spectroscopy (Prokai, Zharikova & Stevens, 2005). Until now, the Na^+/K^+ ATPase subunits have only been examined at single time points or with pellet implanted animals which prevented an accurate assessment of the decay of tolerance back to baseline. We examined the α_1, α_3, and β_1 subunits in the brainstem and the α_3 subunit in the LM/MP. We observed no change in any subunit in the brainstem but there did appear to be a trend for a decrease in the abundance of the α_3 subunit with morphine treatment that returned to baseline by 4 days after the treatment ended. Although statistical significance could not be achieved, the magnitude of the decrease was similar to that previously reported in the literature (Li, Maguma, Thayne, Davis & Taylor, 2010; Prokai, Zharikova & Stevens, 2005). The lack of a change in the expression of the α_3 subunit in the brainstem was not expected and may be due to the fact that there are a larger proportion of neurons in that brain area that would not be expected to participate in the response to morphine thereby masking a decrease in expression. It may also reflect a difference in the way that the brainstem develops tolerance compared to the LM/MP. Further investigation will be necessary to explain this discrepancy.

The final set of proteins examined were the γ and ε isoforms of PKC. Expression of these two isoforms has been reported to increase in tolerant animals. The results obtained in the present study indicated that PKC_γ is not present in the LM/MP, which is consistent with previous reports in the literature (Aley & Levine, 1997). Therefore, PKC_ε was examined in the LM/MP and, while present in the tissue, was not observed to significantly change at any time point measured. However, a trend for an increase in expression of that protein was observed as

treatment length increased. Though not statistically significant, there appeared to be trend for a decrease in the abundance of both isoforms of PKC in the brainstem. This observation is not consistent with most of the reported literature. The cause of this discrepancy could be the fact that whole brainstem homogenates were employed instead of specific nuclei within the brainstem that may be more integral to the nociception pathway. It may be that PKC does increase in specific nuclei that are involved with nociception, but neurons in other brain nuclei that are not involved in nociception respond to chronic treatment with morphine differently and decrease. Because the trend is not statistically significant and an opposing trend was observed in the LM/MP, the trend may not reflect anything beyond biological variability. Another possibility that could explain the difference between the brainstem and LM/MP is that these two tissues develop tolerance by different mechanisms, resulting in a decrease in the α_3 subunit Na^+/K^+ ATPase in the LM/MP but not in the brainstem, and no change in PKC levels in the LM/MP but a decrease in the brainstem. However, further experiments would be necessary to confirm this.

In summary, this project has provided a time course for the onset and offset of tolerance to chronic morphine treatment following escalating doses of morphine delivered by either intraperitoneal or subcutaneous injections in the guinea pig. A significant level of tolerance begins to develop after only 2 days of treatment. By 4 days of treatment, heterologous tolerance is evident in the LM/MP based on the IC_{50} ratios of DAMGO and 2-CADO. Although there is no significant difference in the magnitude of tolerance that develops in response to chronic morphine between the 4, 7, and 10 day treatments, it does appear to take longer for animals treated for 7 and 10 to return to baseline (4 days) than for animals treated for 4 days (2 days). These data may indicate that more extensive adaptations occurred in the animals treated for longer periods of time. The tolerance observed in those animals is not due to changes in the μ

receptor, or any other receptor measured, in either the LM/MP or the brainstem as determined by western blot analysis. Although nothing significant was observed, there was a trend for a decrease in the level of the α_3 subunit Na^+/K^+ ATPase in the LM/MP, but not the brainstem. There was also a trend for a decrease in the level of both the γ and ε isoforms of PKC in the brainstem but not in the LM/MP. The time course generated here could provide a useful tool for examining the expression of other proteins that have been implicated in the development of opioid tolerance.

6.2 Future Directions

There are several types of experiments that could be performed to further the goal set forth by this project. One interesting experiment would be to change the method of administration of morphine to one that combines the lower animal stress of pellet implantations with the ability to stop dosing at will. There are programmable osmotic mini pumps available now from Alzet that would allow dose increases similar to what was used in our subcutaneous injection schedule by increasing the rate of infusion after a period of time. This method of administrations also allows for continuous infusion of drug, similar to pellet implantation, which prevents the partial withdrawal between doses that the animal experiences with injections but still allows for the dosing to be stopped at a defined point in time. In using this method of administration, it may be possible to show supersensitivity of the LM/MP to nicotine which may have been masked by the stress the injections put on the animals. Another possibility would be to generate concentration response curves for 5-HT or K^+ instead of nicotine, agents that the LM/MP has previously been shown to develop supersensitivity in morphine tolerant animals (Johnson, Westfall, Howard & Fleming, 1978). The ability to demonstrate supersenitivity to excitatory stimuli and subsensitivity to inhibitory stimuli over the time course generated here would provide greater

evidence that tolerance is the result of a generalized change in membrane potential. Such a mechanism would explain why tolerance is observed to the inhibitory effects of several different agonists (in this project; morphine, DAMGO, and 2-CADO) without a change in the receptor populations of any of these agonists.

Another experiment that would be interesting to perform would be activity assays for the Na^+/K^+ ATPase and PKC. Because the protein levels did not change in the way they were expected to, it would be interesting to see if the activity of these proteins changed in the appropriate direction. Additionally analysis of the mRNA of these proteins using quantitative RT-PCR would provide insight into the nature of the change in protein expression. These studies would allow the determination of whether or not the observed changes in the protein levels were due to changes in synthesis or not. Another experiment of interest would be a more thorough examination of the brainstem. Instead of looking at homogenates of whole brainstem, certain portions of the brainstem that play a role in nociceptive signaling, such as the periaqueductal gray, could be excised and examined individually. Such studies may correct the issues with the brainstem analysis that were performed in these studies. Although some mechanistic work has been done with Na^+/K^+ ATPase and PKC (see chapter 1.6.4 and 1.6.6), it would be interesting to do more of it with the time course generated here. For example, one could inhibit the α_3 subunit of the Na^+/K^+ ATPase from a placebo animal using a low (nM) dose of ouabain in the organ bath set up used for the ex-vivo experiments in chapters 3 and 4. If the α_3 subunit of the Na^+/K^+ ATPase was decreased in either expression or activity during the development of morphine tolerance, artificially inhibiting the activity of the pump in a placebo animal and then constructing concentration response curves for DAMGO and 2-CADO in the LM/MP should generate an alteration in responsiveness that is similar to that observed in morphine tolerant

animals. Conversely, overexpression of the α_3 subunit Na^+/K^+ ATPase in morphine tolerant animals should mitigate the development of tolerance to some degree. Similar types of experiments could be done with the α, γ, and ε isoforms of PKC. Some of these types of experiments have been performed (see chapter 1.6.4) but most of that work has not been done in a guinea pig using the LM/MP as a model system.

Of the five criteria that were proposed (Taylor & Fleming, 2001) that must be fulfilled in order to establish a proposed mechanism as truly being able to account for the observed changes in responsiveness, the second criterion regarding the time course is generally lacking in most of the current literature. Most authors tend to focus on single time points, usually 4 or 7 days of treatment, where the animal is known to be tolerant. The work described in these studies has provided a time course which can now be used to verify several of the other mechanisms suggested by other authors (see chapter 1.6).

REFERENCES

Al-Hasani R, & Bruchas MR (2011). Molecular mechanisms of opioid receptor-dependent signaling and behavior. Anesthesiology 115**:** 1363-1381.

Aley KO, & Levine JD (1997). Different mechanisms mediate development and expression of tolerance and dependence for peripheral mu-opioid antinociception in rat. J Neurosci 17**:** 8018-8023.

Allouche S, Noble F, & Marie N (2014). Opioid receptor desensitization: mechanisms and its link to tolerance. Front Pharmacol 5**:** 280.

Alreja M, & Aghajanian GK (1993). Opiates suppress a resting sodium-dependent inward current and activate an outward potassium current in locus coeruleus neurons. J Neurosci 13**:** 3525-3532.

Arttamangkul S, Lau EK, Lu HW, & Williams JT (2012). Desensitization and trafficking of μ-opioid receptors in locus ceruleus neurons: modulation by kinases. Mol Pharmacol 81**:** 348-355.

Barrett DM, Maguma HT, & Taylor DA (2011). Time course of altered sensitivity to inhibitory and excitatory agonist responses in the longitudinal muscle-myenteric plexus and analgesia in the Guinea pig after chronic morphine treatment. Front Pharmacol 2**:** 88.

Bernstein MA, & Welch SP (1998). mu-Opioid receptor down-regulation and cAMP-dependent protein kinase phosphorylation in a mouse model of chronic morphine tolerance. Brain Res Mol Brain Res 55**:** 237-242.

Biser PS, Thayne KA, Fleming WW, & Taylor DA (2002). Na^+, K^+ ATPase a-subunit isoform distribution and abundance in guinea-pig longitudinal muscle/myenteric plexus after exposure to morphineBrain Research, pp 186-193.

Blanco G, & Mercer RW (1997). Regulation of the alpha 2 beta 1 and alpha 3 beta 1 isozymes of the Na,K-ATPase by Ca2+, PKA, and PKC. Ann N Y Acad Sci 834**:** 572-575.

Bohn LM, Dykstra LA, Lefkowitz RJ, Caron MG, & Barak LS (2004). Relative opioid efficacy is determined by the complements of the G protein-coupled receptor desensitization machinery. Mol Pharmacol 66**:** 106-112.

Bot G, Chahl LA, Brent PJ, & Johnston PA (1992). Effects of intracerebroventricularly administered mu-, delta- and kappa-opioid agonists on locomotor activity of the guinea pig and the pharmacology of the locomotor response to U50,488H. Neuropharmacology 31**:** 825-833.

Bunzow JR, Saez C, Mortrud M, Bouvier C, Williams JT, Low M*, et al.* (1994). Molecular cloning and tissue distribution of a putative member of the rat opioid receptor gene family that is not a mu, delta or kappa opioid receptor type. FEBS Lett 347**:** 284-288.

Chakrabarti S, Chang A, & Gintzler AR (2010). Subcellular localization of mu-opioid receptor G(s) signaling. J Pharmacol Exp Ther 333**:** 193-200.

Chakrabarti S, Regec A, & Gintzler AR (2005). Biochemical demonstration of mu-opioid receptor association with Gsalpha: enhancement following morphine exposure. Brain Res Mol Brain Res 135**:** 217-224.

Chakrabarti S, Wang L, Tang WJ, & Gintzler AR (1998). Chronic morphine augments adenylyl cyclase phosphorylation: relevance to altered signaling during tolerance/dependence. Mol Pharmacol 54**:** 949-953.

Collier H (1966). Tolerance, physical dependence and receptors. Adv Drug Res 3.

Crambert G, Hasler U, Beggah AT, Yu C, Modyanov NN, Horisberger JD*, et al.* (2000). Transport and pharmacological properties of nine different human Na, K-ATPase isozymes. J Biol Chem 275**:** 1976-1986.

Daniels DJ, Lenard NR, Etienne CL, Law PY, Roerig SC, & Portoghese PS (2005). Opioid-induced tolerance and dependence in mice is modulated by the distance between pharmacophores in a bivalent ligand series. Proc Natl Acad Sci U S A 102**:** 19208-19213.

De Vries TJ, Tjon Tien Ril GH, Van der Laan JW, Mulder AH, & Schoffelmeer AN (1993). Chronic exposure to morphine and naltrexone induces changes in catecholaminergic neurotransmission in rat brain without altering mu-opioid receptor sensitivity. Life Sci 52**:** 1685-1693.

Doll C, Konietzko J, Pöll F, Koch T, Höllt V, & Schulz S (2011). Agonist-selective patterns of μ-opioid receptor phosphorylation revealed by phosphosite-specific antibodies. Br J Pharmacol 164**:** 298-307.

Doll C, Pöll F, Peuker K, Loktev A, Glück L, & Schulz S (2012). Deciphering μ-opioid receptor phosphorylation and dephosphorylation in HEK293 cells. Br J Pharmacol 167**:** 1259-1270.

Donica CL, Awwad HO, Thakker DR, & Standifer KM (2013). Cellular mechanisms of nociceptin/orphanin FQ (N/OFQ) peptide (NOP) receptor regulation and heterologous regulation by N/OFQ. Mol Pharmacol 83**:** 907-918.

Feng B, Li Z, & Wang JB (2011). Protein kinase C-mediated phosphorylation of the μ-opioid receptor and its effects on receptor signaling. Mol Pharmacol 79**:** 768-775.

Fichna J, Janecka A, Costentin J, & Do Rego JC (2007). The endomorphin system and its evolving neurophysiological role. Pharmacol Rev 59**:** 88-123.

Fields H, & Basbaum A (2005). Central nervous system mechanisms of pain modulation. In Wall and Melzack's Textbook of Pain. eds McMahon S., & Koltzenburg M. Churchhill Livingstone: Edinburgh.

Fleming WW (1999). Cellular adaptation: journey from smooth muscle cells to neurons. J Pharmacol Exp Ther 291**:** 925-931.

Fleming WW, & Taylor DA (1995). Cellular mechanisms of opioid tolerance and dependence. In Pharmacology of Opioid Peptides. ed Tseng L.F. Harwood Academic Publishers: Amsterdam, pp 463-502.

Fujita W, Gomes I, & Devi LA (2015). Heteromers of μ-δ opioid receptors: new pharmacology and novel therapeutic possibilities. Br J Pharmacol 172**:** 375-387.

Fábián G, Bozó B, Szikszay M, Horváth G, Coscia CJ, & Szücs M (2002). Chronic morphine-induced changes in mu-opioid receptors and G proteins of different subcellular loci in rat brain. J Pharmacol Exp Ther 302**:** 774-780.

Gabra BH, Bailey CP, Kelly E, Smith FL, Henderson G, & Dewey WL (2008). Pre-treatment with a PKC or PKA inhibitor prevents the development of morphine tolerance but not physical dependence in mice. Brain Res 1217**:** 70-77.

George SR, Fan T, Xie Z, Tse R, Tam V, Varghese G*, et al.* (2000). Oligomerization of mu- and delta-opioid receptors. Generation of novel functional properties. J Biol Chem 275**:** 26128-26135.

Gintzler AR, & Chakrabarti S (2008). The ambiguities of opioid tolerance mechanisms: barriers to pain therapeutics or new pain therapeutic possibilities. J Pharmacol Exp Ther 325**:** 709-713.

Goldstein A, Lowney LI, & Pal BK (1971). Stereospecific and nonspecific interactions of the morphine congener levorphanol in subcellular fractions of mouse brain. Proc Natl Acad Sci U S A 68**:** 1742-1747.

Goldstein A, & Schulz R (1973). Morphine-tolerant longitudinal muscle strip from guinea-pig ileum. Br J Pharmacol 48**:** 655-666.

Gomes BA, Shen J, Stafford K, Patel M, & Yoburn BC (2002). Mu-opioid receptor down-regulation and tolerance are not equally dependent upon G-protein signaling. Pharmacol Biochem Behav 72**:** 273-278.

Gomes I, Gupta A, Filipovska J, Szeto HH, Pintar JE, & Devi LA (2004). A role for heterodimerization of mu and delta opiate receptors in enhancing morphine analgesia. Proc Natl Acad Sci U S A 101**:** 5135-5139.

Gomes I, Jordan BA, Gupta A, Trapaidze N, Nagy V, & Devi LA (2000). Heterodimerization of mu and delta opioid receptors: A role in opiate synergy. J Neurosci 20**:** RC110.

Gonzalez LG, Masocha W, Sánchez-Fernández C, Agil A, Ocaña M, Del Pozo E*, et al.* (2012). Changes in morphine-induced activation of cerebral Na(+),K(+)-ATPase during morphine tolerance: biochemical and behavioral consequences. Biochem Pharmacol 83**:** 1572-1581.

Granados-Soto V, Kalcheva I, Hua X, Newton A, & Yaksh TL (2000). Spinal PKC activity and expression: role in tolerance produced by continuous spinal morphine infusion. Pain 85**:** 395-404.

Grevel J, & Sadée W (1983). An opiate binding site in the rat brain is highly selective for 4,5-epoxymorphinans. Science 221**:** 1198-1201.

Gupta A, Décaillot FM, & Devi LA (2006). Targeting opioid receptor heterodimers: strategies for screening and drug development. AAPS J 8**:** E153-159.

Gupta A, Mulder J, Gomes I, Rozenfeld R, Bushlin I, Ong E*, et al.* (2010). Increased abundance of opioid receptor heteromers after chronic morphine administration. Sci Signal 3**:** ra54.

Gähwiler BH (1981). Development of acute tolerance during exposure of hippocampal explants to an opioid peptide. Brain Res 217**:** 196-200.

Hanner M, Moebius FF, Flandorfer A, Knaus HG, Striessnig J, Kempner E*, et al.* (1996). Purification, molecular cloning, and expression of the mammalian sigma1-binding site. Proc Natl Acad Sci U S A 93**:** 8072-8077.

He SQ, Zhang ZN, Guan JS, Liu HR, Zhao B, Wang HB*, et al.* (2011). Facilitation of μ-opioid receptor activity by preventing δ-opioid receptor-mediated codegradation. Neuron 69**:** 120-131.

Hislop JN, Henry AG, & von Zastrow M (2011). Ubiquitination in the first cytoplasmic loop of μ-opioid receptors reveals a hierarchical mechanism of lysosomal down-regulation. J Biol Chem 286**:** 40193-40204.

Houshyar H, Gomez F, Manalo S, Bhargava A, & Dallman MF (2003). Intermittent morphine administration induces dependence and is a chronic stressor in rats. Neuropsychopharmacology 28**:** 1960-1972.

Javed RR, Dewey WL, Smith PA, & Smith FL (2004). PKC and PKA inhibitors reverse tolerance to morphine-induced hypothermia and supraspinal analgesia in mice. Eur J Pharmacol 492**:** 149-157.

Johnson EA, Oldfield S, Braksator E, Gonzalez-Cuello A, Couch D, Hall KJ*, et al.* (2006). Agonist-selective mechanisms of mu-opioid receptor desensitization in human embryonic kidney 293 cells. Mol Pharmacol 70**:** 676-685.

Johnson SM, & Fleming WW (1989). Mechanisms of cellular adaptive sensitivity changes: applications to opioid tolerance and dependence. Pharmacol Rev 41**:** 435-488.

Johnson SM, & Pillai NP (1990). Hyperpolarization of myenteric neurons by opioids does not involve cyclic adenosine-3',5'-monophosphate. Neuroscience 36**:** 299-304.

Johnson SM, Westfall DP, Howard SA, & Fleming WW (1978). Sensitivities of the isolated ileal longitudinal smooth muscle-myenteric plexus and hypogastric nerve-vas deferens of the guinea pig after chronic morphine pellet implantation. J Pharmacol Exp Ther 204**:** 54-66.

Jordan BA, & Devi LA (1999). G-protein-coupled receptor heterodimerization modulates receptor function. Nature 399**:** 697-700.

Kelly E (2013). Ligand bias at the μ-opioid receptor. Biochem Soc Trans 41**:** 218-224.

Kenakin T (2011). Functional selectivity and biased receptor signaling. J Pharmacol Exp Ther 336**:** 296-302.

Klee WA, & Streaty RA (1974). Narcotic receptor sites in morphine-dependent rats. Nature 248**:** 61-63.

Kong JQ, Leedham JA, Taylor DA, & Fleming WW (1997). Evidence that tolerance and dependence of guinea pig myenteric neurons to opioids is a function of altered electrogenic sodium-potassium pumping. J Pharmacol Exp Ther 280**:** 593-599.

Koob GF, & Bloom FE (1988). Cellular and molecular mechanisms of drug dependence. Science 242**:** 715-723.

Kramer HK, & Simon EJ (1999). Role of protein kinase C (PKC) in agonist-induced mu-opioid receptor down-regulation: I. PKC translocation to the membrane of SH-SY5Y neuroblastoma cells is induced by mu-opioid agonists. J Neurochem 72**:** 585-593.

Laemmli UK (1970). Cleavage of structural proteins during the assembly of the head of bacteriophage T4. Nature 227**:** 680-685.

Lau EK, Trester-Zedlitz M, Trinidad JC, Kotowski SJ, Krutchinsky AN, Burlingame AL*, et al.* (2011). Quantitative encoding of the effect of a partial agonist on individual opioid receptors by multisite phosphorylation and threshold detection. Sci Signal 4**:** ra52.

Law PY, Hom DS, & Loh HH (1982). Loss of opiate receptor activity in neuroblastoma X glioma NG108-15 hybrid cells after chronic opiate treatment. A multiple-step process. Mol Pharmacol 22**:** 1-4.

Law PY, & Loh HH (1999). Regulation of opioid receptor activities. J Pharmacol Exp Ther 289**:** 607-624.

Leedham JA, Doak N, Taylor DA, & Fleming WW (1989). The development and reversal of the tolerance to morphine in the longitudinal smooth muscle-myenteric plexus preparation of the guinea pig. Life Sci 45**:** 1483-1489.

Leedham JA, Kong JQ, Taylor DA, Johnson SM, & Fleming WW (1992). Membrane potential in myenteric neurons associated with tolerance and dependence to morphine. J Pharmacol Exp Ther 263**:** 15-19.

Levitt ES, & Williams JT (2012). Morphine desensitization and cellular tolerance are distinguished in rat locus ceruleus neurons. Mol Pharmacol 82**:** 983-992.

Li P, Maguma HT, Thayne K, Davis B, & Taylor DA (2010). Correlation of the time course of development and decay of tolerance to morphine with alterations in sodium pump protein isoform abundance. Biochem Pharmacol 79**:** 1015-1024.

Lin HY, Law PY, & Loh HH (2012). Activation of protein kinase C (PKC)α or PKCε as an approach to increase morphine tolerance in respiratory depression and lethal overdose. J Pharmacol Exp Ther 341**:** 115-125.

Lord JA, Waterfield AA, Hughes J, & Kosterlitz HW (1977). Endogenous opioid peptides: multiple agonists and receptors. Nature 267**:** 495-499.

Lutfy K, Brown MC, Nerio N, Aimiuwu O, Tran B, Anghel A*, et al.* (2006). Repeated stress alters the ability of nicotine to activate the hypothalamic-pituitary-adrenal axis. J Neurochem 99**:** 1321-1327.

Maguma H, & Taylor DA (2011). The effect of chronic opioid vs. cannabinoid exposure on the expression of tolerance to morphine- or WIN-55,212-2-induced analgesia and hypothermia in the guinea pig. Eur J Pharmacol 660**:** 334-340.

Manallack D, Beart P, & Gundlach A (1986). Psyhcotomimetic sigma-opiates and PCP. Trends Pharmacol Sci 7**:** 448-451.

Mansour A, Khachaturian H, Lewis ME, Akil H, & Watson SJ (1988). Anatomy of CNS opioid receptors. Trends Neurosci 11**:** 308-314.

Martin WR, Eades CG, Thompson JA, Huppler RE, & Gilbert PE (1976). The effects of morphine- and nalorphine- like drugs in the nondependent and morphine-dependent chronic spinal dog. J Pharmacol Exp Ther 197**:** 517-532.

Masocha W, González LG, Baeyens JM, & Agil A (2002). Mechanisms involved in morphine-induced activation of synaptosomal Na+,K+-ATPase. Brain Res 957**:** 311-319.

Mathoôt RA, Soudijn W, Breimer DD, Ijzerman AP, & Danhof M (1996). Pharmacokinetic-haemodynamic relationships of 2-chloroadenosine at adenosine A1 and A2a receptors in vivo. Br J Pharmacol 118**:** 369-377.

Meng J, Malanga CJ, Kong JQ, Taylor DA, & Fleming WW (1997). Hyperpolarizing effects of morphine, clonidine and 2-chloroadenosine in myenteric neurons associated with tolerance to morphine. J Pharmacol Exp Ther 281**:** 41-47.

Meunier JC, Mollereau C, Toll L, Suaudeau C, Moisand C, Alvinerie P*, et al.* (1995). Isolation and structure of the endogenous agonist of opioid receptor-like ORL1 receptor. Nature 377**:** 532-535.

Mollereau C, Parmentier M, Mailleux P, Butour JL, Moisand C, Chalon P*, et al.* (1994). ORL1, a novel member of the opioid receptor family. Cloning, functional expression and localization. FEBS Lett 341**:** 33-38.

Nestler EJ, & Aghajanian GK (1997). Molecular and cellular basis of addiction. Science 278**:** 58-63.

Nestler EJ, Alreja M, & Aghajanian GK (1994). Molecular and cellular mechanisms of opiate action: studies in the rat locus coeruleus. Brain Res Bull 35**:** 521-528.

Nestler EJ, Erdos JJ, Terwilliger R, Duman RS, & Tallman JF (1989). Regulation of G proteins by chronic morphine in the rat locus coeruleus. Brain Research 476**:** 230-239.

Oka T (1980). Enkephalin receptor in the rabbit ileum. Br J Pharmacol 68**:** 193-195.

Osler W (1910). The Lumleian lectures on angina pectorisLancet I: London, UK, pp 697-702, 839-844, 973-977.

Patierno S, Anselmi L, Jaramillo I, Scott D, Garcia R, & Sternini C (2011). Morphine induces μ opioid receptor endocytosis in guinea pig enteric neurons following prolonged receptor activation. Gastroenterology 140**:** 618-626.

Paton WD (1957). The action of morphine and related substances on contraction and on acetylcholine output of coaxially stimulated guinea-pig ileum. Br J Pharmacol Chemother 12**:** 119-127.

Paul O (1999). Notes on the effects of morphine. In The Caring Physician: The Life of Dr Francis W Peabody. The Francis A. Countway Library of Medicine & The Harvard Medical Alumni Association: Harvard University Press, pp 137, 175-182.

Pert CB, & Snyder SH (1973). Opiate receptor: demonstration in nervous tissue. Science 179**:** 1011-1014.

Pierce KL, Premont RT, & Lefkowitz RJ (2002). Seven-transmembrane receptors. Nat Rev Mol Cell Biol 3**:** 639-650.

Pradhan AA, Smith ML, Kieffer BL, & Evans CJ (2012). Ligand-directed signalling within the opioid receptor family. Br J Pharmacol 167**:** 960-969.

Prokai L, Zharikova AD, & Stevens SM (2005). Effect of chronic morphine exposure on the synaptic plasma-membrane subproteome of rats: a quantitative protein profiling study based on isotope-coded affinity tags and liquid chromatography/mass spectrometry. J Mass Spectrom 40**:** 169-175.

Raehal KM, Schmid CL, Groer CE, & Bohn LM (2011). Functional selectivity at the μ-opioid receptor: implications for understanding opioid analgesia and tolerance. Pharmacol Rev 63**:** 1001-1019.

Randall LO, & Selitto JJ (1957). A method for measurement of analgesic activity on inflamed tissue. Arch Int Pharmacodyn Ther 111**:** 409-419.

Reinscheid RK, Nothacker HP, Bourson A, Ardati A, Henningsen RA, Bunzow JR*, et al.* (1995). Orphanin FQ: a neuropeptide that activates an opioidlike G protein-coupled receptor. Science 270**:** 792-794.

Rodríguez-Muñoz M, de la Torre-Madrid E, Sánchez-Blázquez P, & Garzón J (2011). NO-released zinc supports the simultaneous binding of Raf-1 and PKCγ cysteine-rich domains to HINT1 protein at the mu-opioid receptor. Antioxid Redox Signal 14**:** 2413-2425.

Rodríguez-Muñoz M, de la Torre-Madrid E, Sánchez-Blázquez P, Wang JB, & Garzón J (2008). NMDAR-nNOS generated zinc recruits PKCgamma to the HINT1-RGS17 complex bound to the C terminus of Mu-opioid receptors. Cell Signal 20**:** 1855-1864.

Rodríguez-Muñoz M, Sánchez-Blázquez P, Vicente-Sánchez A, Berrocoso E, & Garzón J (2012). The mu-opioid receptor and the NMDA receptor associate in PAG neurons: implications in pain control. Neuropsychopharmacology 37**:** 338-349.

Rothman RB, Long JB, Bykov V, Xu H, Jacobson AE, Rice KC*, et al.* (1991). Upregulation of the opioid receptor complex by the chronic administration of morphine: a biochemical marker related to the development of tolerance and dependence. Peptides 12**:** 151-160.

Rozenfeld R, & Devi LA (2007). Receptor heterodimerization leads to a switch in signaling: beta-arrestin2-mediated ERK activation by mu-delta opioid receptor heterodimers. FASEB J 21**:** 2455-2465.

Sarnyai Z, Shaham Y, & Heinrichs SC (2001). The role of corticotropin-releasing factor in drug addiction. Pharmacol Rev 53**:** 209-243.

Schulz R, & Goldstein A (1973). Morphine tolerance and supersensitivity to 5-hydroxytryptamine in the myenteric plexus of the guinea-pig. Nature 244**:** 168-170.

Schumacher MA, Basbaum AI, & Way WL (2012). Opioid Analgesics and Antagonists. In Basic and Clinical Pharmacology. eds Katzung B.G., Masters S.B., & Trevor A.J. McGraw-Hill: USA.

Schwinger RH, Wang J, Frank K, Müller-Ehmsen J, Brixius K, McDonough AA*, et al.* (1999). Reduced sodium pump alpha1, alpha3, and beta1-isoform protein levels and Na+,K+-ATPase activity but unchanged Na+-Ca2+ exchanger protein levels in human heart failure. Circulation 99**:** 2105-2112.

Shen J, Benedict Gomes A, Gallagher A, Stafford K, & Yoburn BC (2000). Role of cAMP-dependent protein kinase (PKA) in opioid agonist-induced mu-opioid receptor downregulation and tolerance in mice. Synapse 38**:** 322-327.

Shy M, Chakrabarti S, & Gintzler AR (2008). Plasticity of adenylyl cyclase-related signaling sequelae after long-term morphine treatment. Mol Pharmacol 73**:** 868-879.

Sim LJ, & Childers SR (1997). Anatomical distribution of mu, delta, and kappa opioid- and nociceptin/orphanin FQ-stimulated [35S]guanylyl-5'-O-(gamma-thio)-triphosphate binding in guinea pig brain. J Comp Neurol 386**:** 562-572.

Smith FL, Gabra BH, Smith PA, Redwood MC, & Dewey WL (2007). Determination of the role of conventional, novel and atypical PKC isoforms in the expression of morphine tolerance in mice. Pain 127**:** 129-139.

Smith NJ, & Milligan G (2010). Allostery at G protein-coupled receptor homo- and heteromers: uncharted pharmacological landscapes. Pharmacol Rev 62**:** 701-725.

Sorge RE, Martin LJ, Isbester KA, Sotocinal SG, Rosen S, Tuttle AH*, et al.* (2014). Olfactory exposure to males, including men, causes stress and related analgesia in rodents. Nat Methods 11**:** 629-632.

Stafford K, Gomes AB, Shen J, & Yoburn BC (2001). mu-Opioid receptor downregulation contributes to opioid tolerance in vivo. Pharmacol Biochem Behav 69**:** 233-237.

Su TP, London ED, & Jaffe JH (1988). Steroid binding at sigma receptors suggests a link between endocrine, nervous, and immune systems. Science 240**:** 219-221.

Sweadner KJ (1989). Isozymes of the Na+/K+-ATPase. Biochim Biophys Acta 988**:** 185-220.

Sánchez-Blázquez P, Rodríguez-Muñoz M, de la Torre-Madrid E, & Garzón J (2009). Brain-specific Galphaz interacts with Src tyrosine kinase to regulate Mu-opioid receptor-NMDAR signaling pathway. Cell Signal 21**:** 1444-1454.

Sánchez-Blázquez P, Rodríguez-Muñoz M, & Garzón J (2010). Mu-opioid receptors transiently activate the Akt-nNOS pathway to produce sustained potentiation of PKC-mediated NMDAR-CaMKII signaling. PLoS One 5**:** e11278.

Taylor DA (2011). In Vitro Opioid Receptor Assays. In Current Protocols in Pharmacology. Wiley Online Library, p Unit 4.8.

Taylor DA, & Fleming WW (2001). Unifying perspectives of the mechanisms underlying the development of tolerance and physical dependence to opioids. J Pharmacol Exp Ther 297**:** 11-18.

Taylor DA, Leedham JA, Doak N, & Fleming WW (1988). Morphine tolerance and nonspecific subsensitivity of the longitudinal muscle myenteric plexus preparation of the guinea-pig to inhibitory agonists. Naunyn Schmiedebergs Arch Pharmacol 338**:** 553-559.

Tokhtaeva E, Clifford RJ, Kaplan JH, Sachs G, & Vagin O (2012). Subunit isoform selectivity in assembly of Na,K-ATPase α-β heterodimers. J Biol Chem 287**:** 26115-26125.

Trescot AM, Datta S, Lee M, & Hansen H (2008). Opioid pharmacology. Pain Physician 11**:** S133-153.

Vandevenne M, Vandenbussche H, & Verstraete A (2000). Detection time of drugs of abuse in urine. Acta Clin Belg 55**:** 323-333.

Velázquez KT, Mohammad H, & Sweitzer SM (2007). Protein kinase C in pain: involvement of multiple isoforms. Pharmacol Res 55**:** 578-589.

Wang ZJ, & Wang LX (2006). Phosphorylation: a molecular switch in opioid tolerance. Life Sci 79**:** 1681-1691.

Whistler JL, & von Zastrow M (1998). Morphine-activated opioid receptors elude desensitization by beta-arrestin. Proc Natl Acad Sci U S A 95**:** 9914-9919.

Wong SK, Westfall DP, Fedan JS, & Fleming WW (1981). The involvement of the sodium-potassium pump in postjunctional supersensitivity of the guinea-pig vas deferens as assessed by [3H]ouabain binding. J Pharmacol Exp Ther 219**:** 163-169.

Wu ZQ, Li M, Chen J, Chi ZQ, & Liu JG (2006). Involvement of cAMP/cAMP-dependent protein kinase signaling pathway in regulation of Na+,K+-ATPase upon activation of opioid receptors by morphine. Mol Pharmacol 69**:** 866-876.

Wüster M, Schulz R, & Herz A (1979). Specificity of opioids towards the mu-, delta- and epsilon-opiate receptors. Neurosci Lett 15**:** 193-198.

Yabaluri N, & Medzihradsky F (1997). Down-regulation of mu-opioid receptor by full but not partial agonists is independent of G protein coupling. Mol Pharmacol 52**:** 896-902.

Yaksh TL, & Wallace MS (2011). Opioids, Analgesia, and Pain Management. In Goodman and Gilman's The Pharmacological Basis of Terapeutics. eds Brunton L., Chabner B., & Knollman B. McGraw Hill: New York.

Yekkirala AS, Banks ML, Lunzer MM, Negus SS, Rice KC, & Portoghese PS (2012). Clinically employed opioid analgesics produce antinociception via μ-δ opioid receptor heteromers in Rhesus monkeys. ACS Chem Neurosci 3**:** 720-727.

Yekkirala AS, Kalyuzhny AE, & Portoghese PS (2010). Standard opioid agonists activate heteromeric opioid receptors: evidence for morphine and [d-Ala(2)-MePhe(4)-Glyol(5)]enkephalin as selective μ-δ agonists. ACS Chem Neurosci 1**:** 146-154.

Yoburn BC, Billings B, & Duttaroy A (1993). Opioid receptor regulation in mice. J Pharmacol Exp Ther 265**:** 314-320.

Zagon IS, Goodman SR, & McLaughlin PJ (1989). Characterization of zeta (zeta): a new opioid receptor involved in growth. Brain Res 482**:** 297-305.

Zeitz KP, Malmberg AB, Gilbert H, & Basbaum AI (2001). Reduced development of tolerance to the analgesic effects of morphine and clonidine in PKC gamma mutant mice. Pain 94**:** 245-253.

Zhu Y, King MA, Schuller AG, Nitsche JF, Reidl M, Elde RP*, et al.* (1999). Retention of supraspinal delta-like analgesia and loss of morphine tolerance in delta opioid receptor knockout mice. Neuron 24**:** 243-252.

APPENDIX A: ANIMAL CARE AND USE COMMITTEE APPROVAL LETTER

East Carolina University

Animal Care and Use Commitee
212 Ed Warren Life Sciences Building
East Carolina University
Greenville, NC 27834

252-744-2436 office
252-744-2555 fax

November 6, 2015

David Taylor, Ph.D.
Department of Pharmacology
Brody 6S-10
ECU Brody School of Medicine

Dear Dr. Taylor:

Your Animal Use Protocol entitled, "Cell Signaling and Tolerance to Drugs" (AUP #W201d) was reviewed by this institution's Animal Care and Use Committee on November 6, 2015. The following action was taken by the Committee:

"Approved as submitted"

Please contact Dale Aycock at 744-2997 prior to hazard use

A copy is enclosed for your laboratory files. Please be reminded that all animal procedures must be conducted as described in the approved Animal Use Protocol. Modifications of these procedures cannot be performed without prior approval of the ACUC. The Animal Welfare Act and Public Health Service Guidelines require the ACUC to suspend activities not in accordance with approved procedures and report such activities to the responsible University Official (Vice Chancellor for Health Sciences or Vice Chancellor for Academic Affairs) and appropriate federal Agencies. **Please ensure that all personnel associated with this protocol have access to this approved copy of the AUP and are familiar with its contents.**

Sincerely yours,

Susan McRae, Ph.D.
Chair, Animal Care and Use Committee

SM/jd

Enclosure

APPENDIX B: KREBS – HENSELEIT BUFFER

Stock Solution "A" (10X Stock)

Chemical	Molecular Weight	Grams	Final Concentration
Sodium Chloride	58.44	66.00	1.13 M
Potassium Chloride	74.56	3.54	47 mM
Calcium Chloride	110.99	2.80	25 mM
Magnesium Sulfate	246.5	2.94	12 mM
Dextrose	180.16	10.00	56 mM

Final Volume (bring to with distilled water) 1 L

Store at 4°C

Stock Solution "B" (10X Stock)

Chemical	Molecular Weight	Grams	Final Concentration
Potassium Phosphate Monobasic	136.09	1.61	11.8 mM
Sodium Bicarbonate	84.10	21.00	250 mM

Final Volume (bring to with distilled water) 1 L

Store at 4°C

To make 1 L of the working solution: (1X solution) MAKE FRESH DAILY

1) Add 100 mL of the 10X Stock "A"
2) Add some distilled water
3) Add 100 mL of the 10X Stock "B"
4) Bring volume to 1 L with distilled water
5) Aerate with 95% oxygen/ 5% carbon dioxide

APPENDIX C: PROTEASE INHIBITOR BUFFER

Components

Chemical	Constitution	Concentration	Notes
Phenylmethyl Sulfonyl Fluoride(PMSF)	35.6 mg into 1 mL of isopropanol	204 mM	More concentrated that Sigma recommends. It will go into solution by heating at 55°C for 5 min. **Make fresh daily.**
Bacitracin	50 mg into 500 µL of distilled water then add 500 µL of distilled water	50 mg/mL	May require heating at 55°C for 10-15 min to go into solution. **Store at < 0°C.**
4-Aminobenzamindine	50.4 mg into 1 mL of distilled water	242 mM	**Store at < 0°C.**
Ethylenediaminetetraacetic acid (EDTA)	46.53 g into 500 mL of distilled water	250 mM	**pH to 8.0 and store at room temperature.**

To make the working solution (Make Daily):

Chemical	Amount for full batch	Amount for half batch	Amount for quarter batch	Final Concentration
PMSF	0.5 mL	0.25 mL	0.125 mL	4.08 mM
Bacitracin	500 µL	250 µL	125 µL	1 mg/mL
4-Aminobenzamidine	100 µL	50 µL	25 µL	1 mM
Sucrose	2.14 g	1.07 g	0.535 g	0.25 mM
EDTA	1 mL	0.5 mL	0.25 mL	10 mM
Final Volume (bring to with distilled water)	25 mL	12.5 mL	6.25 mL	

APPENDIX D: WESTERN BLOT BUFFERS

10X Running Buffer

Chemical	Amount	Final Concentration
Tris-Base	30.28 g	0.25 M
Glycine	150.14 g	2 M
Sodium Dodecyl Sulfate (SDS)	10.00 g	1%

pH to 8.6 and bring volume to 1 L with distilled water
Dilute 1:10 for working solution.
Store at room temperature.

10X Phosphate Buffered Saline (PBS)

Chemical	Amount	Final Concentration
Sodium Chloride	80.00 g	1.4 M
Potassium Chloride	2.00 g	2.6 mM
Sodium Phosphate Dibasic	14.40 g	101.4 mM
Potassium Phosphate Monobasic	2.40 g	17.6 mM

pH to 7.4 and bring volume to 1 L with distilled water
Dilute 1:10 for working solution.
Store at room temperature.

1X Phosphate Buffered Saline – 0.1% Tween 20 (PBS-T)

1) 100 mL 10X PBS
2) 1.0 mL Tween-20
3) Bring volume to 1 L with distilled water. Store at room temperature.

1X PBS-T with 0.02% SDS

1) 500 mL of 1X PBS-T
2) 0.1 g of Sodium Dodecyl Sulfate (SDS). Store at room temperature.

Sample Buffer (Laemmli, 1970)

Components

Chemical	Constitution	Final Concentration	Notes
Tris-HCl	2.364 g into 30 mL of distilled water	0.5 M	**pH to 6.8** Store at room temperature
10% Sodium Dodecyl Sulfate (SDS)	1 g into 10 mL of distilled water	10%	Store at room temperature
Bromophenol Blue	0.000157 mg into 10 mL of distilled water	15.7 µM	Store at room temperature

To make the working solution:

Chemical	Amount
0.5 M Tris-HCl pH 6.8	1.25 mL
10% SDS	2.00 mL
Glycerin	1 g
2-Mercaptoethanol (β-ME)	0.5 mL
Bromophenol Blue	200 µL

Bring to 10 mL with distilled water.
Store at room temperature.

APPENDIX E: ANTIBODIES FOR WESTERN BLOT ANALYSES

Primary Antibodies

Protein	Host	Dilution (LM/MP)	Dilution (Brainstem)	Molecular Weight (kDa)	Antibody Source	Catalogue #
Glyceraldehyde 3-phosphate dehydrogenase (GAPDH)	Rabbit	1:10000	1:10000	36	Sigma	G9545
Glyceraldehyde 3-phosphate dehydrogenase (GAPDH)	Mouse	1:30000	1:30000	36	Millipore	MAB374
β_3 Tubulin	Rabbit	1:2000	N/A	50	Abcam	18207
β_3 Tubulin	Mouse	1:2000	N/A	50	Abcam	118627
μ Receptor	Rabbit	1:2000	1:1000	45	Chemicon	AB5511
A_1 Receptor	Rabbit	1:1000	1:1000	36	Abcam	82477
A_{2a} Receptor	Mouse	1:100	1:100	45	Abcam	ab79714
α_{2b} Receptor	Rabbit	1:5000	1:5000	50	Abcam	ab151727
α_1 subunit of the Na^+/K^+ ATPase	Mouse	1:500	1:1000	110	Abcam	ab7671
α_3 subunit of the Na^+/K^+ ATPase	Mouse	1:500	1:1000	110	ThermoFisher	XVIF9-G10
β_1 subunit of the Na^+/K^+ ATPase	Mouse	1:1000	1:1000	48-55	Millipore	05-382
Protein Kinase C_γ	Rabbit	N/A	1:1000	78	Abcam	71558
Protein Kinase C_ε	Rabbit	1:1000	1:1000	82	Cell Signaling	4376

All primary antibodies were diluted in Odyssey Blocking Buffer with 0.1% Tween 20 and stored at 4°C until use.

Secondary Antibodies

Host	Conjugated Dye	Dilution	Antibody Source	Catalogue #
Goat anti-rabbit	IRDye 680 LT	1:30000	Li-Cor Biosciences	926-68021
Goat anti-mouse	IRDye 800 CW	1:30000	Li-Cor Biosciences	926-32210
Goat anti-rabbit	IRDye 800 CW	1:30000	Li-Cor Biosciences	926-32211
Goat anti-mouse	IRDye 680 LT	1:30000	Li-Cor Biosciences	926-68020

All secondary antibodies were diluted in PBS-T with 0.02% SDS and stored at 4°C until use.

Protect secondary antibody solutions from light.